Optimization of NK cell-based immune therapy strategies against pediatric acute B cell precursor leukemia using a human-murine xenotransplantation model

Dissertation

der Mathematisch-Naturwissenschaftlichen Fakultät

der Eberhard Karls Universität Tübingen

zur Erlangung des Grades eines

Doktors der Naturwissenschaften

(Dr. rer. nat.)

vorgelegt von

Ayline Kübler, geb. Wilhelm

aus Mühlacker

Tübingen

2015

Gedruckt mit Genehmigung der Mathematisch-Naturwissenschaftlichen Fakultät der Eberhard Karls Universität Tübingen.

Tag der mündlichen Qualifikation:	11.11.2015
Dekan:	Prof. Dr. Wolfgang Rosenstiel
1. Berichterstatter:	Prof. Dr. Rupert Handgretinger
2. Berichterstatter:	Prof. Dr. Stefan Stevanović

ZUSAMMENFASSUNG

Killer-immunoglobulin-like Receptors (KIR) auf Natürlichen Killerzellen (NK-Zellen) und deren HLA-Liganden spielen eine wichtige Rolle in der Selbst-und Fremderkennung durch NK-Zellen. In einer inkompatiblen KIR-KIR-Liganden Konstellation (sog. „Mismatch“) wird das Gleichgewicht von inhibitorischen und aktivierenden Signalen zugunsten einer Zytotoxizität gegenüber der Zielzelle verschoben. Bisherige Studien deuten darauf hin, dass die KIR-KIR-Liganden Mismatch-Konstellation bei NK-Zell-basierten Therapieansätzen den Therapieerfolg bei erwachsenen Patienten mit akuter myeloischer Leukämie (AML) deutlich verbessern, während akute lymphatische Leukämien der B-Zellreihe (B-ALL) relativ resistent gegenüber der Zytotoxizität durch NK-Zellen zu sein scheinen. Die Expression von KIR Molekülen wird über Promotormethylierung reguliert, was die Expression sensibel für DNA-Methyltransferase (Dnmt)-Inhibitoren macht. Mithilfe eines NOD-*scid* IL2Rgamma^{null} (NSG) Xenotransplantationsmodels wurden in dieser Arbeit zwei Arten von NK-Zell-basierter Therapie für die pädiatrische B-Zell-Vorläufer-Leukämie (BCP-ALL) untersucht: Erstens der adoptive Transfer von reifen, Zytokin-aktivierten NK-Zellen in leukämietragende Mäuse und zweitens Transplantat-versus-Leukämie Effekte (graft-versus-leukemia, GvL), die durch aus dem Transplantat entstehende NK-Zellen vermittelt werden. Experimente mit adoptivem NK-Zell-Transfer zeigen, dass die pädiatrische BCP-ALL *in vivo* durch reife NK-Zellen angreifbar ist. Darüber hinaus liefert diese Arbeit substantielle Hinweise dafür, dass die KIR-KIRL-Konstellation für das Ausmaß der Zytotoxizität eine wichtige Rolle spielt. Sortierexperimente mit NK-Zellen die einen KIR-KIRL Mismatch aufweisen, zeigen eine erhöhte Funktionalität von KIR$^+$ gegenüber KIR$^-$ NK-Zellen, was sich in der KIR-KIRL kompatiblen Match-Situation umkehrt. Mechanistisch lässt sich dies auf eine erhöhte Funktionalität der „alloreaktiven“ KIR$^+$ NK-Zell Subpopulation zurückführen. In humanisierten, also stammzelltransplantierten NSG-Mäusen (huNSG) finden sich unter den sich aus dem Transplantat entwickelnden NK-Zellen interessanterweise hauptsächlich unreife KIR$^-$ NK-Zellen. Dies ähnelt daher ideal der NK-Zell-Entwicklung in Patienten nach hämatopoetischer Stammzelltransplantation (HSCT). Durch die Supplementation von Zytokinen können in huNSG Mäusen relevante GvL-Effekte gegenüber primären B-Zell-Vorläufer-Leukämiezellen nachgewiesen werden, was darauf hinweist, dass wahrscheinlich unreife, sich aus dem Transplantat entwickelnde NK-Zellen zur Alloreaktivität beitragen. Der Dnmt-Inhibitor 5-Azacytidin (5-AzaC) hat in diesem Modell überraschenderweise nicht die KIR-Expression auf NK-Zellen erhöht, wie dies für reife NK-Zellen *in vitro* beschrieben ist, sondern zu einem erhöhten Vorhandensein von unreifen und auch reifen NK-Zell-Subpopulationen und einer damit einhergehenden erhöhten anti-leukämischen Antwort geführt. Es kann daher davon ausgegangen werden, dass eine 5-AzaC Behandlung früh nach HSCT die Differenzierung von NK-Zellen fördert, die wiederrum zu einem relevanten GvL-Effekt *in vivo* beitragen können. Im Ergebnis könnte die NK-Zell-vermittelte Immunantwort in der Therapie von rezidivierenden kindlichen BCP-ALL Patienten in Zukunft berücksichtigt werden.

SUMMARY

Killer-immunoglobulin-like (KIR)-receptors on natural killer (NK) cells and their corresponding HLA ligands play an important role in self-/non-self-discrimination of NK cells. In mismatched KIR-KIR ligand constellations the balance of inhibitory and activating signals is shifted towards target cell lysis. Previous studies indicate that these KIR-KIR ligand mismatch constellations significantly increase the outcome for patients suffering from adult acute myeloid leukemia whereas adult acute B cell lymphocytic leukemia (B-ALL) seems to be relative resistant to NK cell-mediated cytotoxicity. Expression of KIR molecules is regulated via promoter methylation rendering expression susceptible for DNA methyltransferase (Dnmt) inhibitors. Using a NOD-*scid* IL2Rgamma^{null} (NSG) xenotransplantation model two modes for NK cell-based therapies in pediatric B cell precursor ALL (BCP-ALL) were explored: First, the adoptive transfer of mature cytokine-activated NK cells into leukemia-bearing mice and second graft-versus-leukemia effects (GvL) mediated by transplant–emerging NK cells. Adoptive transfer experiments show that pediatric BCP-ALL can be targeted by mature NK cells *in vivo*. Furthermore, this work provides substantial evidence that mismatched KIR-KIRL constellations are superior in this setting. Sorting experiments reveal that mismatched KIR$^+$ NK cells display enhanced functionality compared to KIR$^-$ NK cells, which is reversed in matched constellations. Mechanistically, superior alloreactivity of KIR-KIRL mismatched compared to KIR-KIRL matched NK cells can be attributed to the KIR$^+$ 'alloreactive' subset. Considering graft-emerging NK cells mainly immature KIR$^-$ NK-cells in stem cell transplanted NSG mice ("humanized NSG") can be detected, thus ideally resembling human NK cell ontogeny of patients post hematopoietic stem cell transplantation (HSCT). Under cytokine support there are relevant GvL effects towards primary B cell precursor leukemia in huNSG mice providing evidence that also early graft-emerging immature NK cells might contribute to alloreactivity. The Dnmt-inhibitor 5-azacytidine (5-AzaC) surprisingly does not increase KIR expression on NK cells as previously described for mature NK cells *in vitro*. 5-AzaC distinctly enhances immature and mature NK cell subsets and along with this the anti-leukemic response. It can therefore be proposed that 5-AzaC treatment early after HSCT promotes differentiation of NK cells which can contribute to relevant GvL effects *in vivo*. As a result, future protocols might consider exploitation of NK cell-mediated immune-responses for relapsing pediatric BCP-ALL patients.

ABBREVIATIONS

5-AzaC	5-Azacytidine, trade name Vidaza
5-AzadC	5-Aza-2'deoxycytidine, decitabine, trade name Dacogen
aKIR	Activating KIR
ALL	Acute lymphocytic leukemia
AML	Acute myeloid leukemia
APC	Antigen-presenting cell
Bcl-2	B cell lymphoma 2
BCP-ALL	Acute B cell precursor leukemia
BrdU	5-Bromo-2'deoxyuridine
CCR7	Chemokine (C-C motif) receptor 7
CD	Cluster of differentiation
cDNA	Complementary DNA
C_t	Threshold cycle
CFSE	Carboxyfluorescein diacetat succinimidyl ester
CML	Chronic myeloid leukemia
CMML	Chronic myelomonocytic leukemia
DAP12	DNAX activation protein of 12 kDa
DC	Dendritic cell
DLI	Donor lymphocyte infusion
DMSO	Dimethyl sulfoxide
DNA	Deoxyribonucleic acid
DNAM-1	DNAX accessory molecule 1
Dnmt	DNA methytransferase
E:T ratio	Effector-to-target ratio
EMA	European Medicines Agency
ETS	E26 transformation-specific
FAB	French-American-British cooperative group
FasL	Fas ligand (TNF superfamily, member 6)
FCS	Fetal calf serum
FDA	U.S. Food and Drug Administration
FFP	Fresh frozen plasma
FLT3L	FMS-like tyrosine kinase 3 ligand
GalC	Galactosylceramidase
gDNA	Genomic DNA
GFP	Green fluorescent protein
GMP	Good manufacturing practice
GvHD	graft-versus-host disease
GvL	Graft versus leukemia
h	hour/hours
HLA	Human leukocyte antigen
HSC	Hematopoietic stem cell
HSCT	Hematopoietic stem cell transplantation
HuNSG	Humanized NOD.Cg-*Prkdc*^{Scid}*IL2Rg*^{tmWjl}*/Sz* mice
iKIR	Inhibitory KIR

i.p.	Intraperitoneal
i.v.	Intravenous
IFN-γ	Interferon-γ
Ig	Immunoglobulin
IL	Interleukin
IL-15Rα	IL-15 receptor α chain
IL2R	IL-2 receptor
ILC	Innate lymphoid cell
iNK cell	Immature NK cell (stage 3)
ITIM	Immune tyrosine-based inhibitory motifs
kDa	Kilo dalton
KIR/KIRL	Killer immunoglobulin-like receptor /KIR ligand
LFA-1	Leukocyte function-associated antigen 1
mAb	Monoclonal antibody
MDS	Myelodysplastic syndrome
MICA/MICB	MHC class I polypeptide-related sequence A/B
mNK cell	Mature NK cell (stage 4)
MRD	Minimal residual disease
NCAM	Neural cell adhesion molecule
NCR	Natural cytotoxicity receptor
NK cells	Natural killer cells
NKAES	NK cell activation and expansion system
NKAES cells	NK cells expanded according to the protocol 'NK cell activation and expansion system'
NKG2D-L	NKG2D ligand
NS mice	NOD/*scid* mice
NSG mice	NOD.Cg-Prkdc^{scid} IL2rg^{tmWjl}/SzJ mice, also termed NOD-*scid* IL2Rgamma^{null} mice
o/n	Overnight
PAMP	Pathogen associated molecular pattern
PBMC	Peripheral blood mononuclear cell
PFA	Paraformaldehyde
pre-NK cell	Precursor NK cell (stage 2)
pro-NK cell	Progenitor NK cell (stage 1)
PVR	Poliovirus receptor
RNA	Ribonucleic acid
SCF	Stem cell factor
TCRαβ	T cell receptor α and β chain
Tdt	Terminal deoxynucleotidyl transferase
TLR	Toll-like receptor
T_m	Melting temperature
TNF	Tumor necrosis factor
TRAIL	TNF-related apoptosis-inducing ligand
ULBP	UL16-binding protein

TABLE OF CONTENTS

1 INTRODUCTION

Leukemia constitutes about one third of all childhood cancers diagnosed at the age of 0-14 (Howlader et al., 2014). Acute lymphoblastic leukemia (ALL) is a hematologic malignancy which is characterized by uncontrolled proliferation of lymphoid progenitor cells, in most cases of the B cell lineage. ALL accounts for 81% of childhood leukemias (Howlader et al., 2014).

Remarkable progress has been made in therapy of a subtype of ALL, the childhood acute B cell precursor leukemia (BCP-ALL). Current therapy protocols including combination chemotherapy has led to 5-year event-free survival rates of about 80% (Moricke et al., 2009; Pui and Evans, 2013; Freireich et al., 2014). Despite this progress further research is required to improve therapy options especially for children with high risk features. Patients with bone marrow relapse during conventional therapy have a 5-year survival estimate of only approximately 25% (Rivera et al., 2005).

Aim of this study was to identify natural killer (NK) cell-based therapy options for high risk childhood BCP-ALL patients with poor prognosis. The potential of adoptive NK cell transfer has not yet been fully exploited, the benefit of NK cell-based therapies has been shown for acute myeloid leukemia (AML) but as described later, is still a matter of debate for ALL (see 1.3.1 and 1.3.2). Therefore, NK cell efficiency in this disease entity was exploited and criteria for beneficial NK cell donor selection were examined. A further focus of this work was the modulation of graft-versus-leukemia (GvL) effects towards BCP-ALL by the methyltransferase inhibitor 5-azacytidine (5-AzaC). The following introduction will give an overview on acute childhood leukemias, NK cell biology with a focus on killer cell immunoglobulin-like receptors (KIRs), NK cells in leukemia therapy, as well as mechanisms of action and current applications of 5-AzaC.

1.1 Acute childhood leukemia

In acute leukemias immature hematopoietic precursor cells undergo malignant transformation resulting in maturation arrest and enhanced proliferation. These leukemic cells are released from the bone marrow and can accumulate in organs as for example spleen. In chronic leukemias which are rare in children no such clear maturation arrest occurs (Zwaan and M. van den Heuvel-Eibrink, 2011). Acute leukemias are subdivided in AML and ALL depending on the origin of the malignant cell. They make up about one third of all childhood cancers (Annesley and Brown, 2015). In current classification systems for acute leukemia (AML and ALL) more than 20% of cells in the bone marrow or peripheral blood are blasts (Vardiman et al., 2009; Abdul-Hamid, 2011). ALL is the most common leukemia in childhood. It can according to the WHO classification of 2008 be subdivided into 3 main diagnoses: acute leukemias of ambiguous lineage, B lymphoblastic leukemia/lymphoma and T lymphoblastic leukemia/lymphoma (Vardiman et al., 2009). T-ALL accounts for approximately 25% in children (Chiaretti and Foà, 2009), most ALLs are of the B cell lineage (B-ALL).

5-year-event-free survival for childhood AML ranges between 49 and 63% (Pui et al., 2011). Prognosis for ALL has over the past decades improved to 5-year event-free survival rates of about

80% (Moricke et al., 2009; Pui and Evans, 2013; Freireich et al., 2014), but about 20% of ALL cases relapse leading to a poor prognosis for the affected child (Annesley and Brown, 2015). For an overview of acute childhood leukemias see Table 1.

Table 1: Overview of acute childhood leukemias. FAB: French-American-British cooperative group.

	AML	**ALL**
Origin of malignant cells	Common myeloid precursors	Lymphoid progenitor cells
Incidence in childhood	10.1 per million at the age <5 (Ries, 1999) 15-20% of childhood leukemia (Zwaan and M. van den Heuvel-Eibrink, 2011)	58.2 per million at the age <5 (Ries, 1999) 81% of childhood leukemias (Howlader et al., 2014), T-ALL accounts for 25% of ALLs (Chiaretti and Foà, 2009), most ALLs are of the B cell lineage
Prognosis	5-year-event-free survival between 49 and 63% (Pui et al., 2011)	5-year-event-free survival of about 80% (Moricke et al., 2009; Pui and Evans, 2013; Freireich et al., 2014)
Subclassification	Dependent on degree of maturation; M0-M7 (FAB classification). M0 AML with minimal differentiation, M1–2 AML with minimal or moderate granulocytic differentiation, M3 acute promyelocytic leukemia (APL), M4 AML with mixed myelomonocytic differentiation, M5 acute monoblastic leukemia, M6 "eryhtroleukemia", and M7 acute megakaryoblastic leukemia (Abdul-Hamid, 2011)	Dependent on morphology (L1-L3, FAB) or subclassification in B-or T-ALL with further distinction according to degree of maturation. Pro B-ALL, Common ALL, Pre B-ALL, Mature B-ALL. Pro T-ALL, Pre T-ALL, Cortical T-ALL or Thymic ALL, mature T-ALL (Abdul-Hamid, 2011)
Leukemia propagating potential	Relatively low number of immature leukemia-initiating cells can be identified; hierarchical model (Lapidot et al., 1994; Dick, 2008)	Leukemia-propagating potential detected by blasts with different stages of maturation, almost all blasts have initiating capacity (le Viseur et al., 2008)
Susceptible to NK cell-based therapies	Several studies show beneficial effects, see section 1.3.	Only limited data available adult B-ALL seems to be resistant, see section 1.3.

Flow cytometric analysis can help to subclassify leukemic cells to the stage of development where leukemia transformation happened (McGregor et al., 2012, see Table 2), B-ALLs can be subdivided into 4 groups: Pro B-ALL, Common ALL, Pre B-ALL and mature B-ALL (reviewed in Abdul-Hamid, 2011). B-ALLs of the B cell precursor subtype (BCP-ALL) are the most common type of acute leukemia in childhood (Pui et al., 2008).

Table 2: Immune-phenotype of B lymphocyte progenitors, modified from (McGregor et al., 2012)

B lineage	CD10	CD19	CD22	CD79a	Tdt	Ig
Early precursor (pro-B)	-	+	+	+	+	-
Intermediate (common)	+	+	+	+	+	-
Pre-B	±	+	+	+	+	C-mu

1.1.1 Risk classification for B-ALL

To optimally choose the treatment regimen it is important to assess and classify patients according to their risk for relapse. Patients suffering from low or standard risk B-ALL receive less intense treatment than high risk patients (Pui et al., 2008). After initial categorization of the ALL cells into B or T cell lineage, leukocyte count and age were shown to be a prognostic factor for patients suffering from B-ALL (Smith et al., 1996). Patients between 1 and 9 years of age having a white blood count <50 000 cells per µl at diagnosis can be categorized to standard risk whereas the remaining leukemias are categorized to be of high risk (Smith et al., 1996). Furthermore there are cytogenetic factors that allow further categorization of the outcome for B-ALL patients. Chromosomal translocations can lead to activation of transcription factors or kinases involved in differentiation or proliferation. For example the Philadelphia chromosome or t(4;11) with MLL-AF4 fusion is associated with a poor prognosis as well as hypodiploidy (Pui et al., 2008). Treatment response is increasingly evaluated by quantification of the minimal residual disease (MRD) using PCR or flow cytometry that can detect 1 ALL cell among 10 000 to 100 000 other cells (Campana, 2010). Presence of MRD is the most powerful prognostic marker in ALL that applies to all subgroups (McGregor et al., 2012). Hypodiploidy, remission induction failure or MRD >1% are associated with a poor outcome for patients (Pui et al., 2008). For such high risk patients new therapeutic strategies as NK cell-based approaches in adjunct to HSCT could be a promising additive therapy approach.

1.2 Natural killer cells

NK cells are part of the innate immune system that were originally named *natural killer* cells because of their ability to spontaneously kill target cells without prior priming or peptide restriction. Recent studies indicate that NK cells nevertheless need an education and maturation process (e.g., North et al., 2007; Thomas et al., 2013). NK cells comprise about 10-15% of all lymphocytes and are able to recognize transformed or virus-infected cells by germline-encoded receptors (reviewed in Cooper et al., 2001; Caligiuri, 2008). They mediate direct cytotoxicity or modulate immune responses by the secretion of cytokines. Commonly they are defined as $CD3^-$ and $CD56^+$ which is the 140 kDa isoform of neural cell adhesion molecule (NCAM) that is also present on natural killer T cells, a minority of T cells and some myeloid leukemias (Lanier et al., 1989). Recently, more subsets of innate lymphoid cells (ILCs) have been defined and conventional NK cells are part of group 1 ILCs (ILC1) which are producers of interferon-γ (IFN-γ) (Spits et al., 2013). The definition of NK cells has become more difficult due to the presence of e.g., CD56 and NKp46 (a natural cytotoxicity receptor, NCR) on human IL-22-producing ILCs (Spits et al., 2013).

In the peripheral blood 90% of human NK cells have a low density expression of CD56 ($CD56^{dim}$) and a high expression of the Fcγ receptor III (CD16) (Cooper et al., 2001). This subset has been described to be the main cytotoxic subset (Lanier et al., 1986), whereas the remaining 10% are $CD56^{bright}CD16^{-/dim}$ NK cells are potent producers of IFN-γ. They are the predominant NK cell subset in lymph nodes (expressing high levels of L-selectin and CCR7 for homing to the lymph node and the high affinity receptor IL2Rαβγ), where an interaction with antigen-presenting cells/dendritic cells and T cells in a dynamic bidirectional manner can occur (Fehniger et al., 2003). Human NK cells seem to have a turnover rate of about two weeks in the peripheral blood (Zhang et al., 2007; Castillo et al., 2009).

Cytotoxicity mediated by NK cells is triggered by a change in the balance of activating and inhibitory signals that are sensed by specific receptors on the NK cells. Inhibitory receptors as KIRs, which are specific for HLA class I molecules, provide an inhibitory signal for 'self-molecules'. 'Missing self' (Karre et al., 1986) by for example virus-mediated or tumor-associated downregulation of HLA I molecules can change the equilibrium of signals. Activating receptors recognize e.g., stress-induced ligands as MICA/B or viral proteins and are necessary additional to 'missing self' to trigger NK cell cytotoxicity (Fig. 1, Raulet and Vance, 2006).

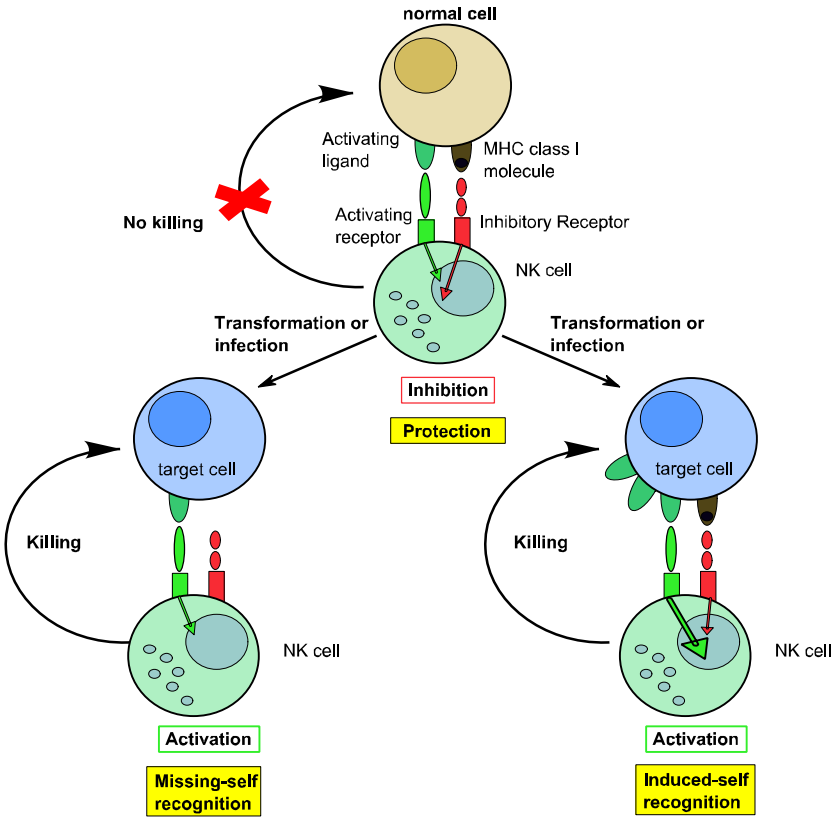

Fig. 1: Cytotoxicity of NK cells is triggered by a change in the balance of activating and inhibitory signals. Normal autologous cells are protected from killing by inhibitory interactions that dominate activating signals. In case of infection or transformation MHC I molecules can be downregulated (left side, 'missing-self') and inhibition by self-MHC I molecules is lost resulting in NK cell activation. Induced expression of stimulatory ligands can change the balance towards NK cell activation and cytotoxicity despite of self-inhibition (right side, 'induced-self'). Figure adapted from (Raulet and Vance, 2006).

Cytotoxicity of NK cells is mainly mediated by the targeted release of vesicles containing perforin and granzymes. Perforin enables the entry of granzymes into the target cell, where e.g., granzyme B can directly activate caspases and induce apoptosis of the target cell (reviewed in Pardo et al., 2009). A marker to quantify granule secretion is lysosome-associated membrane glycoprotein-1 (LAMP-1 or CD107a). It co-localizes with perforin in secretory vesicles and can be detected at the cell surface after degranulation. Furthermore, NK cells are able to induce Fas or TNF-related apoptosis-inducing ligand (TRAIL)-dependent apoptosis (Arase et al., 1995; Kayagaki et al., 1999). The expression of Fas ligand or TRAIL on NK cells can, by binding to respective receptors on target cells, induce apoptosis via aggregation of cytoplasmic death domains, recruitment and activation of caspases (Thorburn, 2004).

Besides cytotoxicity, NK cells also modulate immune responses by the release of cytokines. They are an important source of IFN-γ and TNF. TNF e.g., activates macrophages and vascular endothelium and induces the production of IL-1 and IL-6 (O'Shea et al., 2002). IFN-γ production is mainly triggered by the release of IL-12 and IL-18 from antigen-presenting cells (APCs) and has direct antiviral effects as well as immune-regulatory functions. It for example enhances MHC class I and II antigen presentation and promotes the development of Th1 cells and leukocyte trafficking (Schroder et al., 2004).

1.2.1 NK cell receptors

As mentioned above, NK cell effector functions are triggered by a change in the balance of activating and inhibitory signals that are sensed by specific receptors. The family of KIR molecules plays a central role in self-/non-self recognition via inhibition by HLA class I molecules. They are described in more detail in section 1.2.3. Before KIR expression occurs in NK cell development, the inhibitory receptor NKG2A is an important element for self-tolerance (see section 1.2.2, 1.2.3). Natural cytotoxicity receptors (NCR) are structurally unrelated but share the ability to highly activate the cytolytic potential of NK cells. NKp30 and NKp46 are constitutively expressed, whereas NKp44 expression is induced after NK cell activation (Sanchez-Correa et al., 2011). The first identified NCR ligands were viral proteins but recently, also tumor-associated antigens have been identified to activate NCR (e.g., NKp30-B7-H6, Brandt et al., 2009). But still, many ligands are unknown. A further important activating receptor triggering blast lysis by NK cells is the C-type lectin–like homodimeric receptor NKG2D. 55% of AMLs were shown to express the NKG2D-Ls MICA/B (Sanchez-Correa et al., 2011). Also DNAM-1 and its ligands CD112 and CD155 seem to be relevant for NK cell-mediated cytotoxicity towards leukemia, especially for NKG2D-L-negative blasts (Pende et al., 2005). Further selected receptor-ligand pairs and their effect involved in target recognition and cytotoxicity of NK cells are shown in Table 3.

Table 3: Selected overview of receptors expressed on NK cells, their respective ligands, and effect of the interaction. 21spe-MLL5: Exon 21spe-containing isoform (21spe) of mixed lineage leukemia-5 (MLL5) protein; AICL: activation-induced C-type lectin; DNAM-1: DNAX accessory molecule 1; N.D. not determined; PAMP: pathogen associated molecular pattern, PVR: Poliovirus receptor; TLR: toll-like receptor; ULBP: UL16-binding protein. Modified from (Sivori et al., 2014; Raulet and Vance, 2006).

Receptor	Ligand(s)	Ligand expressing cells	Effect
KIR-family members	Various MHC class I molecules (see also 1.2.3)	Almost all nucleated cells of the body	Inhibitory and activating family members
LFA-1	ICAM-1, ICAM-2 (Bryceson et al., 2005)	Target cells	Adhesion, polarization of granules (prerequisite for effector functions)
DNAM-1 (CD226)	CD112 (Nectin-2), CD155 (PVR) (Bottino et al., 2003)	Tumor and infected cells, stress-induced	Activation
NKp30 (NCR)	B7-H6 (Brandt et al., 2009)	Tumor cells (membrane)	Activation
	Viral heamagglutinin (Jarahian et al., 2011)	Infected cells (ectromelia virus)	Inhibition
NKp44 (NCR)	21spe-MLL5 (Baychelier et al., 2013)	Tumor cells	Activation
	Viral heamagglutinin (Arnon et al., 2001)	Infected cells	Activation
NKp46 (NCR)	N.D. (Sivori et al., 1999)	Tumor cells	Activation (cytokine/cytotoxicity)
	Viral heamagglutinin	Infected cells	Activation

	(Mandelboim et al., 2001)		
NKp80 (C-type lectin–like homodimeric receptor)	AICL (Welte et al., 2006)	Myeloid-specific receptor expressed by monocytes, macrophages and granulocytes	Involved in the activating crosstalk between NK cells and myeloid cells
NKG2D (C-type lectin–like homodimeric receptor)	ULBPs, MICA/MICB Reviewed in (Huergo-Zapico et al., 2014)	Ligands induced by stress and/or DNA damage (transformed and infected cells)	Activation
CD94-NKG2 heterodimer	HLA-E (Braud et al., 1998)	HLA-E binds peptides cleaved from the signal peptides of many classical MHC I molecules	NKG2A- Inhibition NKG2C,E – Activation
FcγRIII (CD16)	IgG (Perussia et al., 1989)	Antibody-coated target cells	Activation/antibody-dependent cytotoxicity (ADCC)
2B4 (CD244)	CD48 (Brown et al., 1998)	Normal hematopoietic and target cells, role in self-tolerance	Inhibition or stimulation, dependent on associated signaling molecules
TLR (2,3,5,7/8,9)	PAMPs (Reviewed in Sivori et al., 2014)	Bacterial/viral structures	Activation/synergy with cytokines

1.2.2 NK cell development

NK cells are lymphoid cells that are derived from hematopoietic stem cells ($CD34^+$). The main side of NK cell maturation is thought to be the bone marrow (Colucci et al., 2003). The cytokine milieu and stromal cells are able to provide the microenvironment for the first steps of maturation. Precursor NK (pre-NK) cells but probably also other NK cell stages may traffic to other tissues (spleen, lymph nodes, (fetal) thymus, (fetal) liver) for further maturation (Freud and Caligiuri, 2006; Huntington et al., 2007).

Freud and colleagues defined four main functionally distinct successive developmental stages that give rise to mature $CD56^+$ NK cells in the secondary lymphoid tissue (SLT; see Table 4; Freud and Caligiuri, 2006; Freud et al., 2006).

Table 4: Developmental NK cell stages. Summarized are stages of NK cell development as defined by Freud and colleagues (Freud and Caligiuri, 2006; Freud et al., 2006). Note that the CD markers mentioned here are only a minimal panel for discrimination of the stages.

	Developmental stage	**Surface antigen expression**
Stage 1	Progenitor NK cells (pro-NK cells)	$CD34^+$ $CD117^-$ $CD94^-$ $CD56^-$
Stage 2	Precursor NK cells (pre-NK cells)	$CD34^+$ $CD117^+$ $CD94^-$ $CD56^{(+)/-}$
Stage 3	Immature NK cells (iNK cells)	$CD34^-$ $CD117^+$ $CD94^-$ $CD56^{(+)/-}$

Stage 4	Mature CD56^{bright} NK cells (mNK CD56^{bright} cells)	CD34^{-}CD117$^{+/-}$CD94^{+}CD56^{bright} Nkp46^{+}CD16^{-}
	Mature CD56^{dim} NK cells (mNK CD56^{dim} cells)	CD34^{-}CD117$^{+/-}$CD94$^{+/-}$CD56^{dim} Nkp46^{+}CD16^{+}

For the first commitment of stage 1 cells, stromal cells or cytokines such as stem cell factor (SCF, also c-KIT ligand), fetal liver kinase 2 ligand also known als FMS-like tyrosine kinase 3 ligand (FLT3L) and IL-7 are necessary (Colucci et al., 2003). Commitment to the NK cell lineage goes along with expression of the IL-2Rβ chain (CD122), thereby inducing IL-2 and IL-15 responsiveness. The E26 transformation specific (ETS) family member PU.1, E4BP4 and later EOMES, ID2 (inhibitor of DNA binding) and T-bet are important transcription factors in NK cell development (Yokota et al., 1999; Colucci et al., 2001; Gordon et al., 2012; Male et al., 2014). PU.1 regulates early commitment of the myeloid and lymphoid lineage, e.g., c-KIT is a molecular target of PU.1 (Colucci et al., 2003). E4BP4 directly regulates Eomes and ID2 expression (Male et al., 2014) that play an important role in iNK to mNK cell transition.

NK cell development from stage 2 on is driven by IL-15 and IL-2, but IL-2 seems to be dispensable as for example in IL-2-deficient patients and mice NK cell numbers are normal and NK cell-mediated cytotoxicity is lower but inducible (DiSanto et al., 1990; Kundig et al., 1993). IL-15 is commonly presented in *trans* as complex of IL-15/IL-15Rα to cells expressing the IL-2Rβ-γc complex (Dubois et al., 2002) and is essential for NK cell development, expansion, and homeostasis via the anti-apoptotic factor Bcl-2 *in vivo* (Kennedy et al., 2000; Ranson et al., 2003).

In contrast to pro-NK and pre-NK cells, stage 3 iNK cells have lost the developmental potential for T cell or DC development. Despite the commitment to the NK cell lineage iNK cells seem neither to display perforin-dependent cytotoxic activity nor to produce IFN-γ. These functions are acquired at stage 4 (mature NK cells) along with the expression of other NK cell receptor such as NKG2D or Nkp46 (Freud and Caligiuri, 2006).

In stage 4 expression of CD94 (which forms a heterodimer with NKG2 receptors) occurs earlier in development than KIR expression. For the final maturation steps it is assumed that CD56^{dim}NKG2A^{-} KIR^{+} are the most mature NK cells and that they develop from CD56^{dim} NKG2A^{+} KIR^{-} cells to CD56^{dim} NKG2A^{+} KIR^{+} cells and finally to CD56^{dim} NKG2A^{-} KIR^{+} cells (Miller and McCullar, 2001). In this sequence self-tolerance via inhibition of NKG2A by HLA-E is achieved before KIRs are expressed.

1.2.3 Killer Ig-like receptors

Killer Ig-like receptors (KIRs) play a central role in NK cell recognition and self-inhibition. In case of 'missing-self', e.g., caused by virally or tumor-associated MHC-I downregulation to escape from CD8^{+} T cell recognition, inhibition by self-KIRs and NKG2A is lost. NKG2A recognizes a conserved signal sequence of most HLA class I molecules which are bound to HLA-E. KIRs are a highly

polymorphic receptor family that bind specific HLA class I alleles or HLA class I determined binding motifs (reviewed in Vilches and Parham, 2002). An overview of KIRs and their respective ligands is shown in Table 5.

Table 5: KIR family members and their respective HLA ligands. The HLA-C group 2 epitope contains lysine in position 80, whereas HLA-C group 1 epitopes share an asparagine in position 80. *note: KIR2DL4 transduces activating signals despite of its long cytoplasmic tail (Rajagopalan et al., 2001). #*KIR2DL5* gene is encoded by two separate loci (duplication). *KIR2DP1* and *KIR3DP1*are pseudogenes and not explicitely mentioned in the table. Adapted from (Campbell and Purdy, 2011).

	Gene name	CD designation	Number of alleles	Recognition motif on HLA ligands
Inhibitory receptors	***KIR2DL1***	CD158a	26	HLA-C group 2
	KIR2DL2	CD158b1	15	HLA-C group 1 and some HLA-C group 2 and HLA-B
	KIR2DL3	CD158b2	11	HLA-C group 1 and some HLA-C group 2 and HLA-B (weaker affinity than 2DL2)
	KIR3DL1	CD158e1	59	Bw4 epitopes among HLA-B allotypes and some HLA-A: A*23, A*24, A*32 (Stern et al., 2008) KIR3DL1*004 is retained intracellularly (Pando et al., 2003)
	KIR3DL2	CD158k	25	Certain HLA-A allotypes: A*03, A*11
	KIR3DL3	CD158z	56	Unknown
	KIR2DL5A#	CD158f	10	Unknown
	KIR2DL5B#	CD158f	21	Unknown
Activating receptors	***KIR2DL4****	CD158d	27	HLA-G
	KIR2DS1	CD158h	15	HLA-C group 2 (low affinity)
	KIR2DS2	CD158j	20	HLA-C group 1 (low affinity)
	KIR2DS3	No CD assigned	12	HLA-C group 1 (low affinity)
	KIR2DS4	CD158i	30	HLA-C (some group 1 and 2), A*11
	KIR2DS5	CD158g	14	Unkown
	KIR3DS1	CD158e2	16	HLA-Bw4?

KIRs are classified into different groups depending on their structural features. KIRs containing two or three extracellular Ig-like domains are referred to as KIR2D or KIR3D. In addition to a stem and a transmembrane region KIRs either contain a short or long cytoplasmic tail. KIRs containing a short cytoplasmic tail (S, e.g., KIR2DS1) transduce activating signals (aKIR) via the DAP12 adapter molecule (Lanier et al., 1998). KIRs containing a long cytoplasmic tail (L, e.g., KIR2DL1) possess immune tyrosine-based inhibitory motifs (ITIMs) allowing the recruitment of protein tyrosine phosphatases containing a SH2-motif that leads to inhibition of the NK cell (iKIR, Olcese et al., 1996). An exception is KIR2DL4 that, despite of its long cytoplasmic tail, contains arginine in the transmembrane region allowing the transduction of activating signals (Rajagopalan et al., 2001).

The *KIR* genes are encoded on chromosome 19q13.4 in the leukocyte receptor complex and display a high degree of sequence homology (Wende et al., 1999). But still, genetic diversity is enormous due to allelic polymorphism (see Table 5) and the inheritance as haplotypes that exhibit a high variability in number and combination of *KIR* alleles (Uhrberg et al., 1997; Valiante et al., 1997). *KIR3DL3*, *KIR3DP1* (pseudogene), *KIR2DL4* and *KIR3DL2* are present in all haplotypes. KIR haplotypes A share the inhibitory receptors *KIR2DL3*, *KIR2DL1*, *KIR3DL1* and *KIR3DL2*. *KIR2DS4* is the only aKIR present within haplotype A. Despite of this defined KIR content, haplotypes A have allelic variation leading to diversity. Haplotypes B are even more variable and include *KIR* genes that are not present in haplotype A, including several activating genes (reviewed in Parham and Moffett, 2013).

1.2.3.1 Regulation of KIR expression

The high level of conservation within the putative promoter regions of *KIR* genes led the Uhrberg group to the hypothesis that epigenetic mechanisms might play an important role in the regulation of KIR expression (Santourlidis et al., 2002). Indeed, it has been shown that methylation of respective CpG islands correlates with inhibition of *KIR* expression, and treatment with the DNA methyltransferase inhibitor 5-AzaC induces *KIR* expression. Silent *KIR* genes display a high level of CpG methylation whereas actively transcribed *KIR* genes are largely unmethylated (Santourlidis et al., 2002; Chan et al., 2003; Chan et al., 2005). Furthermore, often only one allele, not both, are expressed within one individual (Chan et al., 2003).

Since direct DNA methylation may influence histone modifications or vice versa, it seems reasonable that also histone modifications and other epigenetic mechanisms play a role in *KIR* expression. Indeed, chromatin accessibility determines transcriptional activity for the *KIR* locus (Chan et al., 2003; Santourlidis et al., 2008). Currently, it is proposed that demethylation of DNA is not required for the acquisition of histone modifications (Santourlidis et al., 2008). Cells that are not expressing KIRs display low levels of active histone marks as acetylated lysine 8 of histone 4 (H4K8ac) and a high level of repressive H3K9 dimethylation. Acquisition of an active histone signature at the *KIR* locus is followed by CpG methylation not vice versa. Probably active histone marks are necessary to poise cells for rapid CpG demethylation and *KIR* expression (Santourlidis et al., 2008). Besides epigenetic regulation, differences in individual KIR expression on cell surfaces can largely not be explained by differences in RNA expression levels and therefore also post-transcriptional mechanisms are supposed to be involved in expression of *KIR* genes (McErlean et al., 2010).

Extending the view from single cells to the NK cell pool within one individual, varying KIR expression between NK cells can be observed. *In vitro* studies have shown that single HSCs lead to NK cell progeny with polyclonal KIR expression patterns that display plasticity for further KIR expression (Miller and McCullar, 2001). In combination with variegated expression of further NK cell receptors this leads to a high number of diverse NK cell subsets within one human individual.

There are indications for KIR expression during NK cell development being a random process not influenced by the HLA genotype (Miller and McCullar, 2001; Andersson et al., 2009). Still, self-tolerance has to be achieved even in NK cells that do not express any KIR for self-HLA class I. This is in part achieved by a process called education.

1.2.3.2 NK cell education

In order to achieve full functionality, NK cells have to undergo a process called 'education'. This is an MHC class I-dependent process resulting in enhanced responsiveness to activating ligands. It has been shown that NK cells not expressing KIRs for self-MHC class I molecules display a mature phenotype, but are functionally hyporesponsive to diverse stimuli as MHC class I-deficient target cells (Anfossi et al., 2006). Thereby autoreactivity is prevented.
In mice, functional competence of uneducated NK cells can be induced by transfer of uneducated mature NK cells from a MHC class I-deficient host into wild-type hosts, whereas the transfer of educated functional NK cells leads to a loss of responsiveness in MHC class I-deficient hosts (Elliott et al., 2010; Joncker et al., 2010). This shows the relevance of MHC class I molecules for functional competence and also the plasticity ('re-education') of mature NK cells.
The relevance of education can also be seen in the human setting which was for example explicitly shown for KIR3DL1 by Kim and colleagues: KIR3DL1 recognizes HLA class I molecules containing the Bw4 epitope. Educated KIR3DL1$^+$ NK cells from HLA Bw4-homozygous donors display increased responsiveness compared to uneducated KIR3DL1$^+$ NK cells from donors with only one *HLA* Bw4 allele or without *HLA* Bw4 genes (Kim et al., 2008).

Education occurs during NK cell development, but due to the lack of surface markers to identify educated NK cells, the exact stage where this process occurs is unclear. Currently, two possible mechanisms for NK cell education are proposed (reviewed in Bessoles et al., 2014):

- 'Disarming' hypothesis:
  Initially responsive NK cells are chronically stimulated in the absence of inhibitory receptors for self-MHC class I molecules. Chronic activation without neutralizing inhibitory signals leads to hyporesponsiveness.
- 'Arming' hypothesis[1]:
  In this model NK cells are initially poorly responsive to activating signals. Engagement of inhibitory receptors by self-MHC class I molecules induces responsiveness.

Regardless of the respective model it is possible that not only *trans* interactions but also *cis* interactions (on the NK cell itself) might play a role in education (Bessoles et al., 2013). It furthermore

[1] Sometimes the terminus ‚licensing' is used in the literature when referring to the arming hypothesis. Others use the term 'licensing' without preference for one of the two models (e.g., Orr et al., 2010, Bessoles et al., 2014). Here in this work the term licensing is also used as synonym for 'education'.

seems that education is not an 'on-off' process but rather a step-wise process ('rheostat model'). According to the 'rheostat model' more possible inhibitory interactions of KIRs with self-MHC class I molecules result in higher responsiveness of the respective NK cell (Brodin et al., 2008; Brodin et al., 2009; Joncker et al., 2009).

Regarding the molecular mechanism of education or licensing it has been shown that the ITIM signaling motif of Ly49A, which is a murine functional KIR homologue, and therefore also the receptor itself is necessary for education (Kim et al., 2005). There are contradicting reports whether the phosphatase SHP-1 downstream of the ITIM is also involved in this process (Lowin-Kropf et al., 2000; Kim et al., 2005). One functional effect of education might be a change in inside-out signaling of LFA-1 leading to less stable NK cell-target conjugates of unlicensed NK cells (Thomas et al., 2013).

1.2.4 KIR-KIRL mismatch and alloreactive NK cell subsets

As mentioned in section 1.2.3, *KIR* genes and KIR expression on NK cell subsets varies considerably among individuals. Diverse combinations of KIRs are present on various NK cell subsets leading to a complex NK cell repertoire. NK cell education by KIR-HLA class I interactions and further inhibitory receptors (e.g., NKG2A) ensure self-tolerance. Transfer of NK cells into a HLA-disparate host can lead to alloreactivity of NK cell subsets due to missing inhibition (KIR-KIRL mismatch, see also Fig. 2). This is the case in the setting of hematopoietic stem cell transplantation (HSCT) when NK cells are transferred into a KIR-KIRL mismatched recipient.

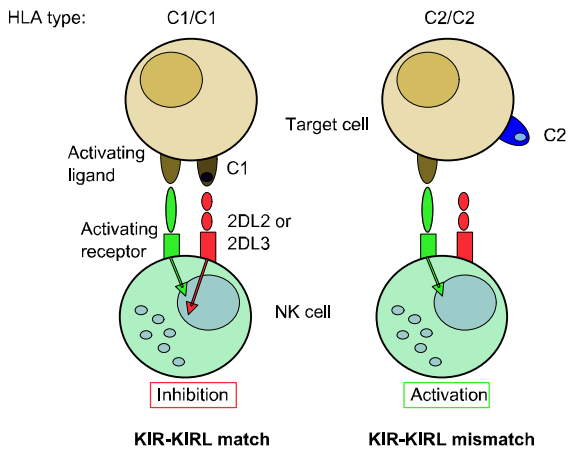

Fig. 2: KIR-KIRL match and mismatch constellations. Shown is an exemplary constellation of a KIR2DL2/L3$^+$ NK cell. Left side: KIR2DL2/L3 interaction with HLA-C1 in a HLA-C1/C1 individual (KIR-KIRL match) leads to NK cell inhibition. On normal cells, KIR-mediated inhibition overrides activating receptor-ligand interactions. Right side: KIR2DL2/L3 do not find a ligand in a HLA-C2/C2 individual (KIR-KIRL mismatch), the inhibiting signal is lost, activation predominates (idea for figure from Parham, 2005).

Since *HLA* class I genes and *KIR* genes are not located on the same chromosome, an individual might also express KIRs for non-self HLA class I molecules. The process of education leads to hyporesponsiveness of NK cells not expressing any self-HLA class I inhibitory receptor. The educated alloreactive NK cell subset is not hyporesponsive and expresses activating receptors but no inhibitory receptors that find a ligand on the respective target cell (Pende et al., 2005; Babor et al., 2013). Taking

this into account, the alloreactive subset can theoretically be predicted as shown in Table 6 for HLA-C-determined KIR ligands. Although the clinical relevance of these considerations has until now only been proven in specific disease entities (as described later in section 1.3.1), studies of KIR-KIRL constellations might help to extend NK cell-mediated GvL effects to further contexts.

Table 6: Exemplified alloreactive NK cell subsets in the context of HLA-C determined KIR-KIRL interactions. aKIRs and other KIR-KIRL pairs are not considered. Modified from (Babor et al., 2013**).**

Donor	Education		Recipient	Alloreactive NK cells	
KIRL	Licensed	Unlicensed	KIRL	Licensed	Unlicensed
C1/C1	KIR2DL2/L3	KIR2DL1	C1/C1	-	KIR2DL1
C1/C2	KIR2DL1 KIR2DL2/L3	-	C1/C1	KIR2DL1	-
C2/C2	KIR2DL1	KIR2DL2/L3	C1/C1	KIR2DL1	-
C1/C1	KIR2DL2/L3	KIR2DL1	C1/C2	-	-
C1/C2	KIR2DL1 KIR2DL2/L3	-	C1/C2	-	-
C2/C2	KIR2DL1	KIR2DL2/L3	C1/C2	-	-
C1/C1	KIR2DL2/L3	KIR2DL1	C2/C2	KIR2DL2/L3	-
C1/C2	KIR2DL1 KIR2DL2/L3	-	C2/C2	KIR2DL2/L3	-
C2/C2	KIR2DL1	KIR2DL2/L3	C2/C2	-	KIR2DL2/L3

1.3 NK cells in leukemia therapy

NK cells are able to lyse malignant cells similar to cytotoxic T cells. Unfortunately, after HSCT T cells from the graft can also attack healthy tissue within the recipient and are a main cause of graft-versus-host disease (GvHD). In contrast, NK cells mediate beneficial anti-leukemic effects (GvL) without causing GvHD (Ruggeri et al., 1999; Ruggeri et al., 2002). Strategies using T cell depletion (CD3, CD3/19 or TCRαβ depletion) from the graft allow co-transplantation of beneficial NK and other effector cells with HSCs which enhances GvL effects, but reduces the GvHD risk (reviewed in Handgretinger, 2012). GvHD can be initiated by stimulation of donor T cells by allogeneic MHC antigens on recipient APCs. But also recipient alloproteins (minor histocompatibility antigens) might be presented by APCs on MHC class I molecules to $CD8^+$ T cells ('cross-priming') and thereby initiating GvHD (reviewed in Auchincloss Jr and Sultan, 1996). Alloreactive NK cells from the graft are able to reduce the GvHD risk by depletion of recipient DCs that are able to trigger GvHD via the mentioned mechanisms (Ruggeri et al., 2002).

Donor selection in HSCT can influence the efficiency of GvL effects mediated by graft-emerging NK cells. For example KIR haplotype B donors seem to be superior compared to KIR haplotype A donors (Oevermann et al., 2014), but more criteria for optimal donor selection need to be defined. NK cells within the graft can also mediate GvL effects; here also donor selection might play an important role. Strategies as CD3/19-depletion from the graft in combination with *ex vivo* IL-15 stimulation could enhance GvL effects from graft-immanent NK cells (Pfeiffer et al., 2012). Adoptive NK cell transfer

includes *ex vivo* NK cell expansion and activation leading to highly potent NK cells which can be transferred to the patient in high numbers. Donor selection and NK cell expansion protocols play an important role for optimal alloreactivity. Clinical data for adoptive NK cell transfer is still very limited and mainly restricted to feasibility studies as described later in section 1.3.2. Another strategy is to enhance endogenous NK cell responses. For example blockade of (inhibitory) KIRs by a monoclonal antibody (1-7F9) might increase the NK cell-mediated anti-leukemic response (Romagné et al., 2009). Drugs and antibodies enhancing NK cell alloreactivity need to be further explored.

1.3.1 NK cell-mediated GvL effects in AML and B-ALL

Donor-recipient HLA matching in HSCT reduces the risk for GvHD (Petersdorf, 2004). But in most cases patients do not have an HLA matched sibling donor and also an unrelated HLA matched donor cannot easily be found (Schipper et al., 1996; Kekre and Antin, 2014). Therefore, haploidentical related donors (up to 50% HLA mismatch) or partially HLA mismatched unrelated donors have to be considered. Under these conditions, enhancing GvL effects by defined KIR-KIRL mismatching is a promising strategy. However, despite the theoretical assumptions shown in the previous section, the benefit of KIR-KIRL mismatched HSCT in leukemia therapy has mainly been shown for AML, but not for ALL.

The prerequisite for NK cell-mediated GvL effects upon HSCT is the observation that KIR expression on NK cells, but probably also education, is donor type-like in the haploidentical setting (Leung et al., 2004; Pende et al., 2009). NK cells developing in a KIR-KIRL mismatched recipient that express KIRs not engaged by the patients KIRLs are surprisingly *not* hyporesponsive. The presence of this alloreactive subset might be explained by the high number of cells infused upon haploidentical HSCT leading to a primarily donor type shaped bone marrow microenvironment (Pende et al., 2009).

In an initial study by Ruggeri et al. 0 of 8 AML, 0 of 5 chronic myeloid leukemia (CML) but 5 of 7 ALL patients relapsed within 6 months after KIR-KIRL mismatched T cell depleted HSCT (Ruggeri et al., 1999). In further *in vitro* experiments lower surface expression of the adhesion molecule LFA-1 on NK cell-resistant ALLs compared to NK cell-susceptible AML or CML was observed. Despite the KIR-KIRL mismatched constellation which could potentially promote GvHD, no such effect was observed after T cell-depleted HSCT. This finding was confirmed in further studies showing a survival benefit of KIR-KIRL-mismatched HSCT in adult AML, but not for ALL, compared to KIR-KIRL matched constellations without increased occurrence of GvHD (Ruggeri et al., 2002; Hsu et al., 2005; Clausen et al., 2007; Ruggeri et al., 2007; Zhou et al., 2014).

In contrast to adult ALL, there is evidence that pediatric ALL is susceptible to NK cell-mediated cytotoxicity (Leung et al., 2004; Pfeiffer et al., 2007; Pende et al., 2009; Pfeiffer et al., 2010). Differential expression of adhesion molecules and HLA class I molecules are hypothesized to be responsible for these differences. Pediatric ALLs express adhesion molecules such as members of the β_1 (CD29, CD49d) and β_2 (LFA-1) integrin family and the Ig superfamily (ICAM-1, LFA-3) (Mengarelli et al., 2001) leading to efficient NK cell-target conjugate formation (Ruggeri et al., 1999).

Furthermore, pediatric blasts with low HLA expression are targeted more efficiently compared to blasts with high HLA expression (Pfeiffer et al., 2007).

Besides *in vitro* experiments showing a relevance of KIR-KIRL constellations for NK cell-mediated cytotoxicity towards pediatric BCP-ALL (Pfeiffer et al., 2007; Feuchtinger et al., 2009) there is only limited clinical data available. Upon haploidentical HSCT Leung and colleagues showed an increased probability of relapse for KIR-KIRL matched donor-recipient pairs in a small cohort of 19 pediatric patients with lymphoid malignancies (Leung et al., 2004). The Perugia group identified alloreactive NK cells that persisted long after transplantation in 10 BCP-ALL patients that underwent haploidentical KIR-KIRL mismatched HSCT (Pende et al., 2009). In this study alloreactivity towards HLA-C1/C1 blasts was mediated by the respective KIR-KIRL mismatched NK cell subset whereas for HLA-C2/C2 blasts the presence of activating KIR2DS1 was relevant.

In line with this data it can be assumed that the disease entity of pediatric BCP-ALL might in contrast to adult B-ALL indeed be a target of NK cell-mediated cytotoxicity and that further investigations are necessary to verify the relevance of KIR-KIRL mismatched constellations.

1.3.2 Adoptive NK cell transfer

Besides GvL effects of graft-emerging NK cells, adoptive transfer of NK cells in therapy was shown to be feasible and safe. Nevertheless, first studies with autologous HLA-matched NK cells were not very promising. In the 1980's, adoptive transfer of autologous lymphokine-activated killer cells in combination with high-dose IL-2 in advanced cancers showed (complete or partial) responses in only about 20% of the cases (Rosenberg et al., 1987). In a further study administration of autologous IL-2 activated NK cells in metastatic breast cancer and lymphoma patients did not lead to an increased survival (Burns et al., 2003). In order to enhance NK cell responses Miller and coworkers transfused haploidentical *ex vivo* stimulated NK cells in immunosuppressed adult AML patients with poor prognosis (Miller et al., 2005). Despite the low amount of T cells that were co-transfused, no signs of GvHD were observed. 3 of 4 patients with a KIR-KIRL mismatch achieved complete remission, whereas only 2 of 13 achieved remission in the KIR-KIRL matched group. They applied a high-dose conditioning regimen and IL-2 administrations leading to *in vivo* expansion of the transferred NK cells that was accompanied with a significant increase in plasma IL-15. In this study the high-dose conditioning and cytokine regimen led to side effects such as pancytopenia or fever. Rubnitz and coworkers therefore applied lower doses of immunosuppressive conditioning and IL-2 doses in pediatric patients (Rubnitz et al., 2010). The infusion of haploidentical KIR-KIRL mismatched NK cells was shown to be feasible and safe in 10 patients in first remission of AML. All 10 patients displayed an event-free survival of at least two years. The Campana group established an efficient NK cell activation and expansion system ('NKAES'; Imai et al., 2005; Fujisaki et al., 2009) to generate highly potent NK cells for future adoptive transfer therapy. K562 feeder cells expressing both, membrane-bound IL-15 and 4-1BBL in combination with soluble IL-2 during culture lead to very efficient expansion and activation of NK cells. 4-1BB engagement by its ligand 4-1BBL was shown to

inhibit activation-induced cell death and co-stimulates activation and proliferation in T cells (Cannons et al., 2001; Habib-Agahi et al., 2007). 4-1BB is also expressed on activated NK cells and 4-1BB stimulation is assumed to enhance anti-tumor activity of NK cells (Dowell et al., 2012). The NKAES protocol constitutes a very promising strategy to generate highly potent alloreactive NK cells for clinical applications (Imai et al., 2005; Fujisaki et al., 2009). For this work NK cells were expanded according to a modified protocol from Fujisaki and colleagues and are in the following termed 'NKAES cells'. Recently, it has been demonstrated that application of *in vitro* IL-15-stimulated CD3/19-depleted haploidentical stem cell boosts in relapsed pediatric patients is safe (Pfeiffer et al., 2012). 8 children with AML, BCP-ALL, or T-ALL in relapse after HSCT were included, IL-15 *ex vivo* stimulation led to proliferation and activation of NK cells within the graft. These NK cells showed an expansion with a maximum at day 10 after infusion and were undetectable at day 30.

In summary, only very limited clinical data is available for children and restricted to feasibility studies mainly performed in AML patients. *Ex vivo* expansion and administration of partially HLA mismatched NK cells does not seem to induce GvHD, and in line with these findings the strategy of adoptive KIR-KIRL mismatched NK cell transfer might be a promising therapy strategy in BCP-ALL.

1.4 The NOD.Cg-*Prkdc*^{Scid}*IL2Rg*^{tmWjl}*/Sz* mouse strain

Immune-deficient mice allow the engraftment of human cells and tissue and are therefore an elegant model to study human cells and complex biological processes *in vivo*. One breakthrough was the establishment of NOD/*scid* (NS) mice that lack mature T and B cells and display impairments in innate immunity (Shultz et al., 1995). But the engraftment of human HSCs or PBMCs is hampered by residual murine NK cell activity and the decreased lifespan of these mice due to the development of thymic lymphomas. These drawbacks were tackled by the development of the NOD.Cg-*Prkdc*^{Scid}*IL2Rg*^{tmWjl}*/Sz* mouse strain (also termed NOD-*scid* IL2Rgamma^{null} mice, NSG) that has an additional homozygous targeted null mutation of the IL-2 receptor common γ-chain locus (*IL2rg)* (Shultz et al., 2005). The common γ-chain is crucial for high-affinity binding and signaling of several cytokines (IL-2, IL-4, IL-7, IL-9, IL-15, IL-21) (Sugamura et al., 1996) and mutation of *IL2rg* in NSG mice prevents any murine NK cell development. The combination of absent mature B and T cells, absence of NK cells, and longer lifespan (NSG mice do not develop thymic lymphomas) leads to a promising mouse model with much better engraftment of human HSCs compared to NS mice (Shultz et al., 2005; Shultz et al., 2007).

Despite IL-7 supplementation and vivid multilineage differentiation of HSCs in sublethally irradiated NSG mice (Shultz et al., 2005), our group demonstrated that there are deficiencies in NK and T cell development in humanized NSG (huNSG) mice (André et al., 2010). Please note that the terminus 'humanized mouse' in this work refers to mice transplanted with human HSCs which is to be distinguished from mice transplanted with human leukemic samples. In huNSG mice developing T cells were mainly $CD4^+$ with a high percentage of $CD45RO^+$ (memory phenotype) while $CD8^+$ T cells were almost absent (André et al., 2010). NK cells did not display KIR expression on the protein level

although mRNA was detectable. In line with these findings the majority of NK cells were of the $CD56^{bright}CD16^{-}$ subset. Despite this phenotype NK cells did not synthesize IFN-γ upon unspecific stimulation and were also not able to mediate cytotoxicity towards K562 *ex vivo* (André et al., 2010). To overcome the deficiencies in NK cell function our group applied IL-15/IL-15Rα complexes according to a treatment regimen from Huntington and colleagues who were able to induce CD16 and KIR expression in humanized $Rag2^{-/-}\gamma c^{-/-}$ mice (Huntington et al., 2009). Indeed IL-15/IL15Rα treatment induced functional competence in huNSG mice, but the majority of NK cells still had the immature $CD56^{bright}CD16^{-}KIR^{-}$ phenotype (André et al., unpublished data). This might be explained by the generation of 'pseudomature lytic NK' cells which can be generated by prolonged culturing of HSCs in the presence of IL-15 and absence of stroma cells (Colucci et al., 2003). These *in vitro*-generated NK cells express CD56 and CD94, but no KIRs analogous to the NK cells generated in huNSG mice.

Besides the generation of NK cells in huNSG mice, NSG mice also readily engraft with primary pediatric leukemic samples. Our group was able to show that leukemic cells retain their characteristic immune-phenotype and gene-expression profile upon transplantation into NSG mice. Furthermore, the clinical outcome of the patients correlates with engraftment rates in NSG mice upon transplantation of low blast numbers (Woiterski et al., 2013).

In summary the NSG mouse strain provides an ideal basis to study donor-patient specific GvL effects and to evaluate the potential of adoptively transferred NK cells *in vivo*.

1.5 5-Azacytidine

5-Azacytidine (5-AzaC) is a cytosine analogue (Fig. 3) that was first synthesized about 50 years ago (Píškala and Šorm, 1964) as direct cytostatic drug acting as nucleoside antimetabolite. Soon it was shown that 5-AzaC is able to inhibit direct DNA methylation leading to the current use as 'epigenetic drug'.

5-AzaC is currently under defined criteria approved for the treatment of the myelodysplastic syndrome (MDS), chronic myelomonocytic leukemia (CMML), and AML by the European Medicines Agency (EMA) and for MDS by the U.S. Food and Drug Administration (FDA) (Kaminskas et al., 2005; Derissen et al., 2013). The *KIR* locus was shown to be methylated as described above (1.2.3.1) and there is some limited data linking NK cell alloreactivity and 5-AzaC treatment (see 1.5.2).

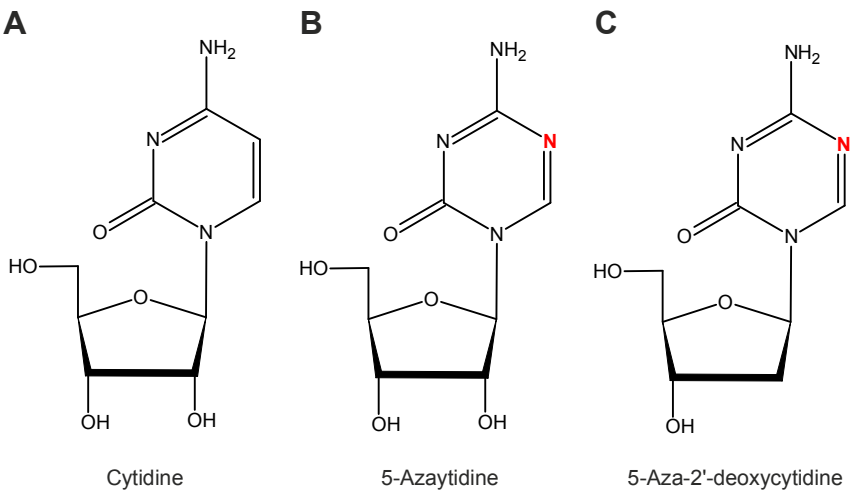

Fig. 3: Structure of cytidine, 5-azacytidine (5-AzaC) and 5-aza-2'-deoxycytidine (5-AzadC). (A) Cytidine (B) 5-AzaC (C) 5-AzadC, which is a metabolite of 5-AzaC.

After triphosphorylation 5-AzaC can be incorporated into DNA and RNA (after reduction by ribonucleotide reductase) leading to inhibition of DNA, RNA, and protein synthesis including tRNA and rRNA processing (reviewed in Christman, 2002). This can lead to DNA damage, cell cycle arrest, and apoptosis. Epigenetic effects of 5-AzaC are mediated by direct irreversible inhibition of DNA methyltransferases (Dnmt); the covalent intermediate product of 5-AzaC and enzyme cannot be released leading to Dnmt depletion (Christman, 2002; Stresemann and Lyko, 2008). Mammalian maintenance methyltransferase Dnmt1, which is assumed to be the major target of 5-AzaC, induces methylation of hemimethylated DNA after replication. Therefore, inhibition of Dnmt1 leads to hemimethylated DNA after one round of replication and at least two cell divisions are necessary to induce demethylation (passive demethylation, Christman, 2002). Low doses of 5-AzaC are sufficient to induce DNA hypomethylation without direct suppression of DNA synthesis (Kaminskas et al., 2005).

1.5.1 Methyltransferase inhibition in cancer therapy

In general, epimutations seem to play an important role in cancer development, for example silencing of the tumor suppressor gene *p16ink4A* is a common event (reviewed in Jones and Baylin, 2007; Issa, 2007). Re-expression of tumor suppressor genes by Dnmt-inhibitors can lead to beneficial effects in cancer treatment. In MDS higher levels of DNA methylation seem to correlate with a worse clinical outcome (Shen et al., 2010) and epimutations in differentiation-associated genes seem to play a role (Issa, 2013).

Linking the tumor-focused concept to immune therapy, it has been speculated that the beneficial effect of combined donor-lymphocyte infusions (DLI) and 5-AzaC treatment in patients with AML/MDS is mediated by epigenetic upregulation of HLA molecules or cancer testis antigens on blasts leading to higher susceptibility to the DLI (Lubbert et al., 2010). Another link is the observation that NKG2D ligands are induced upon 5-AzaC treatment, leading to higher susceptibility of AML cells to NK cell-mediated cytotoxicity (Rohner et al., 2007; Tang et al., 2008).

1.5.2 5-AzaC and NK cell function

As mentioned in section 1.2.3.1 it has been described that *KIR* genes are epigenetically regulated by direct DNA methylation of CpG islands in promoter regions. Demethylation can be induced by 5-AzaC and is correlated with increased KIR expression (Santourlidis et al., 2002; Chan et al., 2003).
NK cell treatment with 1-5 µM 5-AzaC for 72 h induced demethylation-dependent iKIR expression and suppressed cytolytic function of NK92-MI cells towards K562 *in vitro* (Gao et al., 2009). The viability of NK cells was not significantly changed at a dose of 2.5 µM. The induction of iKIR expression seems to contribute to suppressed cytotoxicity since the 5-AzaC-treated KIR3DL1^{+} subset showed much lower cytotoxicity compared to the KIR3DL1^{-} subset.
During short term treatment without IL-2, 5-AzaC also significantly decreased cytotoxicity towards K562 and Raji cells (Schmiedel et al., 2011). 5-AzadC, the deoxy-analogue of 5-AzaC which cannot be incorporated into RNA, induced cytotoxicity and cytokine release but not KIR expression. Schmiedel and colleagues applied non-proliferating conditions without IL-2 supplementation for 24 h and in line with the epigenetic mechanism these effects were probably demethylation-independent.

In these studies only HLA class I-deficient target cell lines were used and the potentially increased expression of aKIRs was not investigated. Specific KIR-KIRL mismatched constellations in combination with aKIR-KIRL interactions might lead to different 5-AzaC effects on cytotoxicity. Furthermore, the effect on of 5-AzaC on NK cell precursors has not been studied yet.

2 AIM OF THIS WORK

Since a beneficial effect of NK cells in the therapy of BCP-ALL has long been neglected, the purpose of this work was to investigate the potential of NK cell-mediated anti-leukemic effects towards pediatric BCP-ALL. Following verification that pediatric BCP-ALL can indeed be a target of NK cells, the aim was to optimize NK cell-based therapeutic strategies. In this regard, systematic NK cell donor selection based on the KIR-KIRL constellation should influence the efficacy of adoptively transferred NK cells in pediatric BCP-ALL. This hypothesis should be examined by exploiting a human-murine NSG xenotransplantation model and by performing NK cell subset analyses. As the KIR locus has been described to be regulated via DNA methylation, the effect of the Dnmt-inhibitor 5-AzaC on NK cell cytotoxicity should additionally be investigated. By using primary leukemic samples, NK cells and hematopoietic stem cells from hypothetical donors, analysis of donor-patient-specific anti-leukemic responses should be performed.

3 MATERIALS AND METHODS

For specific materials not separately mentioned in this section, standard labware was used.

3.1 Cell culture

3.1.1 Cell lines

CELL LINE	DESCRIPTION[2]	MEDIA
K562	Human CML in blast crisis, established from a 53-year old woman in 1970. MHC class I expression negative.	RPMI 1640 complete medium
K562-mbIL15-4-1BBL[3]	Generated by transduction of K562 cells with constructs encoding a 'membrane-bound' form of IL-15 (IL-15 + CD8α transmembrane domain) and human 41BB ligand (both containing GFP) by the Campana group (Imai et al., 2005; Fujisaki et al., 2009). Feeder cell line for NKAES cell expansion.	RPMI 1640 complete medium
Kasumi-1	AML, established from a 7-year-old Japanese boy in 1989.	RPMI 1640 complete medium with 20% FCS
Nalm-16	B cell precursor leukemia, established from a 12-year-old girl with ALL. Cells are described to carry a near haploid karyotype.	RPMI 1640 complete medium
SEM	B cell precursor leukemia, established from a 5-year-old girl with ALL in 1990.	90% Iscoves MDM, 10% FCS, penicillin/streptomycin
MHH-cALL4	B cell precursor leukemia established from a 10-year-old Caucasian boy in 1993.	RPMI 1640 complete medium with 20% FCS

[2] Information according to the DSMZ (Deutsche Sammlung von Mikroorganismen und Zellkulturen) www.dsmz.de

[3] Generously provided from D. Campana, University Children's Hospital, Singapore.

3.1.2 Culturing media

MEDIUM	INGREDIENTS
RPMI 1640 complete medium	10% FCS 100 U/mL penicillin 100 µg/mL streptomycin 2 mM L-glutamine in RPMI 1640 medium
Freezing medium:	20% DMSO 80% human albumin solution 5% w/v mixed 1:1 with cells in RPMI 1640 complete medium (10% final concentration of DMSO)
NKAES medium	10% fresh frozen plasma 100 U/mL penicillin 100 µg/mL streptomycin 2 mM L-glutamine in RMPI 1640 medium

3.1.3 Reagents

REAGENT/PRODUCT	PROVIDER
Cell culture dishes	Corning, USA
Cryogenic vials	Corning, USA
Dulbecco's phosphate buffered saline (PBS)	Sigma Aldrich, Taufkirchen, Germany
Mr. Frosty freezing container	Nalgene/Thermo Fisher Scientific, Waltham, USA
Penicillin/Streptomycin	Biochrom AG, Berlin, Germany
RPMI 1640	Biochrom AG, Berlin, Germany
FCS	Biochrom AG, Berlin, Germany
L-glutamine	Biochrom AG, Berlin, Germany
Venor®GeM classic kit	Minerva Biolabs, Berlin, Germany
DMSO	AppliChem, Darmstadt, Germany
Human albumin solution 5% w/v	CSL Behring GmbH, King of Prussia, USA
Fresh frozen plasma (FFP)	Centre for Clinical Transfusion Medicine Tuebingen

IL-2	(Proleukin®) Novartis Pharma, Basel, Switzerland
NK cell isolation kit human	Miltenyi Biotec, Bergisch Gladbach, Germany
CD56 microbeads, human	Miltenyi Biotec, Bergisch Gladbach, Germany
CD34 microbeads, human	Miltenyi Biotec, Bergisch Gladbach, Germany
5-AzaC	Sigma Aldrich, Taufkirchen, Germany

3.1.4 Experimental procedures in cell culturing

3.1.4.1 Mycoplasma detection

All cell lines used were tested negative for mycoplasma. Testing was performed with the Minerva Biolabs Venor®GeM classic kit according to the manufacturer's instructions.

3.1.4.2 Isolation of human PBMCs

Blood samples were obtained from healthy volunteers or from the Center for Clinical Transfusion Medicine (University of Tuebingen, Germany) either as whole blood or leukocyte concentrates from healthy blood donors. Before density gradient centrifugation on Ficoll/Paque, whole blood sample were diluted 1:1 or 1:4 for leukocyte concentrates with room temperature PBS. After centrifugation at 800 g without brake, the PBMC layer was carefully isolated and PBMCs were washed two times with PBS, counted and further processed or frozen until usage.

3.1.4.3 Magnetic cell isolation

Isolation of cells (NK cells, $CD34^+$ HSCs) with magnetic beads was performed according to the manufacturer's instructions (see above). Purity was measured by flow cytometry using anti-CD34 mAbs after HSC isolation or anti-C56 and anti-CD3 mAbs after NK cell isolation.

3.1.4.4 Expansion of NKAES cells

Expansion of NK cells was performed according to a modified protocol from Imai and colleagues (NKAES cells – expanded according to the modified 'NK cell activation and expansion system' protocol, Imai et al., 2005). Briefly, freshly isolated or thawed PBMCs were incubated with 100 Gy-irradiated K562-mbIL15-4-1BBL (kind gift of D. Campana, University Children's Hospital Singapore) at a ratio of 1 : 1.5 in the presence of 100 IU/ml IL-2 in NKAES medium in a humidified incubator at 37 °C, 5% CO_2. When isolated NK cells were used for expansion, K562-mbIL15-4-1BBL feeder cells were added at a ratio of 1:10 (NK cells : feeder). Cells were splitted every 2-3 days by

adding one volume of fresh medium containing 100 IU/ml IL-2. Cells were harvested after 14 days of expansion and frozen or directly used for experiments. After thawing, NKAES cells were allowed to recover for approximately 20 h in the presence of 100 IU/ml IL-2 before use.

3.1.4.5 5-AzaC treatment in vitro

5-AzaC was prepared as a stock solution of 25 mg/ml in PBS and was stored at -80 °C. Aliquots were handled on ice and were not refrozen after they were thawed. For 5-AzaC *in vitro* treatment of NKAES cells, 1 µM 5-AzaC was added to the cell culture at d7, d9 or d10 and d13 of the NKAES expansion period and harvested at d14 (see 3.1.4.4).

3.1.4.6 Freezing of cells

Up to 50 x 10^6 cells per cryotube in 0.5 ml in RPMI 1640 complete medium were pre-cooled on ice and mixed with 0.5 ml pre-cooled freezing medium. Cryotubes were immediately transferred into pre-cooled freezing containers with a defined cooling rate of -1 °C/minute. After storage at -80 °C o/n, cells were long-term stored in liquid nitrogen. Cryotubes with frozen cells were handled on dry ice.

3.1.4.7 Thawing of cells

Frozen cells were thawed in a 37 °C water bath until only small ice crystals were present. Per 1 ml cell suspension 10 ml of room temperature cell culture medium (depending on cell type) were slowly added, and then cells were spun down for 10 min at 400 g or at 350 g for NK cells. For thawing of $CD34^+$ stem cells, 2 ml of media was added drop-wise to the thawed cell suspension over a period of 2 minutes. Then 8 ml of media was added in 1 ml aliquots, followed by a 35 min resting phase at room temperature before centrifugation. Cells were counted and used for further purposes.

3.2 Q-RT-PCR

3.2.1 Reagents and equipment

REAGENT	PROVIDER
Nanodrop	Peqlab, Erlangen, Germany
RNeasy Mini kit	Qiagen, Hilden, Germany
Qiamp DNA Mini kit	Qiagen, Hilden, Germany
Quantitect Reverse Transcription Kit	Qiagen, Hilden, Germany
KAPA SYBR FAST Biorad iCycler 2x qPCR Mastermix	Peqlab, Erlangen, Germany
Real-time cycler CFX-96	Biorad, Hercules, USA
Reaction dishes (flat cap strips + tube strips white)	Biorad, Hercules, USA
PCR-Cycler for RT reaction	GeneAmp PCR System 9700

Applied Biosystems/Thermo Fisher Scientific, Waltham, USA

3.2.2 Oligonucleotides

Primer sequences for *KIR* detection were taken from the literature (Vilches et al., 2007; Alves et al., 2008). Due to extensive polymorphism of the *KIR* locus, where applicable, two primers for one direction were used in a 1:1 mixture to detect all *KIR* alleles. For *KIR2DS3* the sequence from Vilches and colleagues was used (Vilches et al., 2007).

DENOTATION	**SEQUENCE 5'- 3' Forward**	**SEQUENCE 5'- 3' Reverse**
KIR2DL1	GTTGGTCAGATGTCATGTTTGAA	CCTGCCAGGTCTTGCG
KIR2DL2	AAACCTTCTCTCTCAGCCCA	GCCCTGCAGAGAACCTACA
KIR2DL3	AGACCCTCAGGAGGTGA	CAGGAGACAACTTTGGATCA
KIR2DL4	TCAGGACAAGCCCTTCTGC	GGACAGGGACCCCATCTTTC
KIR2DL5	ATCTATCCAGGGAGGGGAG	CATAGGGTGAGTCATGGAG
KIR2DP1	CGACACTTTGCACCTCAC	GGGAGCTGACAACTGATG
KIR2DS1	TCTCCATCAGTCGCATGAG TCTCCATCAGTCGCATGAA	GGTCACTGGGAGCTGAC
KIR2DS2	TGCACAGAGAGGGGAAGTA	CCCTGCAAGGTCTTGCA
KIR2DS3	CTTGTCCTGCAGCTCCT	GCATCTGTAGGTTCCTCCT
KIR2DS4	GGTTCAGGCAGGAGAGAAT	CTGGAATGTTCCGTKGATG
KIR2DS5	AGAGAGGGGACGTTTAACC	CTGATAGGGGGAGTGAGT
KIR3DL1	CCATYGGTCCCATGATGCT TCCATCGGTCCCATGATGTT	CCACGATGTCCAGGGGA
KIR3DL2	CATGAACGTAGGCTCCG	GACCACACGCAGGGCAG
KIR3DL3	AATGTTGGTCAGATGTCAG	GCYGACAACTCATAGGGTA
KIR3DPf1	GTGTGGTAGGAGCCTTAG	GAAAACGGTGTTTCGGAATAC
KIR3DP1f2	GTACGTCACCCTCCCATGATGTA	GAAAACGGTGTTTCGGAATAC
KIR3DS1	CATCGGTTCCATGATGCG CATCAGTTCCATGATGCG	CCACGATGTCCAGGGGA
Control1 *(Necdin)*	GGCTGCACCTGAGGCTAA	GCCCCAAAAGAACTCGTATTC
Control2 *(GALC)*	TTACCCAGAGCCCTATCGTTCT	GTCTGCCCATCACCACCTATT

3.2.2.1 DNA-Isolation, RNA isolation, and reverse transcription

DNA or RNA was isolated according to the manufacturer's instructions (see above), quality and concentration of DNA and RNA was analyzed using a nanodrop.

For reverse transcription of RNA, 0.5 µg of total RNA was transcribed using the Quantitect RT Kit with an extended 10 minute gDNA wipeout step and reverse transcription for 30 minutes. DNA and cDNA were stored at -20 °C, RNA at -80 °C.

3.2.2.2 Q-PCR conditions

Reaction composition 1x for Q-PCR reaction:

5 µl SYBR green stock 2x

1 µl 0.5 µl forward + 0.5 µl reverse primer (final primer concentration of 0.25 µM each primer or 0.125 µM in case of two primers for one direction)

x µl Template cDNA (according to 25 ng RNA) or 10 ng gDNA

in nuclease-free water to 10 µl

The RT-PCR reaction was carried out using the following conditions:

20 seconds 95 °C

3 seconds 95 °C
20 seconds 64 °C } 32-40 cycles

A melting curve analysis of RT-PCR products was performed between 76 °C - 95 °C to verify product specificity. H_2O was included as negative control, *Necdin* and *GALC* as positive controls. For *KIR2DL2,* product specificity is only guaranteed if the threshold cycle (C_t) is below or equal cycle 32 (validation by Markus Mezger, see also Oevermann et al., 2014)

3.2.2.2.1 KIR-typing (genomic DNA)

GALC primers were used as internal control in a multiplex reaction. Melting curve analysis allowed discrimination of the presence of the specific KIR (T_m between 81-88 °C) and the internal control peak *GALC* (T_m = 75 °C). The B-content score, KIR genotype group and the centromeric and telomeric gene content motif were assessed as described by Cooley and colleagues (Cooley et al., 2010).

3.2.2.2.2 Quantitative analysis of KIR expression (RNA/cDNA)

Relative expression was quantified according to the $2^{-\Delta\Delta Ct}$ (Livak) method (Livak and Schmittgen, 2001) using *GALC* as reference. Controls without reverse transcriptase (-RT control) during the reverse transcription reaction were included to verify the absence of genomic DNA.

3.3 FACS analysis

3.3.1 Reagents and equipment

REAGENT	PROVIDER
Polystyrene FACS tubes	Sarstedt, Nürnbrecht, Germany
Cytometer Software	BD-FACS Diva Software FCS Express 4.0.23.0
Flow Cytometer	BD LSRII, BD Biosciences, Franklin Lakes, USA
Amine-reactive dye (ARD-)Ax350	Invitrogen, Carlsbad, USA
BrdU Flow Kit FITC (including 7-AAD)	BD Biosciences, Franklin Lakes, USA
Rabbit Serum	Invitrogen, Carlsbad, USA
Privigen (human IgG) 100 mg/ml	CSL Behring GmbH, King of Prussia, USA
Fix & Perm kit	An der Grub Bio (ADG) Research GmbH, Vienna, Austria

3.3.2 Buffers and solutions

BUFFER	COMPONENTS
FACS buffer	2% FCS 0.002 M EDTA in PBS
Blocking buffer	10 µg/ml human IgG (Privigen) in FACS buffer

3.3.3 Antibodies

Antibody (anti-human-)	Dilution	Company	Reference	Isotype	Clone
BrdU FITC	1:50	BD Biosciences, Franklin Lakes, USA	BrdU Flow Kit	mouse IgG1	B44
CD3 PE-CF594	1:50	BD Biosciences, Franklin Lakes, USA	562310	mouse IgG1	UCHT1
CD3 PerCP	1:100	BD Biosciences, Franklin Lakes,	345766	mouse IgG1	SK7

		USA			
CD9 APC	1:100	BD Biosciences, Franklin Lakes, USA	341638	mouse IgG1	M-L13
CD10 PE-CF594	1:50	BD Biosciences, Franklin Lakes, USA	562396	mouse IgG1	HI10A
CD10 RPE	1:50	Dako, Denmark	R0848	mouse IgG1	SS2/36
CD13 PerCp-eFluor710	1:25	eBioscience, Frankfurt, Germany	46-0138	mouse IgG1	WM15
CD16 AF700	1:50	BD Biosciences, Franklin Lakes, USA	557920	mouse IgG1	3G8
CD19 APC	1:50	Becton Dicksion	345791	mouse IgG1	SJ25C1
CD19 Brilliant Violet 421	1:25	BD Biosciences, Franklin Lakes, USA	562441	mouse IgG1	HIB19
CD19 Brilliant Violet 785	1:25	BioLegend, San Diego, USA	302239	mouse IgG1	HIB19
CD20 PerCp	1:50	BioLegend, San Diego, USA	302324	mouse IgG2b	2H7
CD24 PE	1:10	BD Biosciences, Franklin Lakes, USA	555428	mouse IgG2a	ML5
CD34 PerCP	1:100	Becton Dickinson	345803	mouse IgG1	8G12
CD38 PE-Cy7	1:25	BioLegend, San Diego, USA	303516	mouse IgG1	HIT1
CD38 APC	1:10	BioLegend, San Diego, USA	303510	mouse IgG1	HIT2
CD45 PE-Cy7	1:100	BD Biosciences, Franklin Lakes, USA	557748	mouse IgG1	HI30
CD54 (ICAM-1) FITC	1:5	Immunotech/Beckman Coulter, Bea, USA	IM0726U	mouse IgG1	84H10
CD56 Brilliant Violet 421	1:50	BioLegend, San Diego, USA	318328	mouse IgG1	HCD56
CD56 Brilliant Violet 711	1:25	BioLegend, San Diego, USA	318335	mouse IgG1	HCD56
CD58 FITC	1:10	BD Biosciences, Franklin Lakes, USA	555920	mouse IgG2a	1C3
CD94 FITC	1:50	BD Biosciences, Franklin Lakes, USA	555888	mouse IgG1	HP-3D9
CD94 PE	1:10	BioLegend, San	305506	mouse IgG1	DX22

		Diego, USA			
CD107a APC	1:20	BD Biosciences, Franklin Lakes, USA	560664	mouse IgG1	H4A3
CD107a Brilliant Violet 421	1:20	BD Biosciences, Franklin Lakes, USA	562623	mouse IgG1	H4A3
CD112 PE	1:50	BioLegend, San Diego, USA	337409	mouse IgG1	TX31
CD117 PE	1:10	BioLegend, San Diego, USA	313204	mouse IgG1	104D2
CD117 Brilliant Violet 421	1:25	BioLegend, San Diego, USA	313216	mouse IgG1	104D2
CD155 PE	1:20	BioLegend, San Diego, USA	337610	mouse IgG1	SKII.4
CD158a/h/i FITC (KIR2DL1/S1/S4)	1:25	BD Biosciences, Franklin Lakes, USA	340531	mouse IgM	HP-3E4
CD158a/h/i PE (KIR2DL1/S1/S4)	1:10	BD Biosciences, Franklin Lakes, USA	556063	mouse IgM	HP-3E4
CD158a PerCp (KIR2DL1)	1:20	R&D Systems, Minneapolis, USA	FAB1844C	mouse IgG1	#143211
CD158b1/b2/j PE (KIR2DL2/L3/S2)	1:50 (1:25*)	Beckman Coulter, Bea, USA	PN IM2278U	mouse IgG1	GL183
CD158b1/b2/j APC (KIR2DL2/L3/S2)	1:100	Beckman Coulter, Bea, USA	A22333	mouseIgG1	GL183
CD158b2 APC (KIR2DL3)	1:10	Beckman Coulter, Bea, USA	FAB2014A	mouse IgG2a	#180701
CD158e1/e2 (KIR3DL1/DS1) PE	1:50 (1:25*)	Beckman Coulter, Bea, USA	PN IM3292	mouse IgG1	Z27.3.7
CD158e APC (KIR3DL1)	1:100 (1:20*)	R&D Systems, Minneapolis, USA	FAB1225A	mouse IgG1	DX9
CD158i (KIR2DS4) APC	1:50	Beckman Coulter, Bea, USA	41116015	mouse IgG2a	FES172
CD226 PE (DNAM-1)	1:5	Miltenyi Biotec, Bergisch Gladbach, Germany	130-092-476	mouse IgG1	Dx11
CD244 FITC (2B4)	1:5	BioLegend, San Diego, USA	329505	mouse IgG1	C1.7
CD304-PE	1:10	BioLegend, San Diego, USA	354504	mouse IgG2a	12C2
HLA Bw4 FITC	1:10	One Lambda	FH0007	IgG2a	
HLA-A,B,C PE	1:50	BioLegend, San	311405	mouse IgG2a	W6/32

		Diego, USA			
IFN-γ BUV395	1:20	BD Biosciences, Franklin Lakes, USA	563563	mouse IgG1	B27
IFN-γ PE	1:50	BD Biosciences, Franklin Lakes, USA	554701	mouse IgG1	B27
NKG2a APC	1:25	Beckman Coulter, Bea, USA	PN A60797	mouse IgG2b	Z199
NKG2A PE-Cy7	1:25	Beckman Coulter, Bea, USA	B10246	mouse IgG2b	Z199
NKG2D APC	1:25	Miltenyi Biotec, Bergisch Gladbach, Germany	130-092-673	mouse IgG1	BAT221
NKp30 PE	1:50	Beckman Coulter, Bea, USA	PN IM 3709	mouse IgG1	Z25
NKp44 PE (CD336)	1:25	Beckman Coulter, Bea, USA	PN IM 3710	mouse IgG1	Z231
NKp46 APC	1:10	BD Biosciences, Franklin Lakes, USA	558051	mouse IgG1	9E2/NKp46
Perforin Pacific Blue	1:20	BioLegend, San Diego, USA	308118	mouse IgG2b	dG9
TNFα Brilliant Violet 605	1:33	BioLegend, San Diego, USA	502935	mouse IgG1	MAb11

* in functional response stainings

Antibody (anti-mouse-)	**Dilution**	**Company**	**Reference**	**Isotype**	**Clone**
CD45 APC-eFluor 780	1:50	eBioscience, Frankfurt, Germany	47-0451-80	mouse IgG2b	30-F11
CD45 FITC	1:50	BioLegend, San Diego, USA	103108	rat IgG2b	30-F11

Isotype controls	**Company**	**Reference**	**Isotype**	**Clone**
IgG1 AF 700	ExBio, Praha, Czech Republic	A7-626-C100	mouse IgG2a	MOPC-21
IgG1 APC	BD Biosciences, Franklin Lakes, USA	555751	mouse IgG1	MOPC-21
IgG1 Brilliant Violet 605 κ	BioLegend, San Diego, USA	400161	mouse(BALB/c) IgG1	MOPC-21
IgG1 Brilliant Violet 421	BD Biosciences, Franklin Lakes, USA	562438	mouse IgG1	X40
IgG1 BUV395	BD Biosciences, Franklin	56356	mouse IgG1	X40

	Lakes, USA			
IgG1 FITC	BD Biosciences, Franklin Lakes, USA	555909	Mouse IgG1	MOPC-21
IgG1 κ PE	BD Biosciences, Franklin Lakes, USA	555749	mouse IgG1	MOPC-21
IgG1-PerCP	BD Biosciences, Franklin Lakes, USA	550672	Mouse IgG1	MOPC-31C
IgG2a APC	BioLegend, San Diego, USA	400219	Mouse IgG2a	MOPC-173
IgG2a control PE	Immuno Tools	21275524	mouse IgG2a	PPV-04
IgG2b Pacific Blue κ Ctrl	BioLegend, San Diego, USA	400331	mouse IgG2b	MPC-11
IgG2b-APC	ExBio, Praha, Czech Republic	1A-801-C020		PLRV219
IgM FITC	Invitrogen, Carlsbad, USA	MGM01	mouse IgM	CTDk

Antibodies for surface staining using secondary fluorochrome-labeled antibodies

Antibody (anti-human-)	**Dilu-tion**	**Company**	**Reference**	**Isotype**	**Clone**
pan-NKG2D-L:					
MICA	1:100	kindly provided by Alexander Steinle	(Welte et al., 2003)	mouse IgG1	AMO1
MICB	1:50			mouse IgG1	BMO1
ULBP1	1:100			mouse IgG1	AUMO3
ULBP2	1:100			mouse IgG1	BUMO1
ULBP3	1:100			mouse IgG1	CUMO3
KIR3DL2	1:5	kindly provided by Daniela Pende, Perugia		mouse IgM	Q66
sheep-anti-mouse-RPE F(ab)2	1:50	Sigma Aldrich, Taufkirchen, Germany	P8547		Polyclonal

3.3.4 Antibody combinations for flow cytometry

Selected multicolour flow cytometric antibody panels used for the respective experiments are shown below. Only complex antibody panels are shown in this section. All antibody panels were stained in combination with a live-dead-discriminating dye as described later. Antibodies have anti-human specificity, unless otherwise indicated (mouse).

Antibody panel for Fig. 7B. Detection of NK cells, AML and BCP-ALL cells after adoptive transfer *in vivo*

Anti-	Clone
mouse CD45 FITC	30-F11
CD10 RPE	SS2/36
CD13 PerCp-eFluor710	WM15
CD45 PE-Cy7	HI30
CD56 Brilliant Violet 421	HCD56
CD19 Brilliant Violet 785	HIB19

Antibody panel for Fig. 9B. Detection of NK cells and BCP-ALL cells after adoptive transfer *in vivo*

Anti-	Clone
CD45 PE-Cγ7	HI30
mouseCD45 APC-eFluor 780	30-F11
CD19 APC	SJ25C1
CD10 RPE	SS2/36
CD56 Brilliant Violet 421	HCD56
CD16 AF 700	3G8
CD3 PerCP	SK7

Antibody panel for Fig. 11B. IPH2102 *in vivo*, detection of BCP-ALL blast (P23T) in huNSG (SSC18U)

Anti-	Clone
CD38 PE-Cy7	HIT2
mouseCD45 APC eFluor 780	30-F11
CD304 PE (for bone marrow samples)	12C2
CD24 PE (for spleen samples)	ML5
CD9 APC	M-L13
CD20-PerCp	2H7
CD58 FITC	1C3
CD19 Brilliant Violet 421	HIB19
CD10 PE-CF594	HI10A

Antibody panel for Fig. 13, Fig. 16 Antibodys for discrimination of the alloreactive/KIR subsets. In combination with functional response staining

Anti-	Clone
CD56 Brilliant Violet711	HCD56
CD3 PE-CF594	UCHT1
NKG2A PE-Cy7	Z199
CD158 a PE	HP-3E4
CD158e1/e2 (KIR3DL1/DS1) PE	Z27.3.7
CD158e APC (KIR3DL1)	DX9
CD158b1/b2/j APC (KIR 2DL2/L3/S2)	GL183

Antibody panel for Fig. 24C. Differentiation of NK cells in huNSG

Anti-	Clone
CD94 FITC	HP-3D9
CD117 PE	104D2
CD34 PerCP	8G12
NKp46 APC	9E2/NKp46
CD16 AF 700	3G8
CD56 Brilliant Violet 421	HCD56
CD45 PE-Cy7	HI30

Antibody panel for Fig. 25. Proliferation after 5-AzaC treatment in huNSG mice

Anti-	Clone
BrdU-FITC	B44
CD94-PE	DX22
CD3 PE CF 594	UCHT1
CD34 PerCP	8G12
NKp46 APC	9E2/NKp46
CD16 AF 700	3G8
CD117-Brilliant Violet421	104D2
CD45 PE-Cy7	HI30
CD56 Brilliant Violet 711	HCD56
mouseCD45 APC-eFluor 780	30-F11
Rabbit Serum	10 µl/Test

Antibody panel for Fig. 25. Cell cycle analysis after 5-AzaC treatment in huNSG mice

Anti-	Clone
BrdU FITC	B44
CD117 Brilliant Violet421	104D2
CD94 PE	DX22
mouse CD45 APC-eFluor 780	30-F11
7-AAD	

3.3.5 Experimental procedures

3.3.5.1 Staining of surface antigens (directly labeled antibodies), live-dead staining with an amine-reactive dye

Up to 5 x 10^6 cells or 10 x 10^6 cells for FACS sorting experiments were resuspended in 50 µl FACS buffer containing the respective diluted antibody-fluorochrome conjugates. Cells were incubated for 10 min at room temperature or for 20 min at 4 °C in the dark. For discrimination between live and dead cells, cells were afterwards washed with PBS and incubated with 39.4 µM ARD-Ax350 for 10 min at room temperature in the dark and washed three times with FACS buffer. Cells were either directly analyzed or fixed with 0.5% PFA for analysis on the following day. Centrifugation steps were performed at 400 g for 4 min. Cells were analyzed with a BD LSR II. Live, vital cells were selected and doublets excluded based on scatter characteristics and low (auto-) fluorescence intensities.

3.3.5.2 Staining of surface antigens (using secondary fluorochrome-labeled antibodies)

Blocking was perfomed for 30 min at room temperature using 10 µg/ml human IgG in FACS buffer. Primary antibodies (for pan-NKG2D-L: combination of MICA, MICB and ULBP1-3) were stained for 20 min at room temperature in blocking buffer. After three washing steps with FACS buffer, the secondary antibody was stained in FACS buffer for 15 min at room temperature in the dark. Optionally further surface antigens were stained as described in 3.3.5.1. Cells were either directly analyzed or fixed with 0.5 % PFA for analysis on the following day. Centrifugation steps were performed at 400 g for 4 min. Cells were analyzed at a BD LSR II. Live, vital cells were selected and doublets excluded based on scatter characteristics and low (auto-) fluorescence intensities.

3.3.5.3 Functional response staining after co-culture experiments

For co-incubation conditions see 3.4.2.4. Fluorescently labeled anti-CD107a antibody was added to the NK cells for 1 h at 37 °C before addition of Golgi Plug and target cells. After further 6 h of co-culture, cells were washed twice with FACS buffer and surface antibodies were stained in 50 µl per well in FACS buffer for 20 min at 4 °C in the dark. After two washes with FACS buffer, cells were incubated with 39.4 µM ARD-Ax350 for 10 min at room temperature in the dark and washed twice times with FACS buffer. For fixation cells were resuspended in 100 µl Reagent A (fixation medium) per well and incubated for 20 min at 4 °C. After two washes with FACS buffer, intracellular epitopes were stained by incubating the cells with the respective antibodies in 100 µl Reagent B (permeabilization medium) per well for 45 min at 4 °C. After two final washes cells were either directly analyzed by flow cytometry or fixed with 0.5% PFA and analyzed the next day. Isotype controls and a baseline (NKAES cells only) as reference were always included.

3.3.5.4 Staining of incorporated BrdU

BrdU staining was perfomed according to the manufacturer's protocol (see above) with additional cell surface staining and live-dead staining with ARD-Ax350 as described in 3.3.5.1 before the BrdU-staining procedure. During establishment, non-BrdU-treated cells and huNSG mice were included to verify the specificity of the staining. For later stainings, only isotype controls (for cell surface antigens and IgG1-FITC for anti-BrdU-FITC) were included.

3.4 Further *in vitro* methods

3.4.1 Reagents and equipment

REAGENT	PROVIDER
Carboxyfluorescein(diacetat) succinimidyl ester (CFSE)	Vybrant CFDA SE Cell Tracer Kit®, Invitrogen, Carlsbad, USA
Ficoll/Biocoll density 1.077 g/ml	Biochrom AG, Berlin, Germany
IPH2102	KIR-blocking mAb, clone 1-7F9, generously provided by Bristol-Myers Squibb, Princeton, USA
Cell sorter	BD FACS Aria, BD Biosciences, Franklin Lakes, USA
Golgi Plug	BD Biosciences, Franklin Lakes, USA
Diaclone Perforin ELISA KIT	Active Bioscience, Hamburg, Germany

3.4.2 Experimental procedures

3.4.2.1 Determination of in vitro cytotoxicity

Target cells or cell lines were labeled with 0.5 µM CFSE one day prior to the assay and cultured o/n in RPMI 1640 complete medium for cell lines or RPMI 1640 complete medium containing 20% FCS for primary leukemic cells. NKAES cells were thawed, cultivated o/n in RPMI 1640 complete containing 100 U/ml IL-2. For primary leukemic cells a density gradient centrifugation on Ficoll/Paque was performed to remove dead cells directly before co-culture. Co-incubation was performed in triplicates at the ratios 10:1 (100 000 NK cells + 10 000 targets), 5:1 (50 000 NK cells + 10 000 targets) and 2:1 (50 000 NK cells + 25 000 targets) in a final volume of 200 µl in RPMI 1640 complete medium for 5 h at 37 °C in U-bottom 96-well plates. For live-dead discrimination cells were afterwards stained with ARD-Ax350 (as described in 3.3.5.1), washed, and analyzed directly or fixed with 0.5% PFA and analyzed up to one day later. In order to exclude spontaneously occurring cell death, target cell monoculture controls were included in every experiment. The percentage of specific target cell lysis was calculated as follows: $\frac{\%CFSE^+ARD^+ \text{dead targets} - \%CFSE^+ARD^+ \text{ spontaneously dead targets}}{(100 - \%CFSE^+ARD^+ \text{ spontaneously dead targets})} \text{x } 100\%$

3.4.2.2 Treatment with the KIR-blocking mAb IPH2102

For *in vitro* treatment NK cells were pre-incubated with 30 µg/ml IPH2102 for 30 min at 37 °C. Blockade of CD158a/h/i and CD158b1/b2/j was verified via flow cytometry (see also 4.2.3).

3.4.2.3 Sorting of KIR^+ and KIR^- NKAES cells

NKAES cells were thawed, cultivated o/n in RPMI 1640 complete medium containing 100 U/ml IL-2 or used from freshly expanded cultures at d13-d15. Cells were stained with the following antibodies: anti-CD3 PECF594, anti-CD56 bv711 for NK cell identification and anti-CD158a/h/i-PE (clone HP-3E4 recognizing KIR2DL1/S1/S4), anti-CD158b1/b2/j-PE (clone GL183 recognizing KIR2DL2/L3/S2) and anti-CD158e-PE (clone DX9 recognizing 3DL1) to discriminate KIR^+ and KIR- NK cells. Up to 10 x 10^6 cells were stained in a final volume of 50 µl containing 20% rabbit serum to block unspecific binding of antibodies. Sorting was performed with a BD FACS Aria cell sorter. After sorting, purity was analyzed (ranging between 91% and 99%); KIR^+ and KIR^- NK cells were cultured o/n in the presence of 100 IU/ml IL2 and then used for further experiments.

3.4.2.4 Co-culture experiments for functional response staining

Thawed NKAES cells were incubated o/n in RPMI complete + 10% human serum and 200 U/ml IL-2 at ca. 2 x 10^6 cells/ml. The next day, 0.5 x 10^6 NKAES cells in 100 µl RPMI 1640 containing 10% human serum and 1% L-Gln per well were incubated with fluorescently labeled CD107a antibody for 1h at 37 °C. Then Golgi Plug (1:250) and the respective target cells at an E:T ratio of 1:2 (1 x 10^6 target cells) were added to the NKAES cells. After 6 h incubation at 37 °C the intracellular staining was performed as described in 3.3.5.3. Isotype controls to allow specific gating were included, all percentages were normalized to the baseline levels of NKAES cells cultured in medium only. Specificity of Perforin staining was verified by ELISA according to the manufacturer's protocol.

3.4.2.5 HLA-typing

HLA class I genotyping was performed at 4-digit resolution by sequence-based typing (SBT) by the lab of Prof. Dr. C. Müller (University of Tuebingen, Germany).

3.5 *In vivo* methods

3.5.1 Mice

NOD.Cg-Prkdc^{scid} IL2rg^{tmWjl}/SzJ, also termed NOD-*scid* IL2Rgamma^{null} (NSG) mice were purchased at The Jackson Laboratory (Bar Harbor, ME, USA), breeded and maintained under specific pathogen-free conditions in the research animal facilities of the University Children's Hospital Tuebingen,

Germany. All animal procedures were approved and conducted according to German federal and state regulations (Regierungspräsidium Tuebingen, permission numbers K4/10, K3/12, K1/13 and §10a permission Witte 01.10.2010).

3.5.2 Primary patient material

HSCs and leukemic cells were obtained at the University Children's Hospital Tuebingen as mentioned in the respective paragraphs. The donation was approved by the local ethics committee with the following project numbers: 23/2007, 199/2010BO1, 029/2013BO1, and 213/2014BO2.

3.5.3 Buffers

BUFFER	COMPONENTS
ACK lysis buffer	8.29 g ammonium chloride 1 g potassium hydrogen carbonate 0.0372 g $Na_2EDTA \cdot 2H_2O$ ad 1 l

3.5.4 Reagents and equipment

REAGENT	PROVIDER
ACK lysis buffer	University Pharmacy Tuebingen, Germany
^{137}Cs irradiator	Gammacell 1000 Elite; MDS Nordion, Fleurus, Belgium
IL-15	CellGenix, Freiburg, Germany
IL-15Rα	R&D Systems, Minneapolis, USA
Fc-IL-7	generously provided by Merck, Darmstadt, Germany
poly (I:C) (HMW)	Invivogen
BrdU	Sigma Aldrich, Taufkirchen, Germany
Glucose	Sigma Aldrich, Taufkirchen, Germany
Cell strainer 0.45 µm	BD Biosciences, Franklin Lakes, USA

3.5.5 Experimental procedures

3.5.5.1 Source and mobilization of HSCs

HSCs were either donated from parents of children diagnosed with various malignancies prior to planned HSCT at the University Children's Hospital Tuebingen or were purchased from healthy

donors from Keybiologics (Memphis, TN, USA). The donation at the University Children's Hospital was approved by the local ethics committee and parents gave informed consent to donate up to 5% for transplantation into NSG mice and to use leukapheresis products for research purposes in case the patient deceased prior to HSCT (see also 3.5.2). As described in (André et al., 2010), peripheral blood HSCs were mobilized by administration of 10 mg/kg/d G-CSF five days before leukapheresis. $CD34^+$ cells were selected using magnetic beads (see 3.1.4.3), purity of the HSCs was evaluated using a LSR II flow cytometer.

3.5.5.2 Processing of mouse tissue

Peripheral blood from living animals was taken from the retrobulbar venous plexus under CO_2/O_2 narcosis. For lysis of erythrocytes, peripheral blood (~ 50 µl) was incubated with 5 ml ACK lysis buffer. After 7 min 5 ml PBS were added to stop lysis followed by two washing steps with cold PBS. After sacrificing mice, spleen and bone marrow were isolated. To obtain single cell suspensions, cells were thoroughly pressed through a 0.45 µm cell strainer and washed in cold PBS. Splenic cells were, in case of high erythrocyte content, subjected to 30s of incubation with ACK lysis buffer.

3.5.5.3 Transplantation of HSCs into NSG mice

As described in (André et al., 2010); 8- to 12-week old female NSG mice were sublethally irradiated (200 cGy). Four hours later, 1-2 x 10^6 $CD34^+$ HSCs were transplanted via intravenous injection into the tail vain. To support engraftment, mice were intravenously injected with 20 mg Fc-IL-7/week/mouse. Engraftment was regularly analyzed in the peripheral blood by flow cytometry.

3.5.5.4 Induction of patient-specific leukemia in NSG mice

As described in (Woiterski et al., 2013); 1-5 x 10^6 leukemic cells derived from bone marrow of children at initial diagnosis or relapse of BCP-ALL or AML were injected into NSG mice. To monitor and quantify leukemic engraftment, peripheral blood from the mice was analyzed via flow cytometry using pre-defined leukemic surface markers. Animals were sacrificed if engraftment exceeded 60% in the peripheral blood or animals showed signs of leukemic disease (weight loss, ruffled fur, hunched back). Bone marrow and spleen were flow-cytometrically analyzed for leukemic engraftment, blasts were retransplanted into successive mouse generations or frozen and stored in lN_2 for *in vitro* or *in vivo* experiments. The study was approved by the local ethics committee and informed consent was obtained from the parents of the patients (see 3.5.2).

3.5.5.5 Adoptive NK cell transfer in vivo

1-2 x 10^6 blasts were intravenously injected into non-irradiated NSG mice on d0, followed by intravenous injection of 10 x 10^6 NKAES cells 6-8 h later. Further NKAES cell injections were perfomed at the time points indicated in the respective figures. NKAES cells were thawed one day

prior to adoptive transfer and cultured in RPMI 1640 complete medium containing 100 U/ml IL-2. Engraftment was monitored by flow-cytometric analysis of PBMCs using pre-defined leukemia specific surface markers and NK cell markers. In all experiments, the frequencies of patient-specific vital blasts were normalized to vital murine $CD45^+$ cells.

3.5.5.6 Determination of in vivo cytotoxicity

Mice were transplanted with HSCs of the respective donor and weekly injected with Fc-IL-7 as described above. To obtain functional competence of the developing NK cells, 2.5 µg IL-15 and 7.5 µg IL-15Rα in PBS were intraperitoneally injected three times (15, 10 and 5 days prior to analysis) according to (Huntington et al., 2009) and once with 100 µg poly (I:C) intraperitoneally one day prior to leukemia injection (Strowig et al., 2010). 3 x 10^6 blasts were intravenously injected into huNSG mice and the extent of blasts was determined 20 h post injection in the bone marrow using polychromatic (8-11) color flow cytometry. In all experiments, the frequencies of patient-specific vital blasts were normalized to vital murine $CD45^+$ cells (see also Kübler et al., 2014).

3.5.5.7 IPH2102 treatment of huNSG

For treatment of huNSG mice, 250 µg IPH2102 in PBS was intravenously injected once one day before blast injection.

3.5.5.8 In vivo treatment of huNSG mice with 5-azacytidine

For in vivo treatment of huNSG mice with 5-AzaC, huNSG mice were randomly assigned to treatment or control group in week 6 (d39) post transplantation. Therapy with 5-AzaC (0.025 mg/mouse/dose intraperitoneally, twice a week for a total of 4 weeks) was initiated. Both groups were treated with IL-15/IL-15Rα and poly (I:C) as described in 3.5.5.6. 4 weeks later, 3 x 10^6 blasts were intravenously injected into 5-AzaC- or untreated animals. 20 h later, mice were sacrificed and subjected to analysis of NK cell phenotype and for quantification of leukemic burden as already described above (see also Kübler et al., 2014).

3.5.5.9 BrdU treatment of huNSG

For *in vivo* BrdU treatment of huNSG mice, 0.8 mg/ml BrdU and 1mg/ml Glucose were added to the drinking water 7 days before analysis. Drinking water was exchanged every 2-3 days.

3.6 Statistics

Unless mentioned otherwise, a Student's t-test for two samples with equal variance with two-tailed distribution was performed.

Effect size was calculated as follows: $\frac{\text{mean}^{\text{treated}} - \text{mean}^{\text{untreated}}}{\text{standard deviation}^{\text{treated and untreated}}}$

4 RESULTS

4.1 Pediatric BCP-ALL is a target of NK cells

Most data reporting beneficial effects of NK cells in leukemia therapy was obtained in AML patients. Studies from the Perugia group suggest that the differential expression of adhesion molecules leads either to resistance or to susceptibility of ALLs towards NK cell-mediated cytotoxicity (Ruggeri et al., 1999; Ruggeri et al., 2002). In contrast to most adult ALLs, pediatric ALLs express adhesion molecules relevant for NK cell-target conjugate formation (Mengarelli et al., 2001). In line with this observation, preliminary data shows the anti-leukemic effects of NK cells towards pediatric B-ALL (Leung et al., 2004; Pende et al., 2009). As ALL, which is mainly of the B cell precursor type (BCP-ALL), comprises 81% of childhood leukemias (Howlader et al., 2014), more data on the susceptibility of BCP-ALL could help to improve therapy options for children with poor prognosis. In this regard, the aim of this study was to evaluate the capability of expanded NK cells towards BCP-ALL cell lines and primary pediatric samples *in vitro* and *in vivo*.

4.1.1 Pediatric BCP-ALL can be targeted by NKAES cells in vitro

Since NK cell responsiveness is greatly influenced by cytokines (Bonnema et al., 1994), an efficient expansion and stimulation regimen was chosen to maximize anti-leukemic effects. NK cells were expanded according to a modified GMP (good manufacturing practice)-compatible protocol of (Fujisaki et al., 2009), based on a K562-mbIL15-4-1BBL feeder cell line and low-dose recombinant IL-2 (see 3.1.4.4).

To phenotypically compare expanded NKAES cells to resting NK cells, analysis of common NK cell receptors was performed before and after the 14 day expansion period. In line with published data (Fujisaki et al., 2009) NKp44 and NKG2D expression is slightly upregulated in NKAES cells (Fig. 4). In addition, NKAES cells show a slight increase in KIR expression and a significant increase in NKG2A expression.

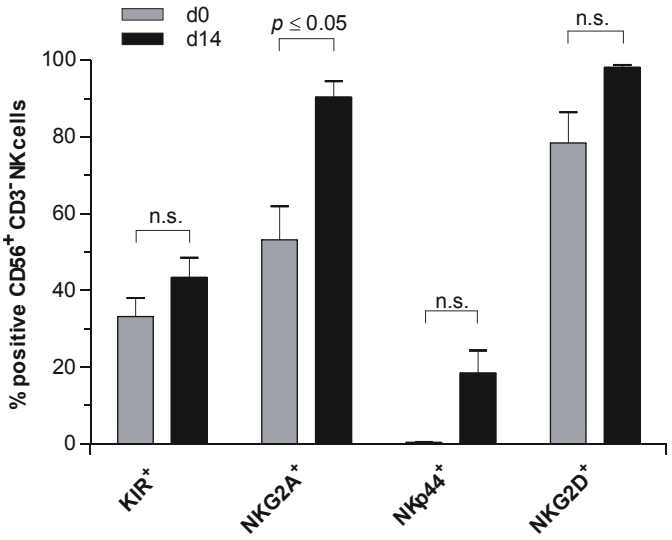

Fig. 4: *In vitro* expanded NKAES cells display increases in NKG2A expression. NK cells were expanded from PBMCs according to a modified protocol from (Fujisaki et al., 2009). Shown is the percentage of receptor positive $CD56^{+}CD3^{-}$ cells as quantified by flow cytometry; KIR: combined staining of KIR2DL1/S1/S4 (clone HP-3E4), KIR2DL2/L3/S2 (clone GL183) and KIR3DL1 (clone DX9); NKG2A, NKp44, NKG2D. (n = 3; statistics: Student's paired t-test with two-tailed distribution)

Since the extent of HLA class I expression has been described to impact NK cell-mediated cytotoxicity (Pfeiffer et al., 2007; Feuchtinger et al., 2009), BCP-ALL cell lines with comparable intermediate HLA class I expression were chosen (Fig. 5; pediatric BCP-cell lines Nalm-16, MHH-cALL4 and SEM, the pediatric AML cell line Kasumi-1 and the HLA class I-deficient CML cell line K562 as a control).

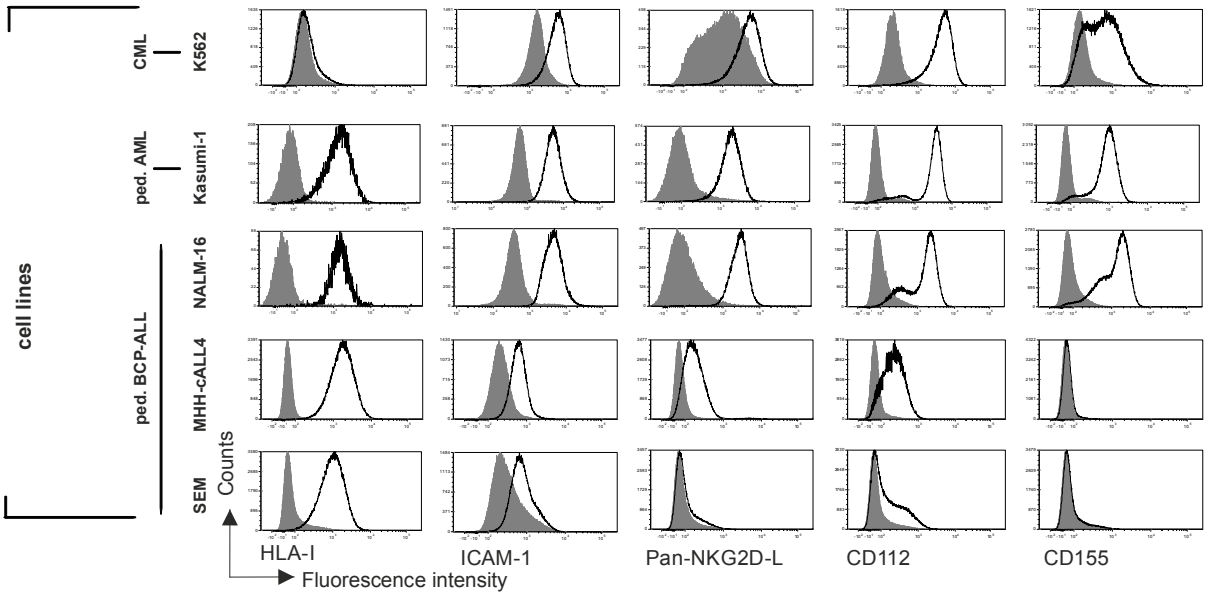

Fig. 5: Phenotypical characterization of selected cell lines by HLA class I, ICAM-1, NKG2D-L, CD112 and CD155 expression. Flow cytometric characterization of important molecules recognized by NK cells on the pediatric BCP-cell lines Nalm-16, MHH-cALL4 and SEM, the pediatric AML cell line Kasumi-1 and the HLA class I-deficient CML cell line K562. Pan-NKG2D-L staining was performed using a cocktail of anti-MICA, anti-MICB and anti-ULBP1-3 antibodies, HLA class I with clone W6/32; for others refer to section 3.3. Grey, filled: isotype; black line: specific antibody staining (Kübler et al., 2014)[i].

Comparison of the cytotoxic potential towards these cell lines shows that pediatric BCP-ALL cell lines can in principle be a target of NKAES cells (Fig. 6). The extent of specific lysis varies and probably reflects the differences in ICAM-1, CD112, CD155 and especially NKG2D-ligand expression (Fig. 5).

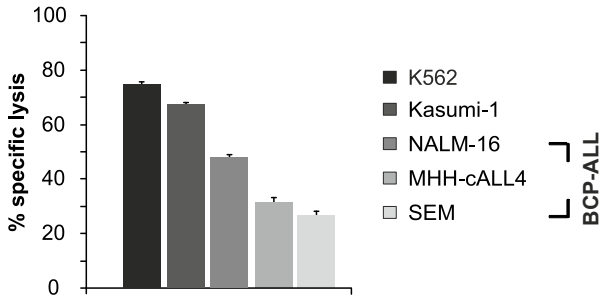

Fig. 6: Surface ligand expression influences killing of BCP-ALL. In vitro cytotoxicity assay performed with SNK15B NKAES cells at an effector to target ratio of 2:1. K562 and Kasumi-1 were used as controls. Shown is the percentage of specific lysis, the assay was perfomed in triplicates (Kübler et al., 2014)[i].

Therefore, in the following experiments investigating the relevance of the KIR-KIRL axis, the expression of ligands potentially relevant for NK cell-mediated cytotoxicity were carefully evaluated on leukemic cells. Furthermore, the expression of important NK cell receptors was analyzed. For all experiments, NK cells and leukemic samples with comparable expression levels were chosen as mentioned in the respective sections (see also Suppl. Fig. 1 and Suppl. Fig. 2).

4.1.2 NKAES cells display significant alloreactivity towards pediatric BCP-ALL *in vivo*

To establish an *in vivo* model of adoptive NK cell therapy a pediatric AML (P18R) and pediatric BCP-ALL sample (P3B) that displayed robust engraftment in NSG mice (data not shown) were chosen. A pooled sample of both was intravenously injected into NSG mice, followed by 4 weekly injections of NKAES cells (for experimental setup see Fig. 7A).

A multicolor flow-cytometric strategy using predetermined CD markers allows discrimination of NK cells, P18R and P3B leukemic cells in the peripheral blood. For all *in vivo* experiments, evaluation of the leukemic burden is given as the number of vital blasts normalized to vital murine $CD45^+$ cells, since murine $CD45^+$ cells are assumed to be a constant population between different mice in cases where the overall abundance of human $CD45^+$ cells is low.

NKAES cells were indeed able to target pediatric BCP-ALL *in vivo* as shown by a significantly decreased leukemic burden in the peripheral blood of NKAES cell-treated compared to untreated animals (Fig. 7B). For phenotypical characterization of blasts and NKAES cells, see Suppl. Fig. 1A and Suppl. Fig. 2. The efficiency of the NK cell-based adoptive transfer strategy is shown by a prolonged survival of treated animals (Fig. 7C). NKAES cells are able to target pediatric BCP-ALL *in vivo* but do not eradicate leukemia under these conditions.

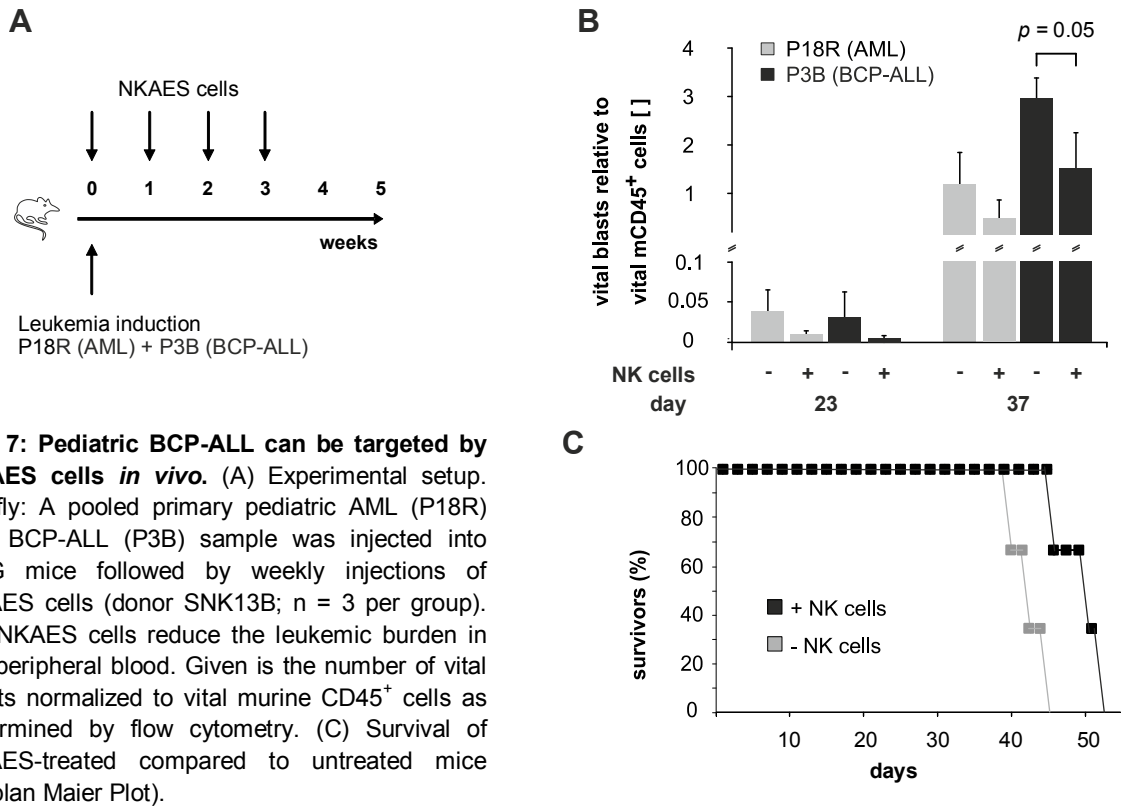

Fig. 7: Pediatric BCP-ALL can be targeted by NKAES cells *in vivo*. (A) Experimental setup. Briefly: A pooled primary pediatric AML (P18R) and BCP-ALL (P3B) sample was injected into NSG mice followed by weekly injections of NKAES cells (donor SNK13B; n = 3 per group). (B) NKAES cells reduce the leukemic burden in the peripheral blood. Given is the number of vital blasts normalized to vital murine $CD45^+$ cells as determined by flow cytometry. (C) Survival of NKAES-treated compared to untreated mice (Kaplan Maier Plot).

4.2 KIR-KIRL mismatches are relevant for cytotoxicity of NK cells towards pediatric BCP-ALL

After having shown that pediatric BCP-ALL can in principal be targeted by NK cells *in vitro* and *in vivo*, the question is whether KIR-KIRL interactions play a major role for the functional outcome of NK cell alloreactivity. To show the relevance of KIR-KIRL mismatches in pediatric BCP-ALL, 7 donors that either exhibit a KIR-KIRL match or mismatch towards specific pediatric BCP-ALLs were chosen (Table 7). For detailed HLA and KIR-typing, see Suppl. Table 1 and Suppl. Table 2, phenotypical characterization of NKAES cells and blasts see Fig. 5, Suppl. Fig. 1 and Suppl. Fig. 2.

Table 7: KIR-KIRL constellations of selected NK cell donors and pediatric BCP-ALL samples. NK cell donors (SNK) and BCP-ALL patient samples (P) are anonymized by an internal code. Shown is the KIRL status, donor education of relevant iKIRs and educated KIRs specific for the missing KIRL of the target to identify the educated alloreactive subset towards the given BCP-ALL. The KIRL HLA-C1 is recognized by KIR2DL2/L3, HLA-C2 by KIR2DL1, HLA-Bw4 epitopes by KIR3DL1, HLA-A3 and HLA-A11 by KIR3DL2. For detailed HLA and KIR-typing of the respective donors and patient samples see Suppl. Table 1 and Suppl. Table 2. *the cell line NALM-16 has a near haploid genome. ** Note that this donor does not express KIR3DL1 on the RNA and protein level (Suppl. Fig. 1,Suppl. Table 2) (Kübler et al., 2014)[i].

		Donor education of iKIRs		**Educated KIRs specific for the missing KIRL in the target**		
Donor	**KIRL**	**Educated**	**Uneducated**	**P3B** ***Bw6/Bw6 C1/C1***	**P31G** ***A3/A3 Bw4/Bw6 C2/C2***	**Nalm-16** ***Bw4 C1****
SNK9A	**Bw6/Bw6 C1/C1**	2DL2, 2DL3	2DL1, 3DL1, 3DL2	/	2DL2, 2DL3	/
SNK10P	**Bw6/Bw6 C1/C1**	2DL2, 2DL3	2DL1, 3DL1, 3DL2	/	2DL2, 2DL3	/
SNK21BC	**A3 Bw6/Bw6 C1/C1**	2DL2, 2DL3, 3DL2	2DL1, 3DL1	3DL2	2DL2, 2DL3	3DL2
SNK13B	**ABw4 Bw4/Bw4 C2/C2**	2DL1, **	2DL2, 2DL3, 3DL2	2DL1, **	/	2DL1
SNK14B	**ABw4 Bw4/Bw4 C2/C2**	2DL1, 3DL1	2DL2, 2DL3, 3DL2	2DL1, 3DL1	/	2DL1
SNK15B	**Bw4/Bw4 C2/C2**	2DL1, 3DL1	2DL2, 2DL3, 3DL2	2DL1, 3DL1	/	2DL1
SNK20B	**A3 Bw4/Bw4 C2/C2**	2DL1, 3DL1, 3DL2	2DL2, 2DL3	2DL1, 3DL1, 3DL2	/	2DL1, 3DL2

4.2.1 KIR-KIRL mismatch constellations enhance cytotoxicity towards pediatric BCP-ALL *in vitro*

To evaluate the potential of the different NK cell donor groups with given KIR-KIRL constellations towards selected BCP-ALLs (Table 7), specific lysis of the primary pediatric BCP-ALL sample P3B relapse (Bw6/Bw6 C1/C1) and P31G (A3/A3 Bw4/Bw6 C2/C2) was determined. Bw6/Bw6 C1/C1 donors (SNK9A, SNK10P, SNK21BC) exhibit a KIR-KIRL match towards P3B relapse and a KIR-KIRL mismatch towards P31G. For Bw4/Bw4 C2/C2 donors (SNK13-15B) the constellation is vice versa (for detailed information see Table 7).

All donors are able to target the MHC-deficient K562 cell line to a similar extent, showing that the general cytotoxic potential of the NKAES cells is comparable (Fig. 8, left columns). In contrast, primary pediatric BCP-ALL samples are significantly better targeted by NKAES cells in the presence of a KIR-KIRL mismatch in comparison to the matched KIR-KIRL constellation (Fig. 8). The effect of KIR-KIRL mismatching is reversible within the same donor groups towards the two pediatric BCP-ALL samples (P3B relapse and P31G). Therefore it can be assumed that indeed KIR-KIRL interactions are relevant for increased alloreactivity of KIR-KIRL mismatched NK cells.

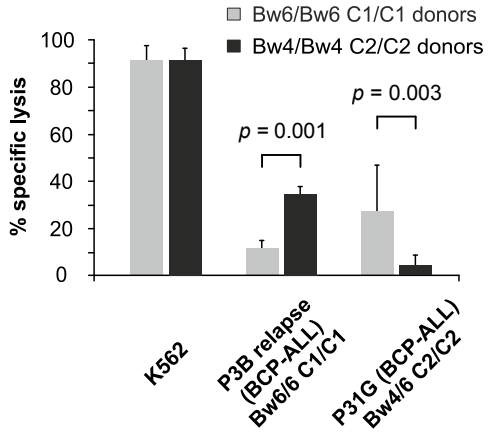

Fig. 8: KIR-KIRL constellations are relevant for the cytotoxic potential of NK cells towards pediatric BCP-ALL *in vitro*. *In vitro* cytotoxicity of KIR-KIRL matched or mismatched NKAES cells against primary pediatric BCP-ALL samples, the K562 cell line was included as positive control. Shown is the % specific lysis at an E:T ratio of 10:1. For more detailed information on KIR-KIRL constellations of Bw6/Bw6 C1/C1 donors (SNK9A, SNK10P, SNK21BC) and Bw4/Bw4 C2/C2 donors (SNK13-15B) see Table 7. For phenotypical characterization of blasts and NKAES cells see Suppl. Fig. 1A and Suppl. Fig. 2, for HLA type Suppl. Table 1 and KIR genotype Suppl. Table 2. Data represents two independent experiments performed in triplicates (Kübler et al., 2014)[i].

4.2.2 KIR-KIRL mismatched NKAES cells display superior *in vivo* cytotoxicity towards BCP-ALL

To examine the relevance of KIR-KIRL mismatches for a potential adoptive NK cell transfer therapy, naïve NSG mice were injected with a primary pediatric BCP-ALL sample (P3B relapse). Weekly injections of either KIR-KIRL matched (SNK10P) or mismatched (SNK13B) NKAES cells lead to a reduction of the leukemic burden in the peripheral blood of the mice (Fig. 9). The reduction is significant for KIR-KIRL mismatched NKAES cells but not for KIR-KIRL matched NKAES cells.

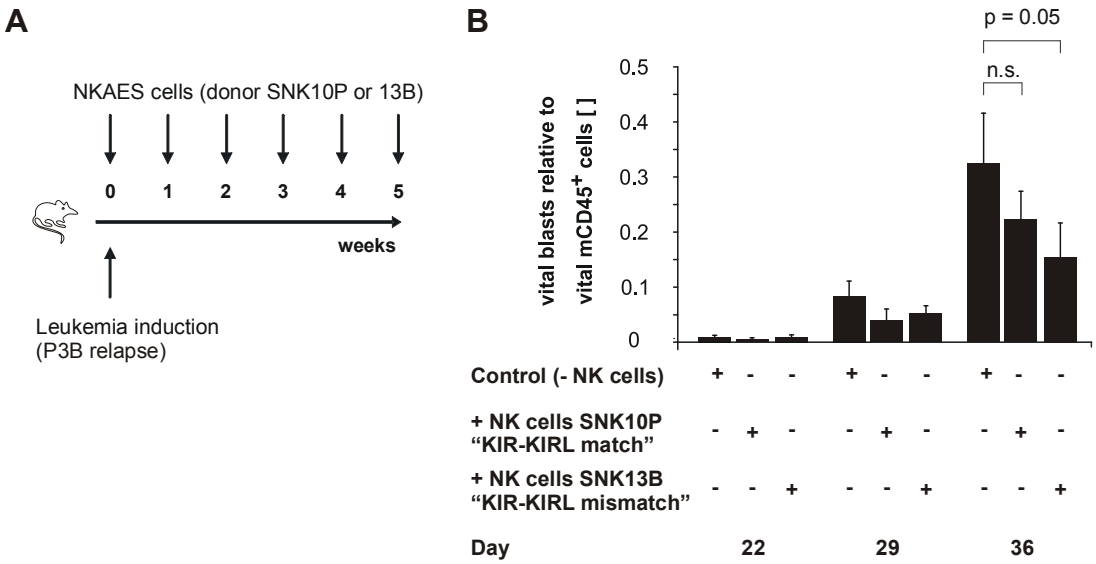

Fig. 9: KIR-KIRL mismatched NKAES cells display superior cytotoxicity towards pediatric BCP-ALL *in vivo*. (A) Experimental setting, briefly: NSG mice were injected with BCP-ALL cells (P3B relapse) followed by weekly injections of KIR-KIRL matched (SNK10P) or mismatched (SNK13B) NKAES cells. (B) Leukemic burden in the peripheral blood was determined by multicolor flow cytometry, shown is the number of vital blasts relative to vital mCD45$^+$ cells. Mice injected with KIR-KIRL mismatched NKAES cells display a significantly lower leukemic burden in vivo compared to untreated controls. For phenotypical characterization of blasts and NKAES cells see Suppl. Fig. 1A and Suppl. Fig. 2, for HLA-type Suppl. Table 1 and KIR genotype Suppl. Table 2. Data represents one experiment performed with 11 mice (Kübler et al., 2014)i.

4.2.3 Blockade of the KIR-KIRL axis

We next asked whether KIR blockade with a monoclonal antibody (IPH2102) would influence cytotoxicity against BCP-ALL. IPH2102 blocks inhibitory KIR2DL1 and KIR2DL2/L3 but also binds to activating KIR2DS1 and KIR2DS2 and has been shown to enhance cytotoxicity towards AML (Romagné et al., 2009). First, conditions for complete blockade were established and verified by flow-cytometric staining of CD158a/h/i (clone HP3E4, KIR2DL1/S1/S4), CD158b1/b2/j (clone GL183, KIR2DL2/L3/S2), and CD158e (clone DX9, KIR3DL1). When IPH2102 binds to the respective epitope, no staining with fluorescently labeled KIR antibodies is possible (Fig. 10). In line with published data (Romagné et al., 2009), IPH2102 blocks CD158a/h/i and CD158b1/b2/j, but not CD158e.

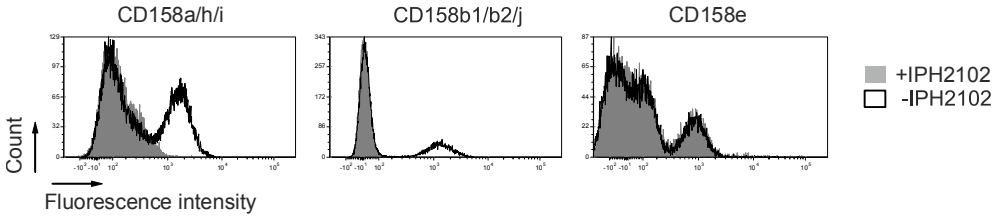

Fig. 10: CD158a/h/i and b1/b2/j are blocked by IPH2102. NKAES cells from 3 donors were incubated at 37 °C for 30 min with 30 µg/ml IPH2102 and with 15 µg/ml for another 5 h. Shown is the flow cytometric analysis of CD158a/h/i (clone HP3E4, KIR2DL1/S1/S4), CD158b1/b2/j (clone GL183, KIR2DL2/L3/S2) and CD158e (clone DX9, KIR3DL1) on CD56$^+$CD3- NK cells after IPH2102-treatment (grey, filled) or untreated (black line). Shown is one representative donor (SNK15B) out of 3.

4.2.3.1 KIR blocking mAb IPH2102 does not enhance GvL effects in huNSG mice which exhibit mainly KIR$^-$ NK cells

HuNSG mice reconstitute diverse human lymphoid and myeloid cells from engrafted human hematopoietic stem cells and are therefore a complex *in vivo* system to study NK cell biology. After sublethal irradiation of NSG mice, transplanted CD34$^+$ HSCs differentiate into the different hematopoietic lineages (Shultz et al., 2005; André et al., 2010). IL-7 and IL-15/IL15Rα supplementation allows the generation of 'pseudomature' lytic NK cells, poly (I:C) treatment one day before injection of a leukemic sample further enhances stimulation of NK cells. By multicolor flow cytometry leukemic cells and cells of the normal hematopoiesis can be discriminated and therefore quantification of the leukemic burden is possible. After having shown that KIR-KIRL mismatched constellations are relevant for adoptive NK cell transfer in BCP-ALL bearing NSG mice, humanized NSG mice were chosen to study the relevance of the KIR-KIRL axis in GvL effects upon HSCT. Treatment of huNSG mice with the KIR-blocking mAb IPH2102 should lead to enhanced NK cell-mediated cytotoxicity depending on the relevance of the KIR-KIRL axis in this setting.

The HSC donor SSC18U was selected as the donor is KIR2DL1$^+$ and KIR2DL3$^+$ and should therefore be able to sustain receptor-ligand interactions with the KIR ligands HLA-C1 and C2 of the primary pediatric BCP-ALL P23T. No activating KIR2DS1 or KIR2DS2 that could be blocked by IPH2102 are present in donor SSC18U (for phenotypical characterization of blasts see Suppl. Fig. 2, for HLA-type Suppl. Table 1 and KIR genotype Suppl. Table 2). Hence there are two iKIR-HLA-interactions with the primary pediatric BCP-ALL P23T that can potentially be blocked by IPH2102 (see also Table 8).

Table 8: KIR-KIRL constellations for the experiment depicted in Fig. 11. *Note that genomic expression of KIR2DL2 is absent in this donor.

	Donor education of iKIRs		**KIR2DS1, 2DS2 expression**	**iKIR-KIRL interaction blockable by IPH2102**
	Educated	**Uneducated**		**P23T**
				A24:02 Bw4/Bw4 C2/C1
SSC18U	2DL1, 2DL3, 3DL1, *	3DL2	/	2DL1, 2DL3

Despite obvious masking of KIR2DL1/S4 and KIR2DL3 on bone marrow- and spleen-residing NK cells (Fig. 11B + C), leukemic burden is comparable in the IPH2102-treated and non-treated group (Fig. 11D).

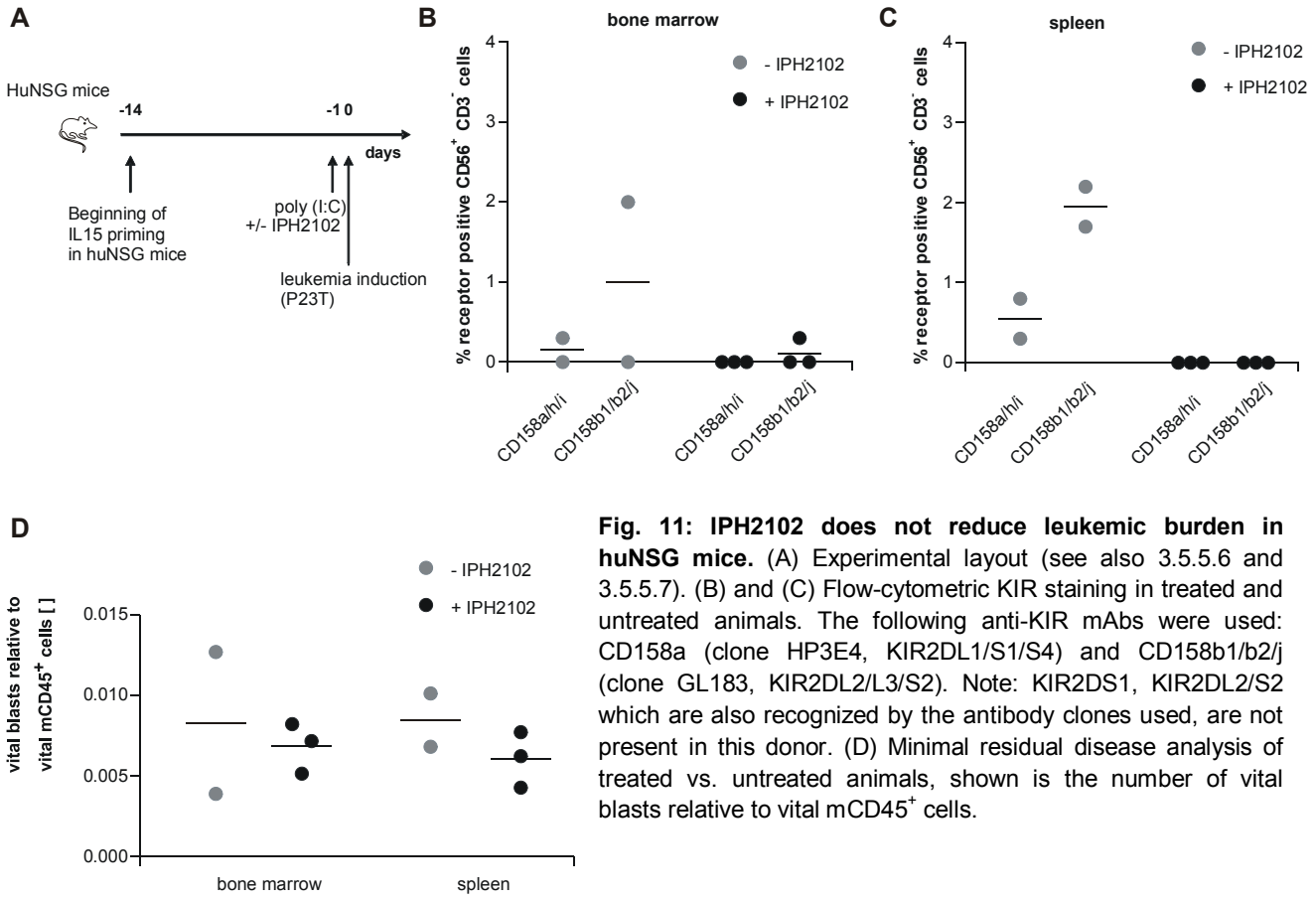

Fig. 11: IPH2102 does not reduce leukemic burden in huNSG mice. (A) Experimental layout (see also 3.5.5.6 and 3.5.5.7). (B) and (C) Flow-cytometric KIR staining in treated and untreated animals. The following anti-KIR mAbs were used: CD158a (clone HP3E4, KIR2DL1/S1/S4) and CD158b1/b2/j (clone GL183, KIR2DL2/L3/S2). Note: KIR2DS1, KIR2DL2/S2 which are also recognized by the antibody clones used, are not present in this donor. (D) Minimal residual disease analysis of treated vs. untreated animals, shown is the number of vital blasts relative to vital mCD45$^+$ cells.

In summary, the preliminary data shown here provides evidence that GvL effects in huNSG mice are not mainly modulated by the KIR-KIRL axis. The abundance of KIR-expressing NK cells is quite low despite of IL-15/IL-15Rα treatment (< 3%, see Fig. 11). In summary, the lack of substantial KIR expression makes the huNSG model unsuitable to investigate the relevance of KIR-KIRL interactions.

4.2.3.2 KIR$^+$ NKAES cells from KIR-KIRL matched donors display significantly enhanced cytotoxicity upon KIR blockade with IPH2102

In line with the data obtained in huNSG mice in the previous section (4.2.3.1) it can be assumed that the abundance of KIR$^+$ NK cells seems to be relevant for the overall effect of KIR blockade with IPH2102. Hence, a subset analysis of KIR$^+$ NK cells might elucidate to which extent cytotoxicity towards BCP-ALL can be modulated by the KIR-KIRL axis. For this purpose sorting of the KIR$^+$ and KIR$^-$ NKAES cell subsets was performed (anti-KIR mAbs used for sorting of KIR$^+$ NK cells: HP-3E4 for KIR2DL1/S1/S4, GL183 for KIR 2DL2/L3/S2, and DX9 for KIR3DL1).

In vitro cytotoxicity of sorted KIR$^+$ NKAES cells from KIR-KIRL matched donors SNK10P and SNK21BC is significantly enhanced in the presence of IPH2102 (Fig. 12). Cytotoxicity of KIR-KIRL mismatched donors is not changed (Fig. 12A) except for SNK14B, where detailed analysis of the respective donors shows a minor enhancement of cytotoxicity (Fig. 12B).

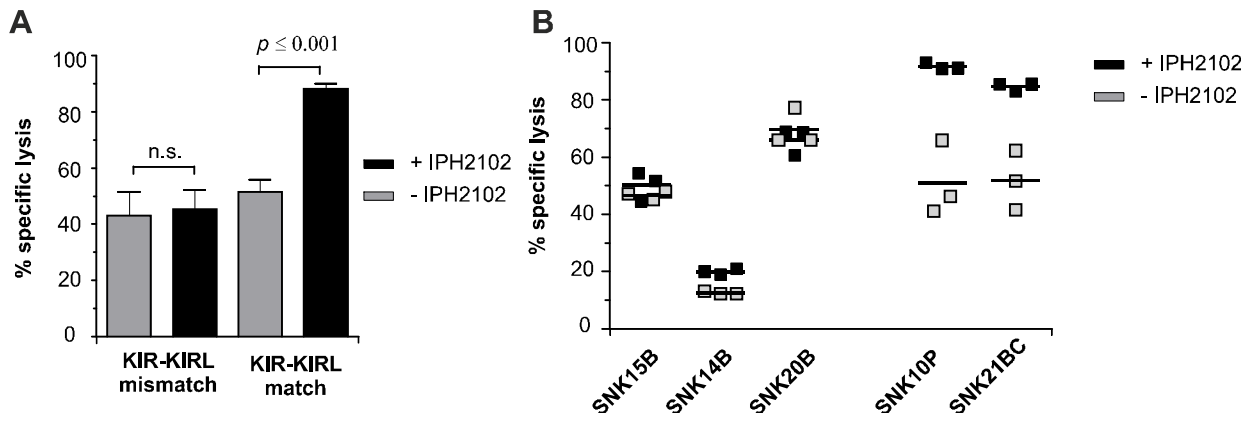

Fig. 12: KIR blocking mAb IPH2102 increases alloreactivity for KIR-KIRL matched donors against BCP-ALL. Specific lysis of the BCP-ALL cell line Nalm-16 after co-culture with sorted KIR$^+$ NKAES cells of the donors SNK14B, SNK15B, SNK20B (KIR-KIRL mismatch) and SNK10P, SNK21BC (KIR-KIRL match) was determined (E:T ratio 2:1) in the presence or absence of the KIR-blocking mAb IPH2102. (A) represents five independent experiments performed in triplicates which are itemized in (B)(Kübler et al., 2014)[ii].

Looking at the KIR-KIRL constellations (Table 9) IPH2102 leads to blockade of educated KIR2DL2/L3 in KIR-KIRL matched constellations and blockade of uneducated KIR2DL2/L3 in KIR-KIRL mismatched constellations. The missing enhancement of cytotoxicity for KIR-KIRL mismatched NK cells by IPH2102 could be explained if uneducated KIR2DL2 and KIR2DL3 are mainly expressed on NK cells that do not express any other self-recognizing inhibitory receptors.

To examine this hypothesis the subset distribution within the donor cells was analyzed. For this purpose NKG2A$^+$ and NKG2A$^-$ NK cells were discriminated and further subgated into KIR2DL2/L3/S2 single positive cells ('others$^-$') or cells co-expressing at least one of the following KIRs: KIR2DL1/S1/S4, KIR3DL1/S1 ('others$^+$'). For the respective NK cell phenotype, see also Suppl. Fig. 1B.

Indeed, the proportion of KIR2DL2/L3/S2$^+$ others$^-$ NK cells is quite high, especially in the NKG2A$^+$ NK cell subset (Fig. 13A). Taking the predominance of the KIR2DL2/L3/S2$^+$ others$^-$ NK cell population into account, the responsiveness of educated and uneducated KIR2DL2/L3/S2$^+$others$^-$ NK cells was analyzed. For this purpose co-culture experiments with K562 were performed. Note that the data shown in Fig. 13 and Fig. 16 were obtained from the same experiment by differing analysis of the primary data.

Table 9: KIR-KIRL constellations for the experiment depicted in Fig. 12. Note that IPH2102 binds to KIR2DL1-3 and KIR2DS1/2. See also supplemental tables.

KIR-KIRL status towards Nalm-16		Donor education of iKIRs		KIR2DS1, 2DS2 expression	possible KIR-KIRL interactions of NK cells with target
					Nalm-16
		Educated	Uneducated		*Bw4 C1*
KIR-KIRL match	**SNK10P**	2DL2, 2DL3	2DL1, 3DL1, 3DL2	/	2DL2, 2DL3, 3DL1
	SNK21BC	2DL2, 2DL3, 3DL2	2DL1, 3DL1	2DS2	2DL2, 2DL3, 3DL1, 2DS2

KIR-KIRL mismatch	**SNK14B**	2DL1, 3DL1	2DL2, 2DL3, 3DL2	2DS2	2DL2, 2DL3, 3DL1, 2DS2
	SNK15B	2DL1, 3DL1	2DL2, 2DL3, 3DL2	/	2DL2, 2DL3, 3DL1
	SNK20B	2DL1, 3DL1, 3DL2	2DL2, 2DL3	2DS2	2DL2, 2DL3, 3DL1, 2DS2

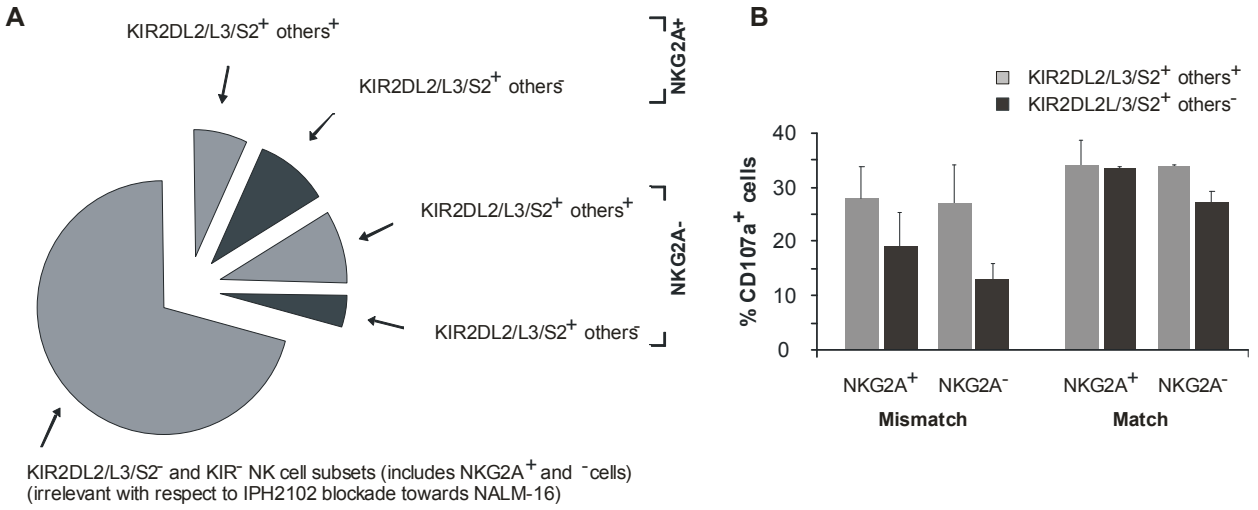

Fig. 13: The KIR2DL2/L3/S2$^+$others$^-$ NK cell subset is predominant in KIR-KIRL mismatched donors and exhibits a low degranulation capacity in response to K562. (A) Shown is the NK cell subset composition with % subset size of KIR2DL2/L3/S2 single positive NKAES cells ('others$^-$') and NKAES cells co-expressing at least one of the following KIRs: KIR2DL1/S1/S4, KIR3DL1/S1 ('others$^+$') in the NKG2A$^+$ and $^-$ subset of KIR-KIRL mismatched C2/C2 donors (B) Shown is the degranulation capacity (% CD107a$^+$ cells after baseline correction) of NK cell subsets shown in (A). In contrast to KIR-KIRL matched donors, the KIR2DL2/L3/S2$^+$others$^-$ NK cell subset degranulates poorly in response to K562 in KIR-KIRL mismatched C2/C2 donors, even in the presence of NKG2A.

Co-culture experiments with K562 show that uneducated NKG2A$^-$ KIR2DL2/L3/S2$^+$ others$^-$ NKAES cells from KIR-KIRL mismatched donors indeed display a remarkably lower degranulation capacity (Fig. 13B) compared to educated NKG2A$^-$ KIR2DL2/L3/S2$^+$ others$^+$. This effect is also present in the respective NKG2A$^+$ subsets. Donors with KIR-KIRL matched constellations do not show major differences in responsiveness of the educated NKG2A$^{+/-}$ KIR2DL2/L3/S2$^+$ others$^-$ and educated NKG2A$^{+/-}$ KIR2DL2/L3/S2$^+$ others$^+$ NK cell subsets.

In summary, KIR blockade by mAb IPH2102 increases cytotoxicitiy of the KIR+ NK cell subset from KIR-KIRL matched but not from KIR-KIRL mismatched NK cell donors towards BCP-ALL. In KIR-KIRL mismatched donors the uneducated hyporesponsive KIR2DL2/L3/S2 single positive NK cell subset is dominant.

4.2.4 Subset analyses reveal functional differences between KIR-KIRL matched and mismatched NK cells

4.2.4.1 The KIR$^+$ subset of KIR-KIRL mismatched donors exerts higher cytotoxicity compared to KIR- NK cells

To further dissect the relevance of KIR-KIRL constellations towards pediatric BCP-ALL, KIR$^+$ and KIR$^-$ subsets of the 7 donors either exhibiting a KIR-KIRL mismatch or match (see also Table 7) towards the BCP-ALL cell line Nalm-16 were sorted. The KIR$^+$ subset includes NKAES cells expressing at least one of the following KIRs: KIR2DL1/S1/S4 (detected by clone HP-3E4), KIR2DL2/L3/S2 (detected by clone GL183) or KIR3DL1 (detected by clone DX9); the KIR$^-$ subset does not express any of the mentioned KIRs. All KIR$^+$ and KIR$^-$ subsets exert comparable cytotoxicity towards the HLA class I-negative K562 cell line (Fig. 14A, triangles), showing that there is no generally lower responsiveness of KIR$^+$ compared to KIR$^-$ NK cells of the different donors. With respect to the HLA-expressing Nalm-16 cell line the KIR$^+$ subset within the KIR-KIRL mismatched donor group displays a clearly superior cytotoxic potential compared to the corresponding KIR$^-$ subset (Fig. 14A). Interestingly, for KIR-KIRL matched NKAES cells the situation is reversed. This effect becomes even more evident upon normalization (Fig. 14B). Lysis of K562 was included as control for overall cytotoxicity (Fig. 14A and B right side).

Despite this clear superiority of KIR$^+$ cells in KIR-KIRL mismatched donors on specific lysis, no such significant effects are observed in cytokine secretion (IFN-γ, TNF), degranulation or perforin levels upon co-culture experiments with Nalm-16 (Fig. 15, data provided by J. Woiterski, see also Kübler et al., 2014).

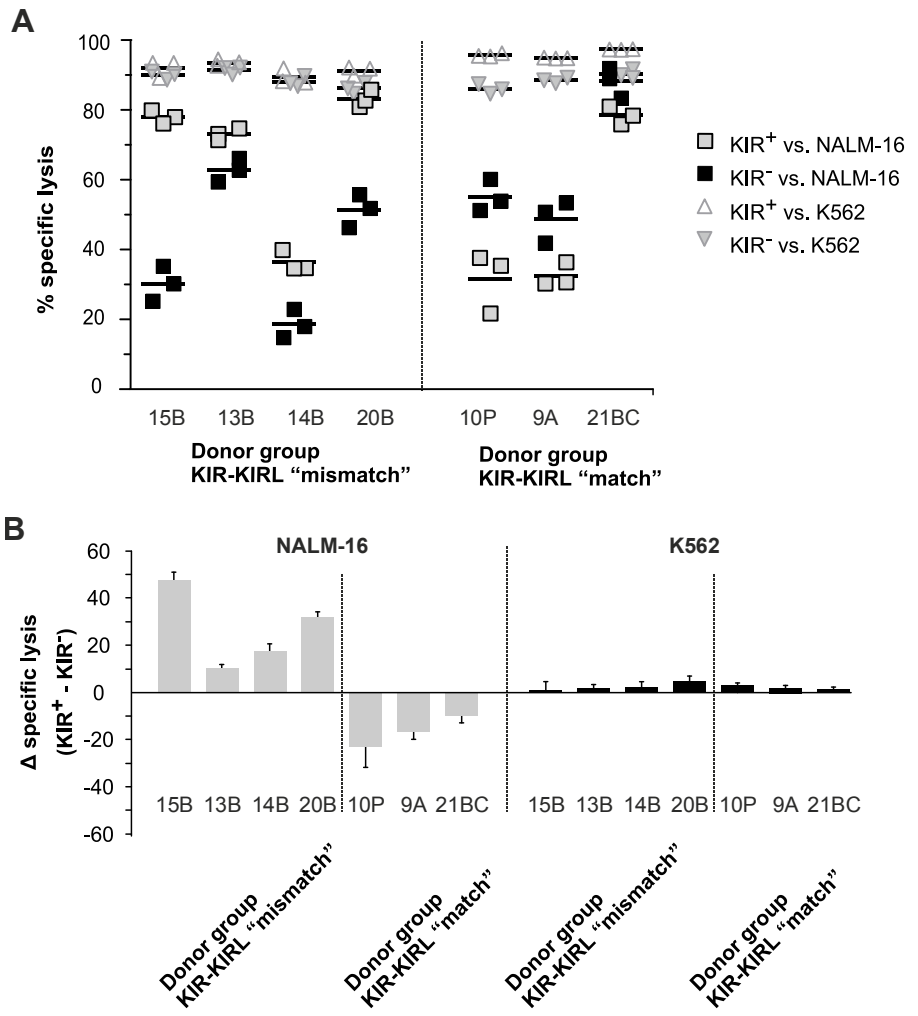

Fig. 14: Sorted KIR$^+$ NK cells of KIR-KIRL mismatched donors but not from KIR-KIRL matched donors display higher cytotoxicity towards pediatric BCP-ALL compared to the corresponding KIR$^-$ subset. (A) Specific lysis of sorted KIR$^+$ and KIR$^-$ NK cells of donors either exhibiting a KIR-KIRL match or mismatch towards Nalm-16 (characterized in Table 7) was determined after co-culture with NALM-16 or K562 cells as a control (E:T ratio 5:1). (B) Data from (A) standardized to the KIR$^-$ subset. Shown is the percentage of specific lysis of the sorted KIR$^+$ subset minus percentage of specific lysis of the sorted KIR$^-$ subset. Data was obtained during six independent experiments performed in triplicates (Kübler et al., 2014)[i].

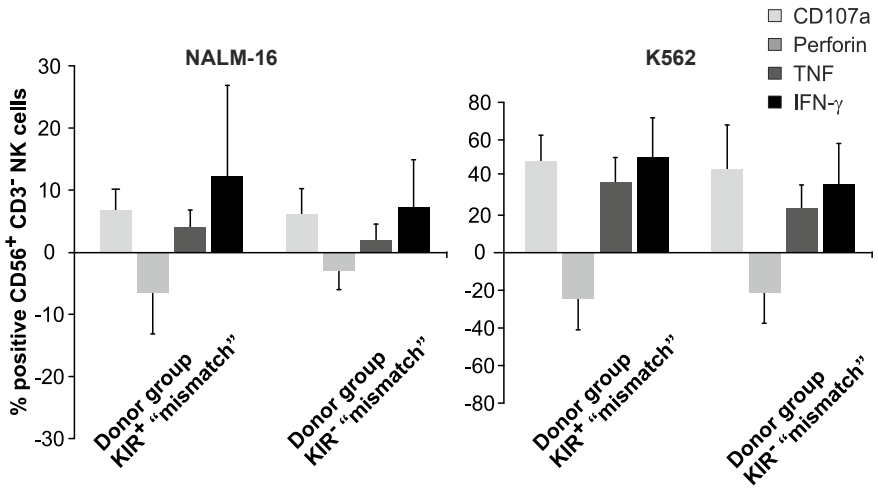

Fig. 15: KIR-KIRL mismatched constellations change the ability for degranulation and cytokine synthesis of KIR$^+$ compared to KIR$^-$ NK cells towards pediatric BCP-ALL. Shown is the degranulation and cytokine synthesis of sorted KIR$^+$ and KIR$^-$ NKAES cells of the donors SNK13-15B and SNK20B (KIR-KIRL mismatch) in response to Nalm-16 (BCP-ALL) or K562 cells (control). The percentages of the respective CD107a, Perforin, TNF and IFN-γ positive populations are normalized to the respective baseline levels of NKAES cells cultured in medium only. Note the different scale of K562 cells which evoke a distinctly higher response. The decline of intracellular perforin was validated to go along with an extracellular release in perforin (measured by ELISA, data not shown) (Kübler et al., 2014)[i].

4.2.4.2 The 'alloreactive' subset of KIR-KIRL mismatched NK cells exhibits a higher degranulation capacity compared to KIR-KIRL matched NK cells

To pinpoint differences in responsiveness within the KIR^+ subsets of KIR-KIRL matched or mismatched donors, an antibody panel that allows assessment of the degranulation potential of KIR^+ 'alloreactive', KIR^+ 'non-alloreactive', and KIR^- cells was designed. According to the literature, the 'alloreactive' subset includes NK cells expressing receptors permissive for target cell lysis (aKIRs and iKIRs that do not find a ligand on the respective target cell). The 'non-alloreactive' subset contains NK cells expressing NKG2A or iKIRs specific for ligands expressed on the target cell (Pende et al., 2005; see also section 1.2.4). Since the expansion protocol highly activates NK cells and leads to expansion of the $NKG2A^+$ subset also 'alloreactive' $NKG2A^+$ cells were considered (for the respective NK cell phenotype see also Suppl. Fig. 1B). The gating strategy is shown in Fig. 16A, exemplary original histogram data in (B) with Nalm-16 as target cells and (C) with K562 as control target.

NK cells expressing KIR2DL1/S1/S4 and/or KIR3DS1 (y-axis) but not KIR2DL2/L3/S2 or KIR3DL1 (x-axis) were assumed to be 'alloreactive' towards Nalm-16 (KIRL Bw4/C1), and indeed, the degranulation capacity of KIR-KIRL mismatched donors upon co-culture is significantly increased compared to the 'non-alloreactive' subset (expresses at least one of the following: KIR2DL2/L3/S2 or KIR3DL1), Fig. 16D. In contrast, 'alloreactive' KIR-KIRL matched donors do not display enhanced degranulation capacity; 'alloreactive' and 'non-alloreactive' NK cells show a similar percentage of $CD107a^+$ cells. This difference can even be seen in $NKG2A^+$ cells (Fig. 16D, right part).

In summary, the superior alloreactivity towards BCP-ALL of KIR-KIRL mismatched compared to KIR-KIRL matched NKAES cells can be attributed to the KIR^+ 'alloreactive' subset.

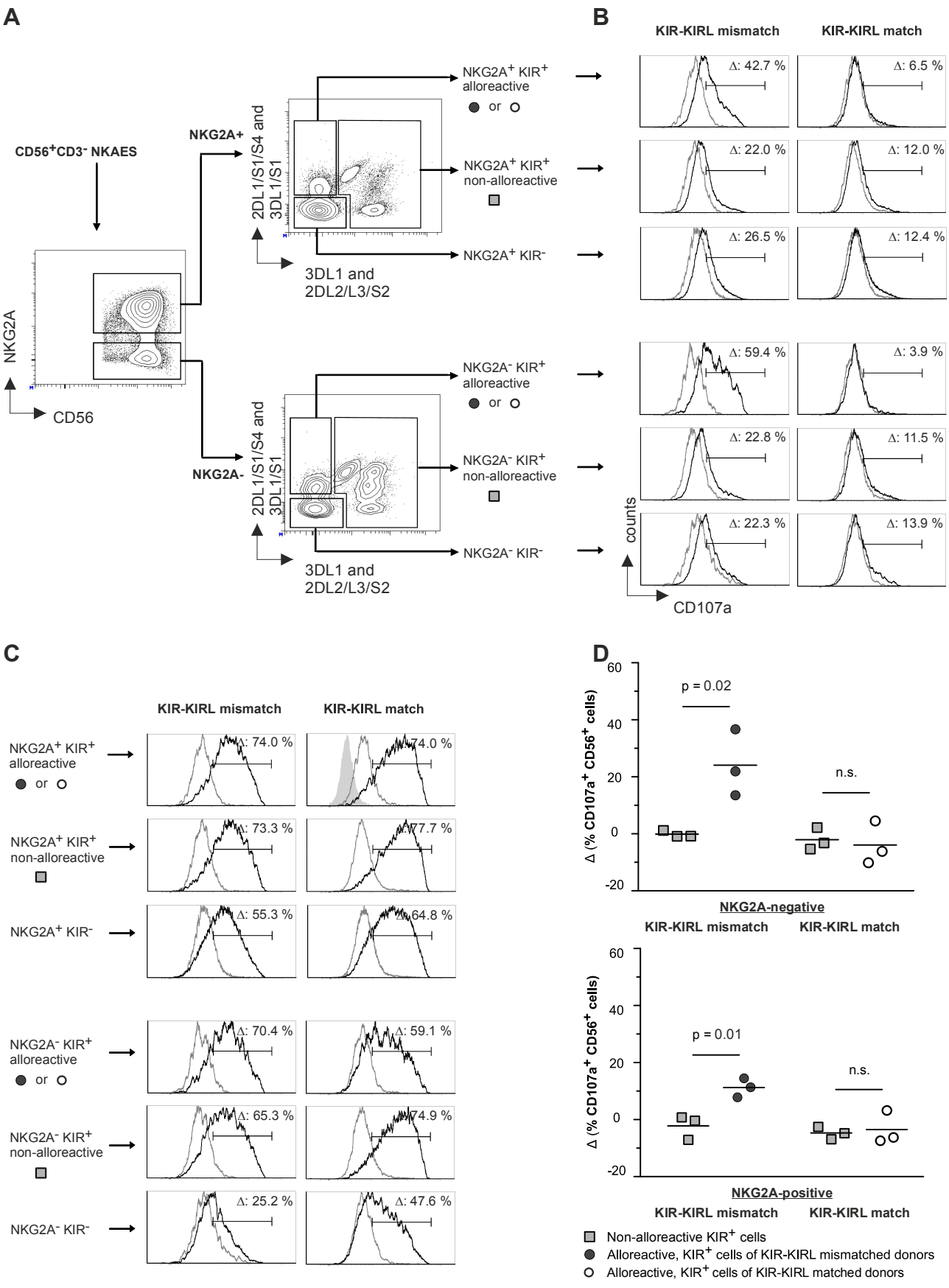

Fig. 16: NK cell subset analysis shows differences in the degranulation capacity of NK cells from KIR-KIRL mismatched and matched donors. NKAES cells from 6 donors either exhibiting a KIR-KIRL mismatch (SNK14B, 15B, 20B) or KIR-KIRL match (SNK9A, SNK10P, SNK21BC) towards Nalm-16 were co-cultured with Nalm-16 or K562 to determine the degranulation capacity of the alloreactive, non-alloreactive and KIR- subset. (A) Exemplified gating strategy for donor SNK15B. The theoretical alloreactive subset towards Nalm-16 (Bw4/C1) includes NK cells expressing

KIR2DL1/S1/S4 and/or KIR3DS1 (y-axis) but not KIR2DL2/L3/S2 or KIR3DL1 (x-axis) (upper left quadrant), whereas the non-alloreactive subset expresses at least one of the following: KIR2DL2/L3/S2 or KIR3DL1 (the combination of clone Z27.3.7 for KIR3DL1/S1 and Dx9 for KIR3DL1 allows identification of the KIR3DL1$^-$3DS1$^+$ subset). (B) + (C) Exemplified CD107a histogram data from SNK15B (KIR-KIRL mismatch) or SNK10P (KIR-KIRL match) of the respective subsets gated according to (A). NKAES cells were either cultured with Nalm-16 (black, open) as shown in (B) or with K562 as control as shown in (C). NKAES cell-only cultures (grey, open) are always included as reference population. The upper right pictogram in (C) (grey, filled) shows the respective isotype control. ΔCD107a is given (% CD107a$^+$ cells in NKAES-tumor co-cultures minus % CD107a$^+$ cells in NKAES cell-only cultures) in each histogram. (D) Pooled data of the degranulation capacity of KIR-KIRL mismatched (SNK14B, SNK15B and SNK20B) or KIR-KIRL matched donors (SNK9A, SNK10P and SNK21BC). Data is normalized to the corresponding KIR$^-$ cells by subtracting the % CD107a$^+$ of the KIR$^-$ population. Symbols: KIR$^+$ alloreactive subset in KIR-KIRL mismatched donors: ●, KIR$^+$ alloreactive subset in KIR-KIRL matched donors: ○, KIR$^+$ non-alloreactive NK cell subset: ■. Data represents one experiment performed with the 6 indicated donors (Kübler et al., 2014)[i].

4.3 Effects of the Dnmt-inhibitor 5-azacytidine on NK cells

The methyltransferase inhibitor 5-Azacytidine is clinically used for treatment of MDS, CMML and AML. At higher doses, direct cytotoxicity e.g., mediated by incorporation into RNA is predominant, whereas lower doses mainly induce DNA hypomethylation by inhibition of Dnmts. Since the KIR-locus has been described to be regulated by direct DNA methylation (Santourlidis et al., 2002), we wanted to use 5-AzaC to modulate NK cell reactivity towards BCP-ALL. Analyses of mature NK cells *in vitro* suggest that 5-AzaC might lead to increased KIR-expression on NK cells also in patients (Gao et al., 2009). But detailed subset analyses or effects on aKIRs have not yet been considered. Furthermore, it is not clear how 5-AzaC affects NK cells and NK cell precursors *in vivo* in a more complex setting including e.g., effects on bystander cells. To tackle these points, *in vitro* subset analyses and complex *in vivo* analyses in huNSG mice were performed.

4.3.1 Modulating KIR expression *in vitro*

For *in vitro* experiments a dose of 1 µM for 7 days was chosen. Doses ≥ 5 µM displayed an anti-proliferative effect on hepatoma cell lines (Venturelli et al., 2007), in neuroblastoma cell lines proliferation was inhibited with an ID_{50} of 10 µM while 4 µM induced demethylation-dependent gene expression (Yang et al., 2010). In NK cells 1 µM 5-AzaC did not affect NK cell viability, but induced KIR expression (Gao et al., 2009). Chan and colleagues applied 1 µM 5-AzaC for 60 h to induce KIR expression in NK cells (Chan et al., 2003). So, the chosen concentration of 1 µM for 7 days in the presence of cytokines should ensure enough cell divisions for passive demethylation without significant decrease in NK cell viability.

4.3.1.1 5-AzaC leads to significantly increased KIR expression but also regulates other NK cell receptors

To establish a suitable *in vitro* model system for analysis of 5-AzaC effects on mature NK cells, 5-AzaC was added to the culture medium at a concentration of 1 µM from d7 until d14 of the NKAES cell expansion protocol. Flow-cytometric analysis of common KIRs (CD158a: KIR2DL1/S1/S4, CD158b1/b2/j:

KIR2DL2/L3/S2, CD158e: KIR3DL1) shows that 5-AzaC leads to an increased abundance of KIR^+ NKAES cells (Fig. 17).

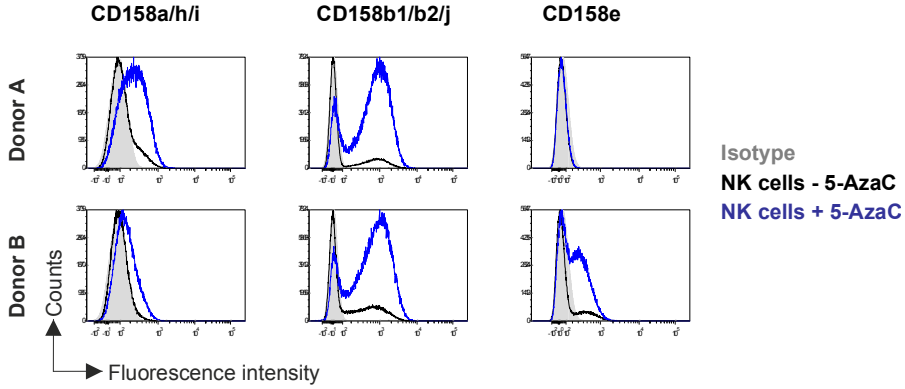

Fig. 17: KIR expression is upregulated by 5-AzaC treatment *in vitro*. NK cells were either treated with 1 µM 5-AzaC from d7-d14 of the NKAES cell expansion protocol (see methods section) or expanded in the absence of 5-AzaC. Shown is the flow cytometric analysis of CD158a/h/i (KIR2DL1/S1/S4, clone HP-3E4), b1/b2/j (KIR2DL2/L3/S2, clone GL183) and e (KIR3DL1, clone DX9) of two donors with different KIR genotypes.

With respect to common KIR expression, the number of receptor-positive cells is significantly increased compared to untreated control NKAES cells (Fig. 18A) without major changes in the median fluorescence intensity (Fig. 18B). Varied expression of common NK cell receptors can also be observed for NKp44 and NKG2D (Fig. 18). The percentage of NKG2A expressing cells is not changed (Fig. 18A) but the decreased median fluorescence intensity shows an approximately halved receptor expression (Fig. 18B).

In summary, 5-AzaC indeed induces KIR expression on NKAES cells at the applied treatment regimen but furthermore induces NKp44 expression and reduces NKG2D expression.

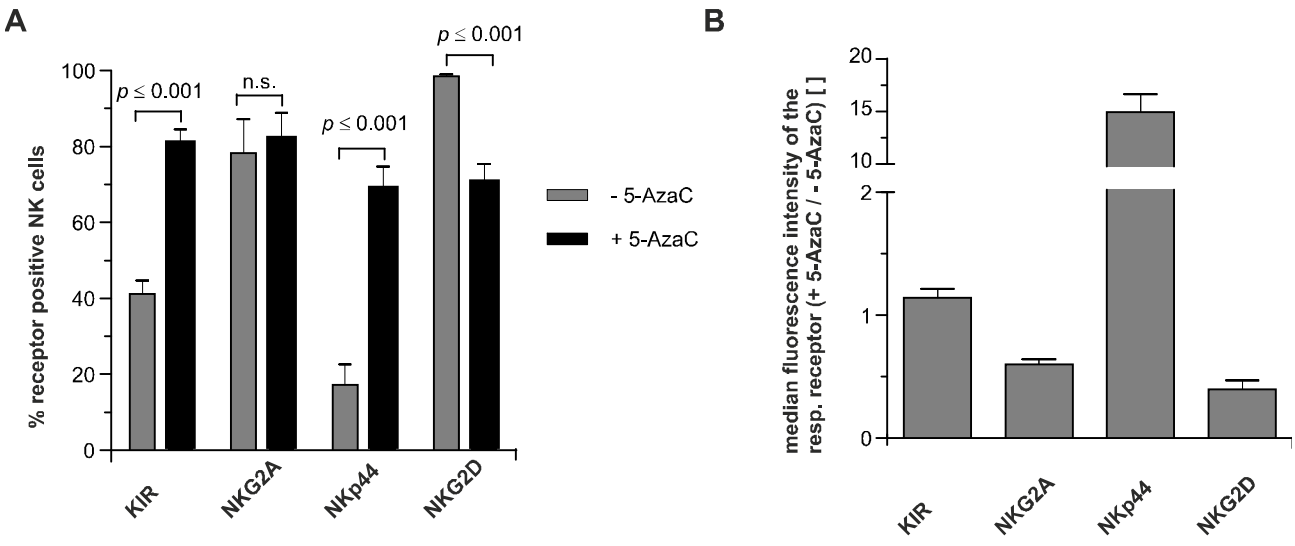

Fig. 18: The number of KIR and NKp44 expressing cells is increased by 5-AzaC whereas the percentage of NKG2D expressing cells and expression level are decreased *in vitro*. NKAES cells were treated with 1 µM 5-AzaC as described in 3.1.4.5. (A) Percentage of KIR, NKG2A, NKp44 or NKG2D positive NK cells is shown as determined by flow cytometry. (B) Median fluorescence intensity of the respective receptor expression of 5-AzaC treated cells was divided by the median of untreated cells to yield an x-fold regulation value. (n = 5 donors, statistics: Student's paired t-test with two-tailed distribution)

4.3.1.2 Upon 5-AzaC treatment, KIR expression is increased on NKG2A$^+$ but not on NKG2A$^-$ cells

As mentioned before, the overall percentage of NKG2A-expressing NKAES cells is not changed upon 5-AzaC treatment on total NKAES cells. But a subset analysis regarding NKG2A KIR double-positive NKAES cells shows that the KIR$^+$NKG2A$^+$ subset is significantly increased but not the KIR$^+$NKG2A$^-$ subset (Fig. 19). As shown in Fig. 19, the data suggests that KIRs are upregulated on NKG2A$^+$ but not on NKG2A$^-$ NK cells.

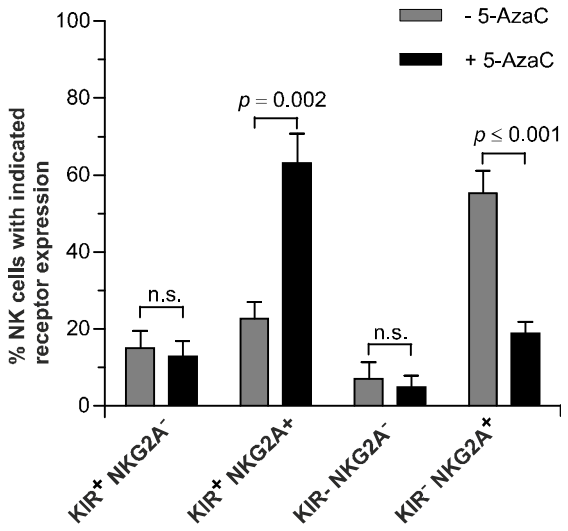

Fig. 19: The abundance of KIR$^+$ NKG2A$^+$ NKAES cells but not KIR$^+$ NKG2A- NKAES cells is increased. NKAES cells were treated with 1 µM 5-AzaC as described earlier. Shown is the percentage of NKAES cells with or without expression of KIR and/or NKG2A as indicated. (n = 5 donors)

4.3.1.3 5-AzaC changes the KIR-expressing NK cell subset distribution with preference for CD158b1/b2/j (co-) expression

Besides the differential effects of 5-AzaC on NKG2A$^{+/-}$ NK cells, the question is whether 5-AzaC also differentially regulates different KIRs or combinations of KIRs. Since many individuals do not express CD158e, 4 donors without CD158e expression and 3 donors expressing CD158e were considered separately (Fig. 20A or B respectively). Looking at CD158a/h/i, b1/b2/j and e, only the total expression of CD158b1/b2/j is significantly increased upon treatment (Fig. 20). Combinatorial subset analysis reveals that besides CD158a/h/i and b1/b2/j double-positive NKAES cells interestingly only the number of CD158b1/b2/j single positive, not of CD158a/h/i single positive NKAES cells is increased (Fig. 20A). This suggests that CD158b1/b2/j is preferentially upregulated on CD158a/h/i single positive cells upon 5-AzaC treatment as well as on KIR$^-$ NK cells. Looking at CD158e$^+$ donors, the number of CD158b1/b2/j-expressing NKAES cells in total is significantly increased in contrast to CD158a/h/i and e expressing cells (Fig. 20B). But the effects on subsets are not significant in this preliminary data and an analysis of more donors might confirm the preference for CD158b1/b2/j co-expression also for CD158e$^+$ individuals.

In summary, the effect of 5-AzaC differentially affects the different KIR expressing subsets with a preference for CD158b1/b2/j (co-)expression.

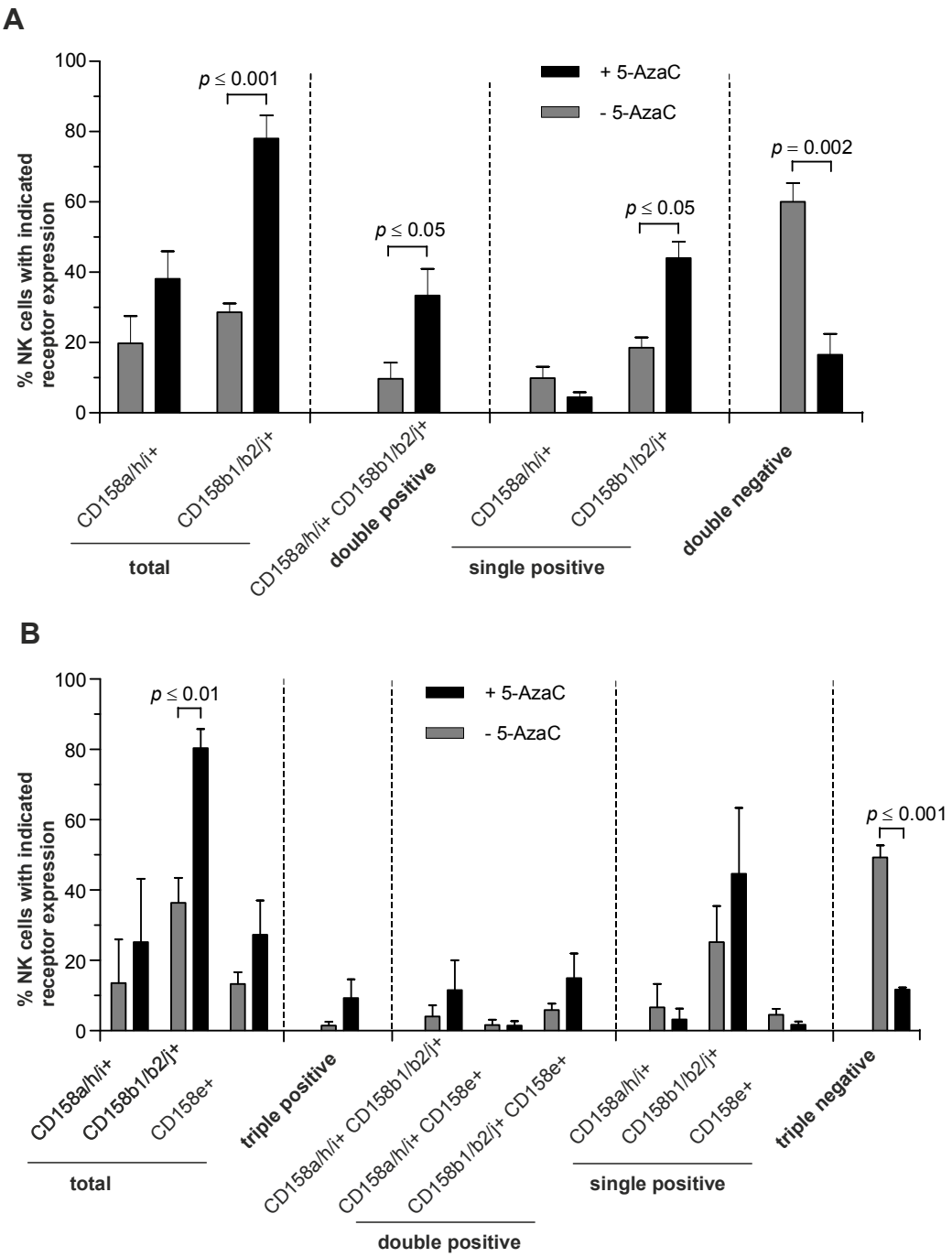

Fig. 20: Increases in KIR expression upon 5-AzaC treatment are not randomly distributed among subsets. NK cells were either treated with 1 µM 5-AzaC from d7-d14 of the NKAES cell expansion protocol or expanded without 5-AzaC treatment. Shown is the flow cytometric analysis of CD158a/h/i, b and e in combinatorial analyzes, where 'total' means the overall percentage of positive cells, 'double' or 'single' positive: exclusive expression of the mentioned KIRs. (A) $CD158e^-$ donors (n = 4 donors) (B) $CD158e^+$ donors (n = 3 donors).

4.3.1.4 aKIR expression is increased upon 5-AzaC treatment of NK cells in vitro

Since only a limited number of KIR-recognizing monoclonal antibodies are available, analysis of more detailed subset distributions is restricted. But KIR-Q-PCR allows analysis of single specific KIRs.

As shown in Fig. 21, not only the expression of iKIRs but also aKIRs is clearly increased upon 5-AzaC treatment *in vitro*.

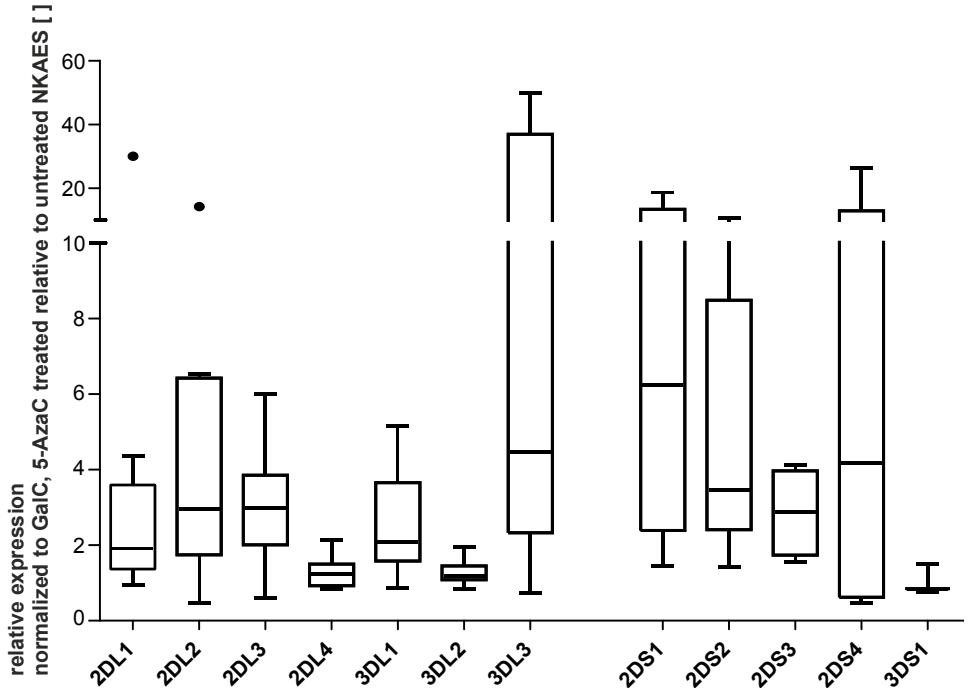

Fig. 21: 5-AzaC increases mRNA expression not only of iKIRs, but also aKIRs. Shown is the relative mRNA expression (5-AzaC treated relative to untreated NKAES cells), normalized to *GALC* in a Box-Whisker-Tukey plot (n = 12 donors)

4.3.1.5 In vitro 5-AzaC treatment of mature NKAES cells decreases cytotoxicity

5-AzaC also increases the expression of aKIRs (see Fig. 21) which in turn might influence cytotoxicity dependent on the KIR-KIRL constellation. In a KIR-KIRL mismatched constellation the increased expression of iKIRs that cannot find a ligand on the target cell should not lead to decreased cytotoxicity. Under these circumstances the increased expression of aKIRs might positively influence the cytotoxic capacity.

For this purpose, KIR2DL1$^+$ SNK13B NKAES cells and K562, Nalm-16, and Kasumi-1 cells were chosen as target cells that do not express the KIR2DL1 ligand HLA-C2. KIR2DL2 and KIR2DL3 are not subject to education in SNK13B and were therefore assumed to be of minor impact. Furthermore, an activating KIR2DS2 interaction of SNK13B NKAES cells with Nalm-1 and Kasumi-1 target cells should be possible (Table 10).

Table 10: KIR-KIRL constellations relevant for Fig. 22.

	Donor education of iKIRs		KIR2DS1, 2DS2 expression	possible KIR-KIRL interactions of NK cells with respective target		
				K562	Nalm-16	Kasumi-1
	Educated	Uneducated		HLA class I-negative	Bw4 C1	Bw6/Bw6 C1/C1
SNK13B	2DL1, **	2DL2, 2DL3, 3DL2	2DS1, 2DS2	/	2DL2, 2DL3, 2DS2	2DL2, 2DL3, 2DS2

Despite these selected constellations cytotoxicity towards the pediatric BCP-ALL cell line Nalm-16 and the pediatric AML cell line Kasumi-1 is decreased (Fig. 22). Cytotoxicity against the HLA class I-deficient K562 cell line also shows decreased cytotoxicity even though no HLA class I-determined KIRL is present.

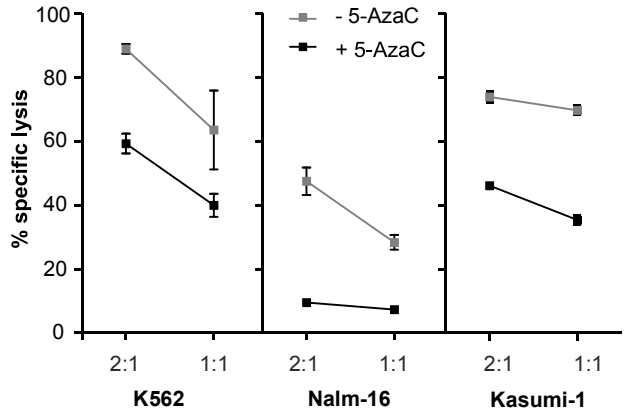

Fig. 22: 5-AzaC treatment of NKAES cells *in vitro* dampens cytotoxicity. Specific lysis upon co-culture of SNK13B NKAES cells and diverse cell lines: K562 (CML), Nalm-16 (ped. BCP-ALL) or Kasumi-1 (ped. AML). Shown is one selected experiment performed in triplicates.

To conclude independent of the individual KIR-KIRL constellation cytotoxicity is reduced in 5-AzaC-treated NKAES cells indicating that phenomena other than KIR induction might have led to the decreased cytotoxic potential.

4.3.2 Low-dose 5-AzaC treatment of huNSG mice increases GvL effects towards pediatric BCP-ALL *in vivo*

5-AzaC treatment *in vitro* shows effects on isolated mature NK cells but does not reflect the very complex situation in a patient where bystander cells but also immature or resting NK cells are present. After HSCT humans first reconstitute a large pool of immature NK cells (Nguyen et al., 2005; Vago et al., 2008). KIR expression is a late event in NK cell development (Miller and McCullar, 2001). Also in the NSG xenotransplantation model established in our laboratory (André et al., 2010) only few NK cells express KIRs despite of IL-15/IL-15Rα supplementation (André et al., unpublished data, and Fig. 11). However, IL-15/IL-15Rα supplementation and poly (I:C) administration in huNSG mice induces functionality of graft-emerging

KIR$^-$ NK cells, probably by the generation of 'pseudomature lytic NK cells' (Colucci et al., 2003) enabling the study of GvL effects *in vivo*. We therefore chose this model as surrogate for the early post-transplantation period of patients. To test whether the effect of 5-AzaC is restricted to the modulation of KIR expression on mature NK cells the effect of 5-AzaC in huNSG mice was assessed.

4.3.2.1 Administration of 5-AzaC in the early post-transplantation period increases NK cell precursor subsets and reduces the leukemic burden in huNSG mice

To investigate epigenetic modulation of KIR$^-$ NK cell precursors, huNSG mice and non-humanized control mice were treated with a low dose of 5-AzaC at an early time after HSC transplantation (experimental outline Fig. 23A). The dose of 1 mg/kg was chosen and administered i.p. twice a week for four weeks. For mice with an average weight of 25 g this results in a single dose of 25 µg and a cumulative dose of 200 µg within 4 weeks. This is in a range that has been investigated in mouse experiments in other contexts (1 mg/kg daily for 12 days in a mouse hepatoma model, cumulative dose of 300 µg (Venturelli et al., 2007), 1 and 10 mg/kg twice a week, 5 times in total in a synovial sarcoma mouse model, cumulative dose 125-1250 µg (Numoto et al., 2010), 150 µg per mouse were administered twice on day 4 and 11 in a mesothelioma xenograft model, cumulative dose 300 µg; Takenouchi et al., 2011). Furthermore, it was described that a dose of 1 mg/kg *in vivo* corresponds to a concentration in the range of 0.1-0.5 µM *in vitro* and yielded best results in terms of survival and GvHD prophylaxis in a GvHD mouse model (Sánchez-Abarca et al., 2009). Taking this into account, the chosen administration regimen should lead to a low *in vivo* dose of 5-AzaC in huNSG experiments. Thereby direct cytotoxic effects should be kept low. The long administration time in combination with cytokine support should additionally enable a sufficient number of cell divisions for epigenetic effects.

5-AzaC treatment was stopped 3 days before injection of a primary BCP-ALL sample. Due to the very short half-life of 5-AzaC (less than 4 h, Troetel et al., 1972) a direct effect of the substance on leukemic cells was assumed to be negligible. To confirm that a direct effect can indeed be neglected, non-humanized but 5-AzaC-treated control animals were included in the experiment. Despite the low-dose 5-AzaC induces a statistically not significant reduction of both human and murine CD45$^+$ cells in the bone marrow (Fig. 23B, C). Using a pre-defined blast-specific antibody panel, flow cytometric quantification of the leukemic burden in the bone marrow was performed (exemplary gating shown in Suppl. Fig. 3). Surprisingly, and in contrast to *in vitro* experiments with expanded mature NK cells, the leukemic burden is significantly decreased in 5-AzaC-treated huNSG mice compared to untreated control huNSG mice (Fig. 23D, F). This effect cannot be observed in non-humanized control mice (Fig. 23E, F) excluding a substantial direct cytotoxic effect of 5-AzaC on leukemic cells.

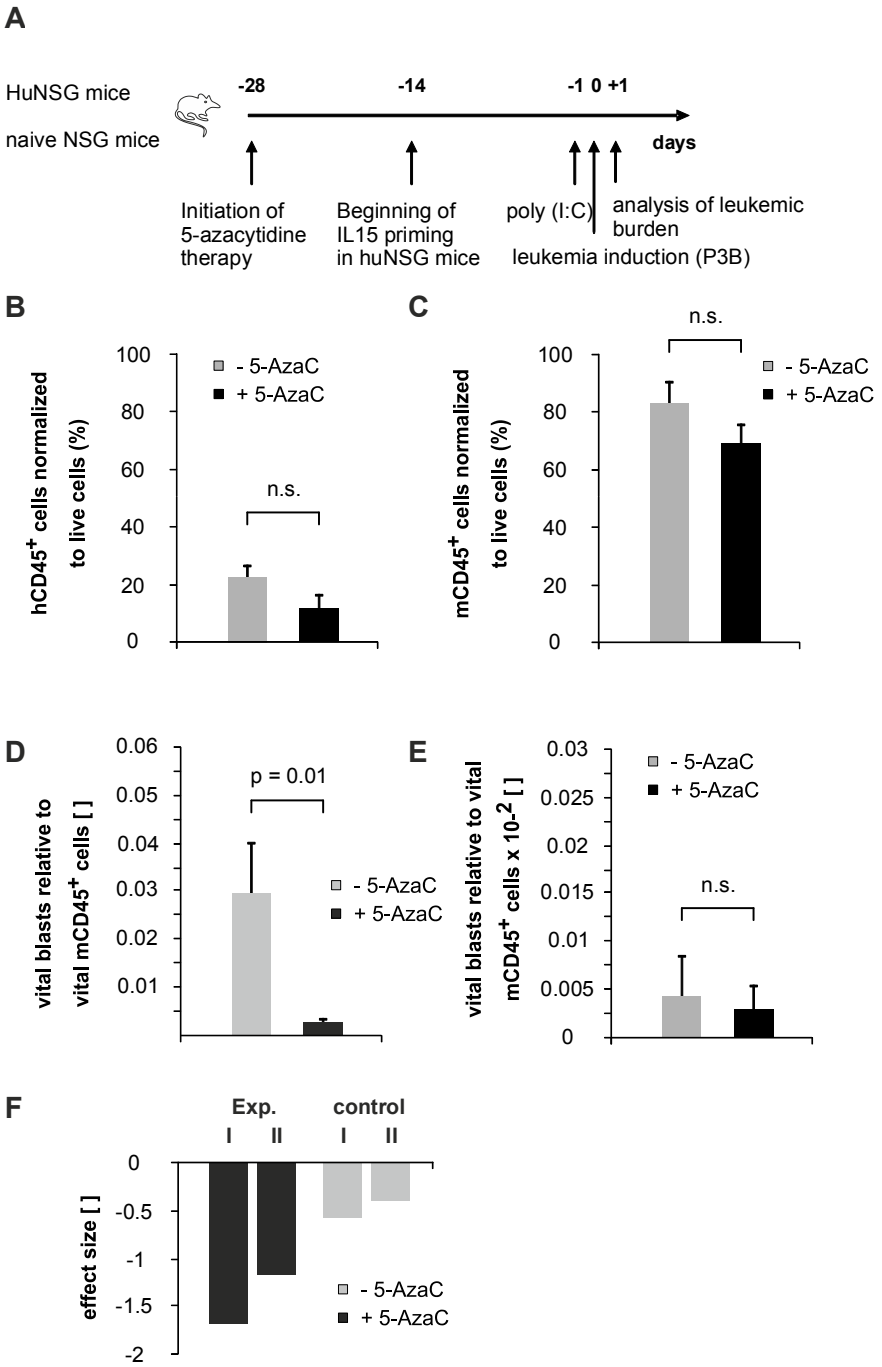

Fig. 23: Low-dose 5-AzaC early after HSC transplantation increases GvL effects towards pediatric BCP-ALL in a huNSG model. (A) Experimental outline, in brief: 5-AzaC treatment was started in week 6 after humanization (donor SSC18U) or with non-humanized control animals, injections were performed i.p. twice a week for 4 weeks before leukemia induction (ped. BCP-ALL P3B). For more detailed description see also section 3.5.5.6 and 3.5.5.8, for HLA genotype see Suppl. Table 1 and for KIR genotype Suppl. Table 2). (B), (C) 5-AzaC treatment leads to non-significant bone marrow cytotoxicity as shown by the percentage of human (B) or mouse (C) $CD45^+$ cells (hCD45 or mCD45 respectively). (D) Leukemic burden of pediatric BCP-ALL blasts (P3B) is significantly reduced upon treatment in huNSG mice. Shown is the number of vital blasts relative to vital $mCD45^+$ cells. (E) In non-humanized control animals the leukemic burden is not significantly reduced by 5-AzaC treatment. (F) Calculated effect size of two independent sets of experiments (I + II), each performed in huNSG ('Exp.') and non-humanized control animals ('control'). Data represents two independent experiments with a total of 11 huNSG mice and 14 non-humanized control NSG mice (Kübler et al., 2014)[i].

In contrast to previously performed *in vitro* experiments, expression of common KIRs (KIR2DL1/S1/S4, KIR2DL2/L3/S2 and KIR3DL1) is not significantly changed on NK cells upon the low dose of 5-AzaC treatment applied (Fig. 24A). Expression of NKp44 and NKG2D is not increased to a significant extent (Fig.

24B). Interestingly, the percentage of both immature NK cell precursors (pre-NK cells $CD34^+CD117^+$ and iNK cells $CD34^-CD117^{low}CD94^-$) and mature ($CD34^-CD117^-CD94^+NKp46^+$ and $CD34^-CD117^-CD94^-NKp46^+$) NK cell subsets (subsets as defined by Freud and Caligiuri, 2006; for exemplary gating strategy see also Suppl. Fig. 4), was significantly increased in the bone marrow of 5-AzaC-treated compared to untreated huNSG mice (Fig. 24C). This indicates that 5-AzaC might have promoted differentiation towards the mature NK cell subsets within the transplanted animals.

In summary, 5-AzaC treatment clearly enhanced NK cell precursors and more mature NK cell subsets within the bone marrow of huNSG mice and along with this reduced the leukemic burden.

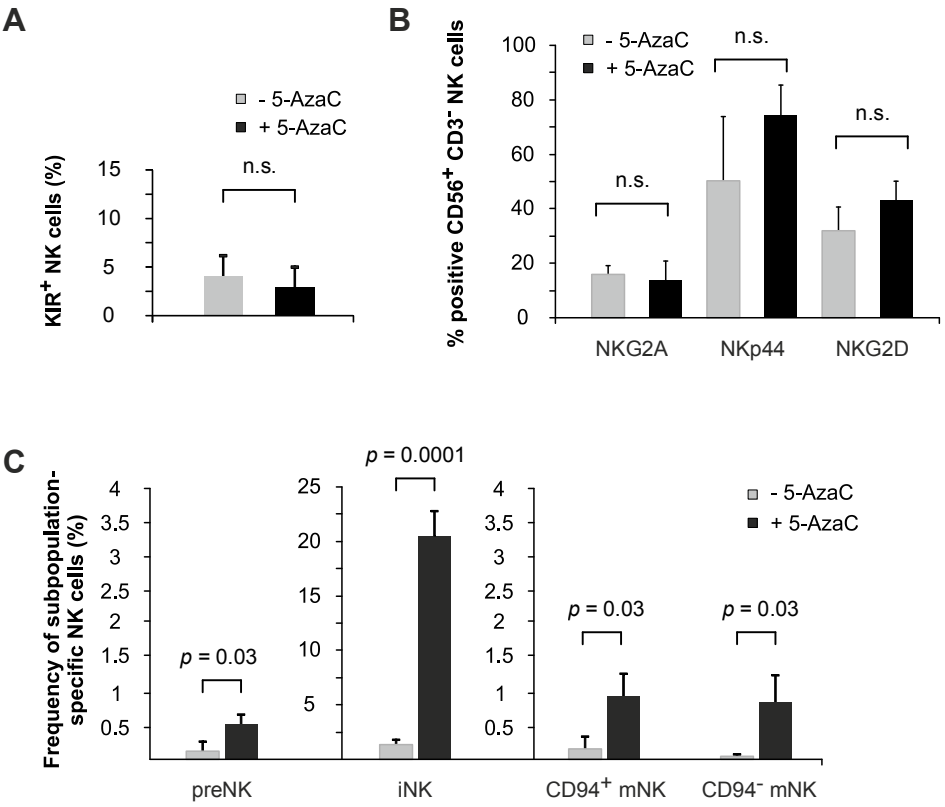

Fig. 24: Low-dose 5-AzaC does not increase KIR expression in a huNSG model *in vivo* but expands NK cell progenitors in the bone marrow. (A) KIR expression (KIR2DL1/S1/S4, KIR2DL2/L3/S2 and KIR3DL1) is not significantly changed in the bone marrow upon 5-AzaC treatment of huNSG mice, as well as the percentage of NK cells expressing NKG2A, NKp44 or NKG2D (B). (C) Frequencies of bone marrow residing NK cell precursors as defined by Freud and Caligiuri, 2006 (preNK cells: $CD34^+CD117^+$, iNK cells: CD34-CD117lowCD94-, $CD94^+$ mNK cells: CD34-CD117-$CD94^+NKp46^+$, CD94- mNK cells: $CD34^-CD117^-CD94^-NKp46^+$) which are significantly increased by 5-AzaC treatment of huNSG mice. Data represents two independent experiments with a total of 11 huNSG mice and 14 control NSG mice (Kübler et al., 2014)[i].

4.3.2.2 5-AzaC treatment increases proliferation of iNK and mNK cell subsets in vivo

The increased frequencies of NK cell precursor subsets observed upon 5-AzaC treatment of huNSG mice (Fig. 24C) might also be a side effect of preferential cytotoxic effects of 5-AzaC on other $hCD45^+$ populations. As huNSG-derived NK cell precursor cell counts had all been normalized to $hCD45^+$ cells, a direct cytotoxic effect of 5-AzaC on other cell lineages would lead to a relative overestimation of NK cell subset numbers. To confirm that NK cell precursors are indeed more abundant upon treatment, an *in vivo* proliferation analysis was performed. As described before huNSG mice were either treated with low-dose 5-AzaC or left untreated (for experimental layout see Fig. 25A). BrdU was added to the drinking water for 7 days before analysis. Flow cytometric analysis of immature, mature $CD94^-$ and mature $CD94^+$ NK cells displays an increased BrdU incorporation in 5-AzaC-treated huNSG mice compared to untreated controls (Fig. 25B). A more detailed cell cycle analysis of either $CD117^+$ cells (Fig**.** 25C) or $CD94^+$ cells (Fig**.** 25D) indicates that the increased BrdU incorporation in the NK cell subsets is indeed accompanied by a decreased number of cells in G0/G1 phase and an increased number of cells undergoing replication in S phase of the cell cycle. This data in summary suggests that the effect of 5-AzaC on NK cell ontogeny is proliferation-dependent.

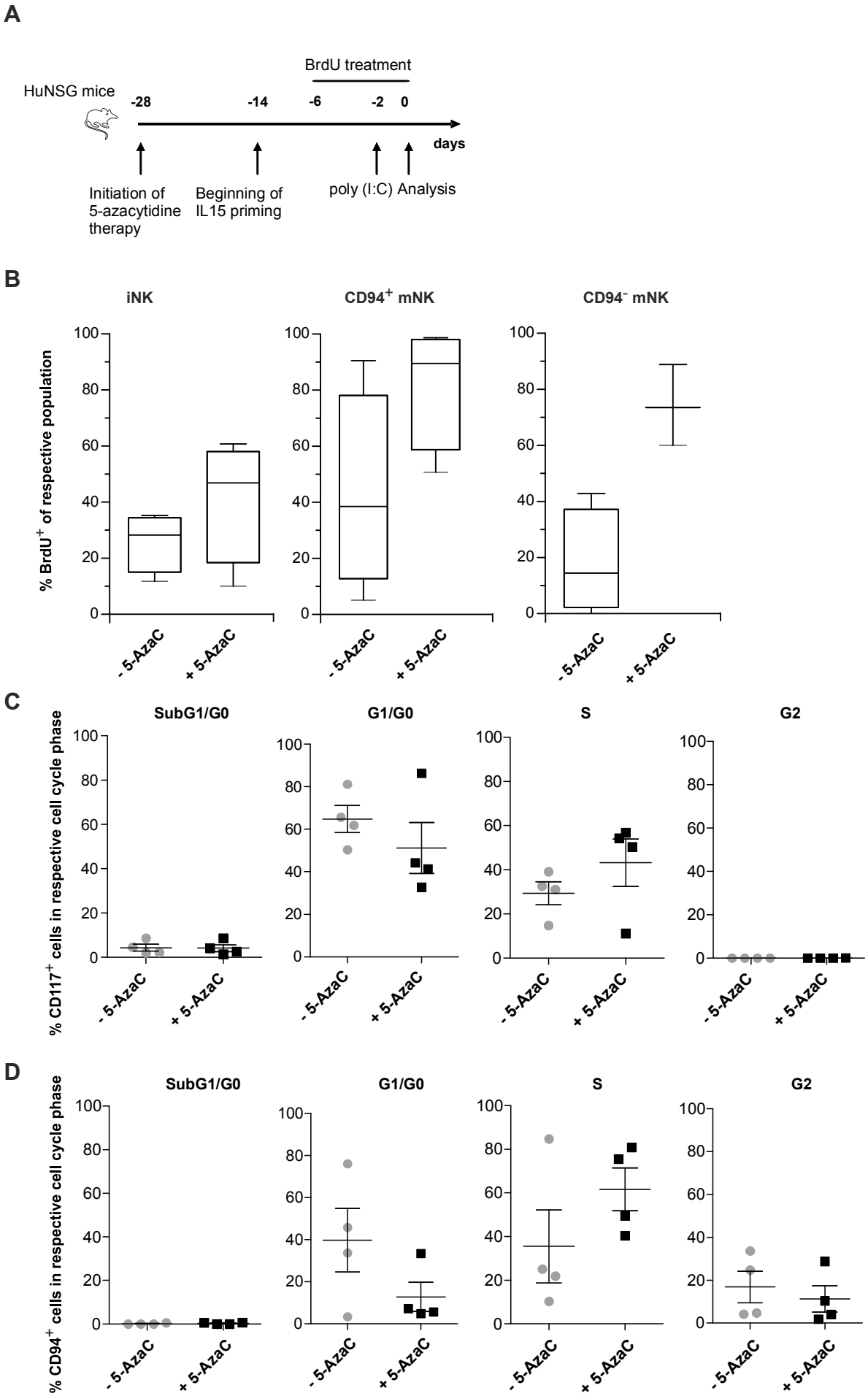
A
BrdU treatment
HuNSG mice
-28
-14
-6
-2
0
days
Initiation of 5-azacytidine therapy
Beginning of IL15 priming
poly (I:C)
Analysis
B
iNK
CD94+ mNK
CD94- mNK
% BrdU+ of respective population
- 5-AzaC
+ 5-AzaC
C
SubG1/G0
G1/G0
S
G2
% CD117+ cells in respective cell cycle phase
D
% CD94+ cells in respective cell cycle phase

Fig. 25: BrdU and cell cycle analyzes show an increased proliferation of NK cell precursors upon 5-AzaC treatment *in vivo*. (A) Experimental layout. BrdU was added to the drinking water of 5-AzaC treated or non-treated huNSG mice for 7 days before analysis. (B) Box-Whisker-Tukey plots illustrating the percentage of $BrdU^+$ cells of the respective NK cell subset (as defined by Freud and Caligiuri, 2006; iNK cells: CD34-CD117lowCD94-, $CD94^+$ mNK cells: CD34-CD117-$CD94^+NKp46^+$, CD94- mNK cells: $CD34^-CD117^-CD94^-NKp46^+$) (C), (D) Cell cycle analysis of $CD117^+$ (C) or $CD94^+$ (D) cells using 7-AAD and BrdU to differentiate between SubG1/G0, G1/G0, S and G2 phase. Data represents one experiment performed with n = 4 huNSG mice per group.

5 DISCUSSION

5.1 Pediatric BCP-ALL is a target of NK cells *in vitro* and *in vivo*

The data on NK cell mediated cytotoxicity towards ALL is scarce and most adult ALLs seem to be resistant (Ruggeri et al., 1999; Ruggeri et al., 2002). This work shows that pediatric BCP-ALL can both *in vitro* and *in vivo* be target of expanded NK cells (Fig. 6, Fig. 7). The better susceptibility of the AML cell line Kasumi-1 compared to the BCP-ALL cell line Nalm-16 (Fig. 6) cannot *per se* be attributed to expression levels of HLA class I molecules, ICAM-1, pan-NKG2D-L, CD112 or CD155 (Fig. 5) as Nalm-16 cells express those ligands to a comparable extent. The different lysis efficiency of the BCP-ALL cell lines (Fig. 6) might be explained by the differential expression of ICAM-1, NKG2D-L, and the DNAM-1 ligands CD112 and CD155 (Fig. 5).

Since *in vitro* experiments only insufficiently reflect primary disease, primary pediatric samples in an *in vivo* xenograft model were used. NSG mice were shown to readily engraft with primary pediatric leukemia retaining the immunophenotype and a similar gene expression profile (Woiterski et al., 2013). Furthermore, the clinical outcome of pediatric patients correlates with engraftment rates in NSG mice. On this basis an *in vivo* model of adoptive NK cell transfer was established. Pediatric AML and BCP-ALL samples were chosen from patients that succumbed to their disease and where blasts displayed robust engraftment in previous transplantations in NSG mice. Adoptively transferred NKAES cells are not able to eradicate leukemia but lead to an increased survival and reduced leukemic burden in NKAES cell-treated mice (Fig. 7). The simultaneous injection of an AML (P18R) and BCP-ALL (P3B) sample shows that BCP-ALL can be a target of NKAES cells *in vivo*. Both P18R and P3B display the HLA-determined KIRL motifs Bw6/Bw6 C1/C1 but vary in the extent of HLA class I, NKG2D-L, and DNAM-1 ligand expression. The slightly higher NKG2D-L expression of P3B might have caused the better susceptibility of the BCP-ALL sample P3B compared to AML P18R.

In summary, pediatric BCP-ALL is shown to be a target of NKAES cells *in vitro* and *in vivo*. The extent to which cytotoxicity is mediated in this disease entity might be influenced by adhesion molecules, NKG2D-Ls and DNAM-1 ligand expression, as in part hypothesized earlier (Ruggeri et al., 2002; Leung et al., 2004). Therefore, for experiments in this study investigating the impact of KIR-KIRL constellations, NK cell receptor expression levels and the respective ligand expression on leukemic samples was carefully evaluated and kept at a comparable level.

5.2 KIR-KIRL mismatched NKAES cells display enhanced cytotoxicity towards pediatric BCP-ALL *in vitro* and *in vivo*

From a T cell perspective, donor-recipient HLA-matching reduces the risk for acute and chronic GvHD upon HSCT and is associated with increased survival. The focus of this work was to describe the extent to which donor selection might contribute to the success of adoptive NK cell transfer in pediatric BCP-ALL. Adoptive NK cell transfer displays the possibility to apply highly purified, expanded and activated NK cells alone or in addition to (haploidentical) HSCT. Using highly purified NK cells allows HLA-mismatching without

increasing the risk for T cell-mediated alloresponses. First studies using *in vitro*-stimulated autologous NK cells did not lead to a significant change in the clinical outcome of patients (Rosenberg et al., 1987; Burns et al., 2003). In contrast, there is evidence that adoptive transfer of haploidentical and therefore partially KIR-KIRL mismatched NK cells improves the clinical prognosis of adult and pediatric AML patients (Miller et al., 2005; Rubnitz et al., 2010). There are contradictory *in vitro* reports whether KIR-KIRL constellations are relevant for blasts with high or low HLA class I expression (Pfeiffer et al., 2007; Feuchtinger et al., 2009). Therefore, cell lines and primary blasts with intermediate HLA class I expression were chosen in this study.

After having shown that pediatric BCP-ALL can indeed be a target of NK cells *in vitro* and *in vivo*, the relevance of KIR-KIRL constellations in NK cell mediated cytotoxicity towards BCP-ALL was investigated in detail. *In vitro* cytotoxicity assays of KIR-KIRL matched and mismatched NKAES cell donor groups towards primary pediatric BCP-ALL samples clearly show enhanced specific lysis of KIR-KIRL mismatched BCP-ALL cells. The MHC-deficient control K562 is targeted to the same extent showing a similar general responsiveness of the NKAES cells in a setting where KIR-KIRL interactions are not relevant (Fig. 8). To further exclude other receptor-ligand interactions that might have influenced the cytotoxic potential, NK cell receptor expression levels were analyzed. Phenotypical characterization of NKAES cells does not show major differences but there are minor differences in the expression of NKG2D-L and DNAM-1 ligands on the BCP-ALL samples used. However, since the effect of KIR-KIRL mismatching on cytotoxicity is reversible by interchanging the respective target cell, it can in summary be assumed that indeed mismatched KIR-KIRL constellations cause enhanced NK cell-mediated cytotoxicity.

The beneficial effect of a KIR-KIRL mismatch constellation is also observed upon adoptive NKAES cell transfer *in vivo*. NSG mice injected with a primary pediatric BCP-ALL sample display significantly decreased leukemic burden compared to untreated mice (Fig. 9). Adoptive transfer of KIR-KIRL matched NKAES cells did not lead to a significant effect on leukemic burden.

In summary, KIR-KIRL mismatched NKAES cells display superior *in vitro* and *in vivo* alloreactivity towards pediatric BCP-ALL. For potential adoptive NK cell therapies, KIR-KIRL constellations play a major role for alloreactivity towards pediatric BCP-ALL, even in highly activated NK cells.

5.2.1 KIR-blocking mAb IPH2102 enhances cytotoxicity of KIR$^+$ NK cells towards BCP-ALL

The KIR-blocking mAb IPH2102 is currently tested in a phase II trial in AML patients. In pre-clinical studies IPH2102 was shown to selectively bind KIR2DL1/L2/L3 and KIR2DS1/S2 and to increase NK cell alloreactivity towards HLA-matched AML blasts *in vitro* and *in vivo* (Romagné et al., 2009). Furthermore, administration of the mAb was shown to be safe with only limited side effects (Vey et al., 2012).

After having shown that the KIR-KIRL axis is relevant for NK cell-mediated cytotoxicity towards pediatric BCP-ALL *in vitro* and in adoptive NK cell transfer *in vivo*, it is surprising that in a humanized NSG mouse model the KIR-blocking mAb IPH2102 does not lead to increased GvL effects (Fig. 11). Data from Romagné and colleagues showed significant effects towards AML cells after adoptive transfer of NK cells that were about 80% KIR2DL1/2/3 receptor positive (Romagné et al., 2009). Furthermore, *in vitro*

experiments in our laboratory indicates that the percentage of KIR expressing NK cells influences the net effect of IPH2102 on NK cell-mediated cytotoxicity (Kübler & André, unpublished data). Despite the IL-15/IL-15Rα treatment of huNSG mice only a very low percentage of graft-emerging NK cells express KIRs (< 5%, see Fig. 11 and Fig. 24). Taking this into account, the missing effect of IPH2102 can here probably be attributed to the low percentage of KIR-expressing NK cells in huNSG mice. This hypothesis is further supported by the significantly increased alloreactivity of sorted KIR^+ NKAES cells from KIR-KIRL matched donors that display increased alloreactivity towards pediatric BCP-ALL upon IPH2102 treatment (Fig. 12). This observation confirms that indeed KIR-KIRL constellations play a major role for NK cell-mediated cytotoxicity towards BCP-ALL.

Surprisingly, IPH2102 does not enhance *in vitro* cytotoxicity of sorted KIR^+ NKAES cells in KIR-KIRL mismatched constellations (Fig. 12). The interaction of NK cells with Nalm-16 cells comprises the interaction of KIR2DL2/L3 receptors with HLA-C1 target cells. In KIR-KIRL matched donors the KIR2DL2/L3 receptors are considered to be educated and – as expected – the blockade with IPH2102 here promoted NK cell functionality. As opposed, KIR2DL2/L3 receptors in NK cells of KIR-KIRL mismatched donors have not been subject to education. Brodin and colleagues describe that the number of possible MHC class I - inhibitory receptor interactions quantitatively tunes the responsiveness of NK cells at a single cell level (Brodin et al., 2008; Brodin et al., 2009). This leads to completely hyporesponsive NK cells when no educating interaction is possible. The higher the inhibitory input during education the higher the resulting responsiveness of the NK cell will be. Thus, in order to explain the lack of an adequate IPH2102 effect it was at this point hypothesized that the KIR-KIRL mismatched donors must possess one large NK cell subset which expresses the uneducated KIR2DL2/L3 as the *only* inhibitory receptor group. As shown in Fig. 13A this indeed is the case. Furthermore, this uneducated KIR2DL2/L3 single positive subset from KIR-KIRL mismatched donors indeed displays a decreased degranulation potential towards K562. The presence of NKG2A on $KIR2DL2/L3^+$ single KIR positive NK cells enhanced the degranulation potential, but not to the level of multiple-KIR positive NK cells. NKG2A therefore seems to have a minor educating effect. Thus, in line with the licensing theory the missing enhancement of cytotoxicity by IPH2102 for KIR-KIRL mismatched donors might be explained by the predominance of the uneducated KIR2DL2/L3 single positive subset that displays decreased responsiveness.

In summary, KIR-blocking mAb IPH2102 might also increase NK cell-mediated cytotoxicity in the disease entity of pediatric BCP-ALL – especially for KIR-KIRL matched constellations. Furthermore, although huNSG mice are a well-suited model to investigate early stages of NK cell development, they might not be ideal to study the relevance of KIR receptors due to the low abundance of KIR^+ NK cells.

5.2.2 Subset analysis reveals functional differences between KIR-KIRL matched and mismatched NK cells

KIR^- and uneducated NK cells were described to be hyporesponsive due to the lacking interaction with MHC class I molecules (Kim et al., 2005; Anfossi et al., 2006; Joncker et al., 2009; Joncker et al., 2010). But it has been shown that MHC-dependent education might be overcome by non-specific post-receptor stimulation

with PMA/Ionomycin. Poly (I:C) treatment or IL-2 are able to partially reverse a deficiency in responsiveness in NK cells from MHC class I negative hosts (Kim et al., 2005; Yokoyama and Kim, 2006). Under inflammatory conditions, both educated and uneducated NK cells were shown to produce IFN-γ upon *Listeria monocytogenes* infection *in vivo* (Fernandez et al., 2005). In murine cytomegalovirus (MCMV) infection also uneducated NK cells become activated by pro-inflammatory cytokines and display even more proliferation than MHC class I-inhibited NK cells. Depletion experiments confirmed that indeed unlicensed NK cells dominate the response to MCMV infection (Orr et al., 2010). So, self-tolerance achieved by education and hyporesponsiveness of NK cells missing self-MHC class I inhibitory receptors might be overcome by pro-inflammatory cytokines. Lanier and colleagues hypothesized that educated NK cells are inhibited and might therefore even display less anti-viral response compared to uneducated NK cells (Orr et al., 2010). These cells might initially also attack healthy cells, but this needs to be confirmed. Exhaustion could also finally diminish the response of uneducated cells.

Cell sorting was performed to dissect the relevance and functional capacity of KIR^+ and uneducated KIR^- NKAES cells in either KIR-KIRL matched or mismatched constellations. Sorted KIR^+ NKAES cells from KIR-KIRL mismatched donors display higher cytotoxicity towards the BCP-ALL cell line Nalm-16 compared to their KIR^- counterparts (Fig. 14). This is reversed for KIR-KIRL matched NKAES cells where KIR^- cells display superior cytotoxicity. The general functionality of KIR^+ and KIR^- NK cells from KIR-KIRL matched and mismatched donors was comparable as seen by the specific lysis of MHC class I-deficient K562 cells. In line with the literature, the cytokine-rich culture conditions during the NKAES expansion protocol leads to responsiveness of uneducated KIR^- NK cells but functional differences between KIR^+ NK cells from different donor groups can still be observed. Despite cytokine stimulation KIR^+ NKAES cells from KIR-KIRL mismatched donors display enhanced cytotoxicity towards Nalm-16 cells compared to KIR^- NKAES cells (Fig. 14). KIR-KIRL matched constellations lead to higher responsiveness of KIR^- cells compared to KIR^+ cells. In summary, these data indicate that the applied cytokine-rich culture conditions only in part reverse the effect of education by turning commonly hyporesponsive KIR^- NK cells responsive. But the effect of KIR-KIRL mismatching is still dominant since only KIR^+ NK cells from KIR-KIRL mismatched donors but not KIR-KIRL matched ones display increased cytotoxicity towards BCP-ALL.

The KIR^+ NK cell subset can further be divided into KIR^+ 'alloreactive' and KIR^+ 'non-alloreactive' NK cells. The alloreactive subset is commonly defined as NK cells expressing activating receptors and only inhibitory receptors permissive for target cell lysis. NK cells expressing KIR2DL1/S1/S4 and/or KIR3DS1 but not KIR2DL2/L3/S2 or KIR3DL1 are assumed to be alloreactive towards Nalm-16 (Bw4/C1). Co-culture experiments and a complex gating strategy allow evaluating the contribution of the different NK cell subsets. The degranulation capacity of alloreactive KIR^+ NKAES cells from KIR-KIRL mismatched donors is indeed superior compared to KIR-KIRL matched donors (Fig. 16).

To conclude, the increased alloreactivity of KIR-KIRL mismatched NKAES cells towards BCP-ALL can be attributed to the increased degranulation potential of the KIR^+ 'alloreactive' NK cell subset.

5.3 Modulation of NK cell functionality with the Dnmt-inhibitor 5-AzaC

The *KIR* locus was described to be regulated by methylation of CpG islands within the promoter region of *KIR* genes (Santourlidis et al., 2002; Chan et al., 2003). In line with this, DNA methyltransferase inhibition was shown to induce KIR expression. Until now, beneficial effects of the Dnmt-inhibitor 5-AzaC in treatment of AML and MDS have been attributed to the epigenetic upregulation of cancer testis antigens or NKG2D-L on blasts leading to higher susceptibility to NK cell-mediated cytotoxicity (Rohner et al., 2007; Tang et al., 2008; Lubbert et al., 2010). Furthermore, methyltransferase inhibitors in cancer therapy can induce the re-expression of tumor suppressor genes (Jones and Baylin, 2007). Besides this tumor-focused concept there is only limited data available about direct effects of 5-AzaC on NK cells.

5.3.1 5-AzaC alters the phenotypical expression pattern of NK cells *in vitro* but decreases cytotoxicity

As already described in the literature (Santourlidis et al., 2002; Chan et al., 2003), 5-AzaC induces KIR expression upon treatment of NK cells *in vitro* (Fig. 17). Furthermore, modulation of other NK cell receptors can be observed (Fig. 18). Interestingly, detailed subset analysis shows a preferential increase of KIR expression mainly on $NKG2A^+$ but not on $NKG2A^-$ NK cells (Fig. 19). The inhibitory receptor NKG2A recognizes HLA-E, and this receptor-ligand interaction plays an important role for self-tolerance. So, especially in KIR^- NK cells, higher frequencies of $NKG2A^+$ cells can be observed (Andersson et al., 2009). From a developmental point of view it has been shown that there is a step-wise maturation process from $CD56^{dim}$ $NKG2A^+KIR^-$ cells that increase KIR expression and decrease NKG2A expression to a finally fully competent $CD56^{dim}NKG2A^-KIR^+$ stage (Béziat et al., 2010). The increased presence of $NKG2A^+KIR^+$ cells but not $NKG2A^-KIR^+$ cells shown in this work might therefore be a consequence of KIR upregulation occurring on the developmentally 'appropriate' precursor only, namely the $NKG2A^+$ NK cells and not $NKG2A^-$ NK cells.

Besides the preference for KIR induction on $NKG2A^+$ NK cells upon 5-AzaC treatment *in vitro,* it was furthermore observed that there is a preference for CD158b1/b2/j (KIR2DL2/L3/S2) expression (Fig. 20).

An *in vitro* study with single umbilical cord blood-derived $CD34^+$/Lin-/CD38- cells, fetal liver, and adult bone marrow showed that these HSCs upon differentiation lead to NK cells with polyclonal KIR expression (Miller and McCullar, 2001). KIR expression frequency was hierarchical: KIR2DL2/L3/S2 > KIR2DL1/S1 ≥ KIR3DL1 (Miller and McCullar, 2001). Most of the cells in the study of Miller and McCullar were KIR^+NKG2A^+, only a small number of cells was KIR^+NKG2A-. The analysis of sorted KIR2DL2/L3/$S2^+$ NK cells revealed that KIR2DL2/L3/S2 expression remained stable and additional KIR3DL1 expression can be induced. The HLA type of the HSCs used did not change the preference for KIR expression. This was also shown by the Malmberg group (Andersson et al., 2009) that furthermore describe that the acquisition probability of KIRs increases with cellular KIR expression. There are further indications for preferential KIR2DL2/L3/S2 reconstitution after HSCT in patients (Pfeiffer et al., 2010).

The data in Fig. 20 showing a preferential (co-)expression of KIR2DL2/L3/S2 observed during 5-AzaC treatment is supported by the observations of several studies (Miller and McCullar, 2001; Andersson et al., 2009; Pfeiffer et al., 2010). At the concentrations used 5-AzaC might not lead to a randomly increased KIR expression, but rather to a conservation of the hierarchical KIR expression order also occurring during NK cell development. This might on a molecular basis be explained by the presence of specific histone modifications that poise KIRs for DNA demethylation and expression (Santourlidis et al., 2008). In contrast to KIR2DL1/S1/S4 or KIR3DL1 expression KIR2DL2/L3/S2 is in most individuals robustly expressed (personal observation). The open chromatin conformation needed for *KIR* expression and high abundance of mRNA transcripts might contribute to the preferential induction of KIR2DL2/L3/S2 expression upon 5-AzaC treatment. However, these hypotheses are speculative and for confirmation further molecular-biologic investigation is needed.

Due to the limited availability of single KIR-specific mAbs data on 5-AzaC effects on aKIR expression is scarce. Applying a Q-PCR-based quantification of aKIRs, this study shows the 5-AzaC-induced induction of inhibitory and also activating KIRs (Fig. 21). Until now the effect of 5-AzaC on NK cell function has mainly been studied in the context of MHC class I-deficient target cell lysis. Gao and colleagues showed a 5-AzaC induced KIR expression on NK cells followed by decreased cytotoxicity towards K562 cells. They attribute this effect to the enhanced inhibition by KIRs and decreased granzyme B and perforin release (Gao et al., 2009). The Salih group also observed diminished cytotoxic potential and IFN-γ release upon treatment of NK cells with 5-AzaC (Schmiedel et al., 2011). However, in this study the exposure of NK cells to 5-AzaC was performed only for a short period of time under non-proliferating conditions. This did not lead to epigenetic modulation as seen by the lack of *KIR* induction. Therefore, experimental conditions cannot be compared.

It has not been investigated whether under certain specific KIR-KIRL constellations the induction of aKIRs might be beneficial. For this purpose, a KIR-KIRL constellation where no educated iKIR-KIRL interaction but rather activating KIR2DS2-HLA-C2 interaction is possible was chosen (Table 10). Despite this selected KIR-KIRL constellation 5-AzaC-treated NKAES cells display decreased cytotoxicity towards a pediatric BCP-ALL and a pediatric AML cell line (Fig. 22). The cytotoxic potential towards the MHC class I-deficient K562 cell line was also decreased. It can therefore be assumed that under the 5-AzaC concentrations applied mechanisms independent of increased inhibition by KIRs lead to a reduced cytotoxic potential of NK cells. Furthermore, the general dampening of cytotoxicity under the given conditions might have outweighed potential functional consequences of aKIR upregulation.

5.3.2 5-AzaC induces proliferation of NK cell progenitors and along with this reduces the leukemic burden in huNSG mice

Low dose 5-AzaC has already been used in a so-called ‘bridging therapy’ in MDS early after HSCT (during the first 3 months) to prevent early occurring relapses (De Lima et al., 2010). In this study toxicity of 5-AzaC when given early after HSCT was acceptable as shown by de Lima and colleagues. Also in AML patients,

there is evidence that 5-AzaC treatment early after HSCT might induce remission (Jabbour et al., 2009). These studies show on one hand the feasibility of low-dose 5-AzaC treatment early after HSCT and on the other hand beneficial anti-leukemic effects in a 'tumor-focused' view.

NK cells are one of the first cell populations recovering in humans upon HSCT and NK cells occur within the first month (Lamb et al., 1998). But these NK cells mainly display an immature phenotype. One month after HSCT, the $CD56^{bright}$ KIR^{-} subset predominates and NK cell-mediated alloreactivity is impaired (Nguyen et al., 2005; Vago et al., 2008). Interestingly, also huNSG mice develop mainly $CD56^{bright}KIR^{-}$ NK cells that are functionally inert (André et al., 2010). This hyporesponsiveness in huNSG mice can be overcome by supplementation of IL-15/IL-15Rα (André et al., unpublished data). Using this humanized xenotransplantation model to study GvL effects upon HSCT is technically challenging and has to our knowledge so far not been attempted by other groups. The application of multi-color flow cytometry-based MRD analysis allows the discrimination of BCP-ALL blasts and graft-emerging B cell-lineage precursors and therefore quantification of GvL effects (Kübler et al., 2014). By using primary patient blast samples the study of donor-patient-specific interactions of graft-emerging NK cells in the presence of bystander cells is possible.

Administration of low-dose 5-AzaC at an early time point after humanization does not increase KIR or other NK cell receptor expression (NKG2D, NKp44, NKG2A) on NK cells (Fig. 24) but intriguingly reduces the BCP-ALL burden (Fig. 23). Non-humanized control NSG mice that received 5-AzaC treatment and blasts do not show a significantly reduced leukemic burden in contrast to huNSG mice. Keeping the short half-life of 5-AzaC in mind, a direct cytotoxic effect of 5-AzaC must therefore have been negligible. The half-life of 5-AzaC and the chosen time point of leukemia induction render it unlikely that regulation of cancer testis antigens or NKG2D ligands on blasts had modulated the immune response. The short time period from blast injection to analysis of only about 20 h should be too short to initiate a T cell-mediated adaptive immune response. In addition, at this early stage after humanization T cells are only present at a very low level (Kübler & André, unpublished data). Most likely, the GvL effect can indeed be attributed to graft-emerging NK cell subsets. To definitively verify this hypothesis, NK cell-depleting experiments would be required. Unfortunately, until now the human NK cell-depleting mAb (anti-Nkp46 mAb from the Moretta group) has not been available to our group.

The observation that 5-AzaC induces clinically relevant *in vivo* GvL effects of NK cells is in sharp contrast to our own *in vitro* data and data published from other groups on mature 5-AzaC-treated NK cells (Gao et al., 2009; Schmiedel et al., 2011). Unlike these studies that have exclusively been performed with mature NK cells, huNSG mice harbor diverse NK cell progenitor cells. 5-AzaC significantly increased the abundance of immature and mature NK cell subsets in the bone marrow of huNSG mice. This increased pool of NK cells might have caused the enhanced GvL effect. Therefore, it can be proposed that 5-AzaC differently affects NK cell progenitors or mature NK cells. A methylome and transcriptome analysis of isolated 5-AzaC treated NK cell progenitors could verify epigenetic effects and potentially identify candidate genes that for example might have induced proliferation or differentiation of NK cells.

5-AzaC was shown to induce cytopenia in a phase III study (Fenaux et al., 2009). Also in huNSG mice 5-AzaC induces a non-significant reduction of human and murine $CD45^+$ cells in the bone marrow (Fig. 23B,C). Therefore, the increased abundance of cells from the NK cell lineage might have been caused by a cytotoxic effect on other human $CD45^+$ populations causing an apparent increase of NK cells. But *in vivo* BrdU analysis shows an increased BrdU incorporation in iNK, $CD94^+$ and $CD94^-$ mNK cells in 5-AzaC-treated huNSG mice compared to untreated animals (Fig. 25). Furthermore, $CD117^+$ and $CD94^+$ cells in 5-AzaC-treated huNSG mice display a percentage of cells in the S phase of the cell cycle. From these findings it can be assumed that 5-AzaC increases the abundance of NK cell progenitors and also mature NK cell subsets in huNSG mice in a proliferation-dependent manner. In conclusion, it can be hypothesized that low-dose 5-AzaC treatment early after HSCT might induce proliferation of NK cells and NK cell progenitors, leading to an enhanced GvL effect.

Mechanistically, several aspects support this hypothesis. Data from embryonal carcinoma cells (Musch et al., 2010) or primary MDS progenitors (Curik et al., 2012) showed that 5-AzaC can indeed promote differentiation. Epigenetically downregulated *PU.1* in high-risk MDS can be re-expressed by 5-AzaC treatment *in vitro* and especially in combination with G-CSF it induced myeloid differentiation of MDS blasts (Curik et al., 2012). This might also be relevant for the NK cell lineage since *PU.1* -deficient fetal liver cells give rise to less NKPs and NK cells after transfer into $Rag2/\gamma c^{-/-}$ mice compared to controls (Colucci et al., 2001). Since *PU.1* influences the differentiation of HSCs to NK cell progenitors and NK cells, low-dose 5-AzaC treatment might induce expression of *PU.1* and thereby promote NK cell differentiation.

The inhibition of Dnmt1 by nucleoside analogues as 5-AzaC might lead to a relatively broad and unspecific passive demethylation of the genome. But Hageman and colleagues showed in cancer cell lines that this is probably not true for all loci as 5-AzaC rather induces a highly specific non-random demethylation pattern. This is partly caused by targeted remethylation of only specific loci or by demethylation resistance of certain loci (Hagemann et al., 2011). It is possible that also transcription factors required for NK cell lineage decisions display specific demethylation patterns after 5-AzaC treatment. Furthermore, Hageman and colleagues show an increased number of cells in S phase after 5-AzaC treatment (1 µM for 24 hours), only higher concentrations led to arrest in G2-phase. So low-dose 5-AzaC might also promote cell cycle progression of NK cells or NK cell progenitors.

Decitabine (5-AzadC) which is the deoxy-ribose analogue of 5-AzaC has been shown to have stem-cell renewing capacities in the context of hematopoietic precursors (Milhem et al., 2004; Hu et al., 2010). Hu and colleagues propose that Dnmt1 depletion before or concurrent with a differentiation-inducing stimulus maintains stem cell self-renewal by preventing the repression of stem cell genes by the differentiation stimulus. In contrast shortly after a differentiation stimulus Dnmt1 depletion augments differentiation (Hu et al., 2010). Taking these data into account for interpretation of the data shown in this work, it is possible that both enhanced stem cell renewal and enhanced terminal differentiation leads to increased NK cell differentiation in our huNSG model. During the first phase of 5-AzaC treatment no IL-15/IL-15Rα was supported which could have led to an enhanced stem cell renewal. During the second phase IL-15/IL-15Rα administration could have increased NK cell differentiation.

iNK cells are significantly enhanced upon 5-AzaC treatment *in vivo* (Fig. 24) and interestingly, *in vitro* generated immature NK cells ($CD161^+$ CD56-) were found to mediate cytotoxic activity towards Jurkat and J23 cells (Zamai et al., 1998). Cytotoxicity of iNK cells, in contrast to mature NK cells, was shown to be Ca^{2+}-independent, therefore independent from granule exocytosis, and independent of Fas/FasL interaction or TNF. iNK cells seem to be able to mediate TRAIL-dependent cytotoxicity. Taking this into account, the enhanced presence of iNK cells after 5-AzaC treatment *in vivo* might also have enhanced GvL effects by direct TRAIL-dependent iNK cell-mediated cytotoxicity.

HuNSG mice provide the basis for multiple complex cell-cell interactions. Besides the differences observed in NK cell differentiation also other cell compartments or interaction partners of NK cells might have contributed to the increased GvL effect upon 5-AzaC treatment. In this sense mature DCs were shown to display varied cytokine expression and properties upon 5-AzaC treatment *in vitro* (Frikeche et al., 2011). Furthermore, it was shown in a B16-melanoma model that low-dose 5-AzadC increases macrophage cytotoxicity, M 1 polarization, DC activation and reduced the number of myeloid-derived suppressor cells (Triozzi et al., 2012). Polarization of macrophages towards M1 can induce tumoricidal activity and prevent polarization to tumor-promoting M2-type (Tang et al., 2013). Effects of 5-AzadC and 5-AzaC cannot directly be compared, nevertheless 5-AzadC is a metabolite of 5-AzaC and also 5-AzaC treatment might also have influenced the myeloid compartment in the huNSG mouse model in this study. Further investigations are necessary to clarify the role of myeloid cell subsets.

Taken together, the present study provides substantial evidence that low-dose 5-AzaC treatment early after HSCT leads to a proliferation-dependent increased abundance of immature and mature NK cell subsets. Along with this the leukemic burden is reduced. Considering earlier studies using 5-AzaC in so-called 'bridging therapies' early after HSCT, the beneficial anti-leukemic effect in these studies might in part also be attributed to enhanced NK cell-mediated GvL effects. Since 5-AzaC was shown to cause little side effects (Jabbour et al., 2009; De Lima et al., 2010), 5-AzaC therapy early after HSCT could improve the outcome for BCP-ALL patients who are at high risk for relapse.

5.4 Conclusion & Outlook

This work shows that pediatric BCP-ALL is a target of NK cells *in vitro* and *in vivo*. Furthermore, optimization of anti-leukemic activity by selecting KIR-KIRL constellations is possible, which will be of high clinical interest. KIR-KIRL mismatched expanded NKAES cells displayed a higher cytotoxicity in a human-murine xenotransplant model of adoptive transfer as compared to KIR-KIRL matched NKAES cells. Sorting experiments, KIR blockade and subset analyses showed substantial functional differences of certain NK cell subsets and as such substantiate the superior anti-leukemic activity of KIR-KIRL mismatched NK cells towards BCP-ALL. These analyses provide the basis for innovative clinical adoptive NK cell transfer strategies for relapsing BCP-ALL patients.

Manipulation of the KIR-KIRL axis by 5-AzaC treatment of mature NK cells led to changes in receptor expression patterns, but decreased *in vitro* cytotoxicity. However, this work provides evidence that low dose 5-AzaC treatment early after HSCT interestingly does not increase KIR expression in a huNSG mouse model

but nevertheless increases GvL effects. The increased GvL effect can presumably be attributed to increased proliferation of immature and mature NK cell subsets resulting in a marked rise in these cell populations. In this regard, more basic research is envisaged such as methylome and transcriptome analyses that would identify transcription factors that are modulated in response to 5-AzaC exposure.

As a consequence of these data pediatric BCP-ALL patients with high risk features (such as remission induction failure or high MRD load) should benefit from HSCT and early low dose 5-AzaC treatment. These strategies could be a promising approach in addition or as alternative to other novel concepts as *in vitro* IL-15 pretreatment of the graft (Pfeiffer et al., 2012), KIR haplotype donor selection (Oevermann et al., 2014) or bispecific antibodies (e.g. Bargou et al., 2008).

6 SUPPLEMENTS

6.1 Supplemental figures

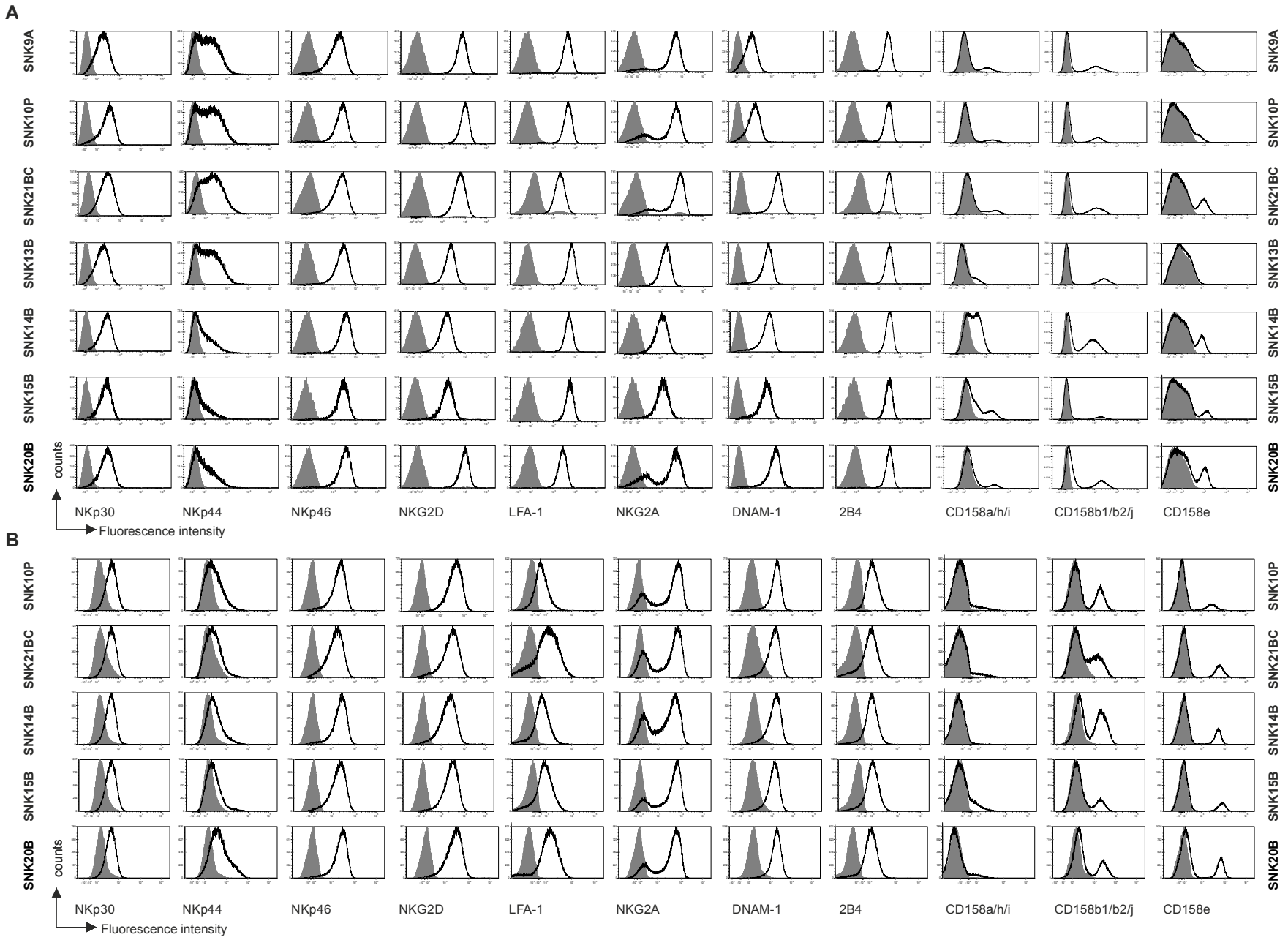
A
SNK9A
SNK10P
SNK21BC
SNK13B
SNK14B
SNK15B
SNK20B
counts
NKp30
NKp44
NKp46
NKG2D
LFA-1
NKG2A
DNAM-1
2B4
CD158a/h/i
CD158b1/b2/j
CD158e
Fluorescence intensity
B
SNK10P
SNK21BC
SNK14B
SNK15B
SNK20B
counts
NKp30
NKp44
NKp46
NKG2D
LFA-1
NKG2A
DNAM-1
2B4
CD158a/h/i
CD158b1/b2/j
CD158e
Fluorescence intensity

Suppl. Fig. 1 (previous page): Receptor expression of selected NKAES cell donors. Expression of selected receptors (NKp30, NKp44, NKp46, NKG2D, LFA-1, NKG2A, DNAM-1, 2B4, CD158a/h/I, CD158b1/b2/j, CD158e) of NKAES cells from donors SNK13-15B, SNK20B, SNK21BC, SNK9A and SNK10P is shown as determined by flow cytometric analysis. Grey, filled: isotype; black line: specific antibody staining. For KIR staining the following clones were used: HP-3E4 (CD158a/h/i), Gl183 (CD158b1/b2/j) and Dx9 (CD158e), for others please refer section 3.3. (A) Phenotype data for experiments shown in Fig. 7, Fig. 8, Fig. 9, Fig. 14, Fig. 15, and SNK9A for Fig. 13, and **Fig.** 16. (B) phenotype data from NKAES cells that were expanded separately for the data shown in Fig. 13, and **Fig.** 16. Note that receptor expression differs to a certain extent, especially for Nkp44, LFA-1 and NKG2A (Kübler et al., 2014)[i].

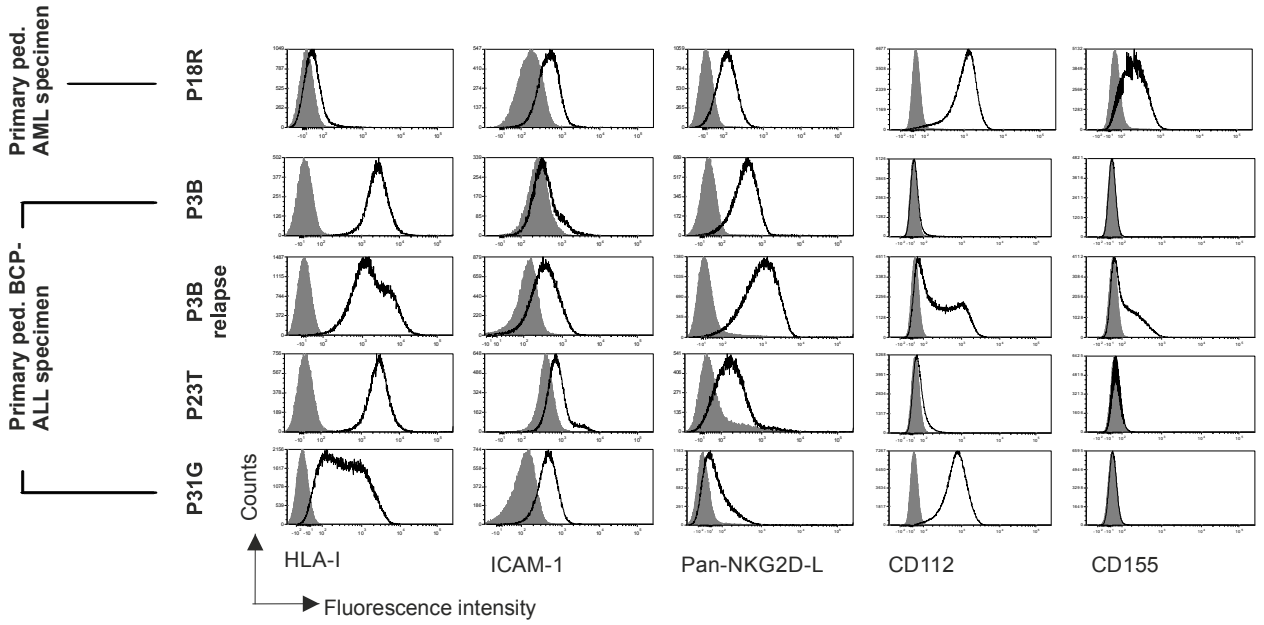

Suppl. Fig. 2: Phenotypical characterization of HLA class I, ICAM-1, NKG2D-L, CD112 and CD155 on selected primary pediatric leukemia samples. Flow cytometric characterization of important molecules recognized by NK cells on the primary pediatric leukemia samples P18R, P3B, P3B relapse, P23T and P31G. Pan-NKG2D-L staining was performed using a cocktail of anti-MICA, anti-MICB and anti-ULBP1-3 antibodies, HLA class I with clone W6/32; for others, please refer section 3.3. Grey, filled: isotype; black line: specific antibody staining (Kübler et al., 2014)[i].

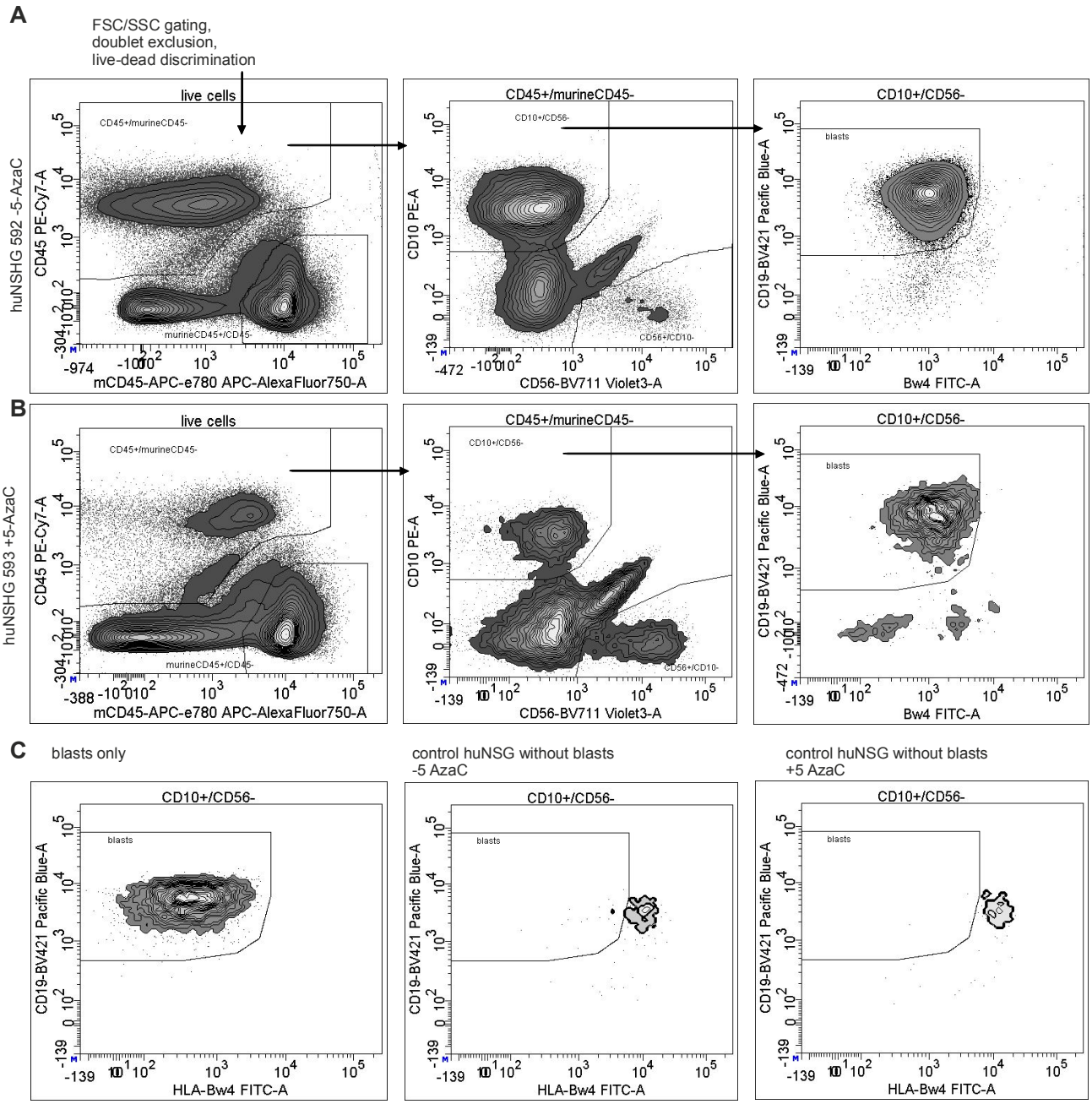

Suppl. Fig. 3: Exemplary gating strategy for blast detection from huNSG mice. Shown is the hierarchical gating strategy for the 5-AzaC *in vivo* experiment shown in **Fig.** 23 by polychromatic flow cytometry using pre-defined CD molecules. (A) Exemplary bone marrow sample from a 5-AzaC untreated huNSG where leukemic cells were injected, (B) exemplary bone marrow sample from a 5-AzaC-treated huNSG that received leukemic cells. The approach shows the exclusion of murine hematopoietic cells and exclusion of non-malignant cells (C).

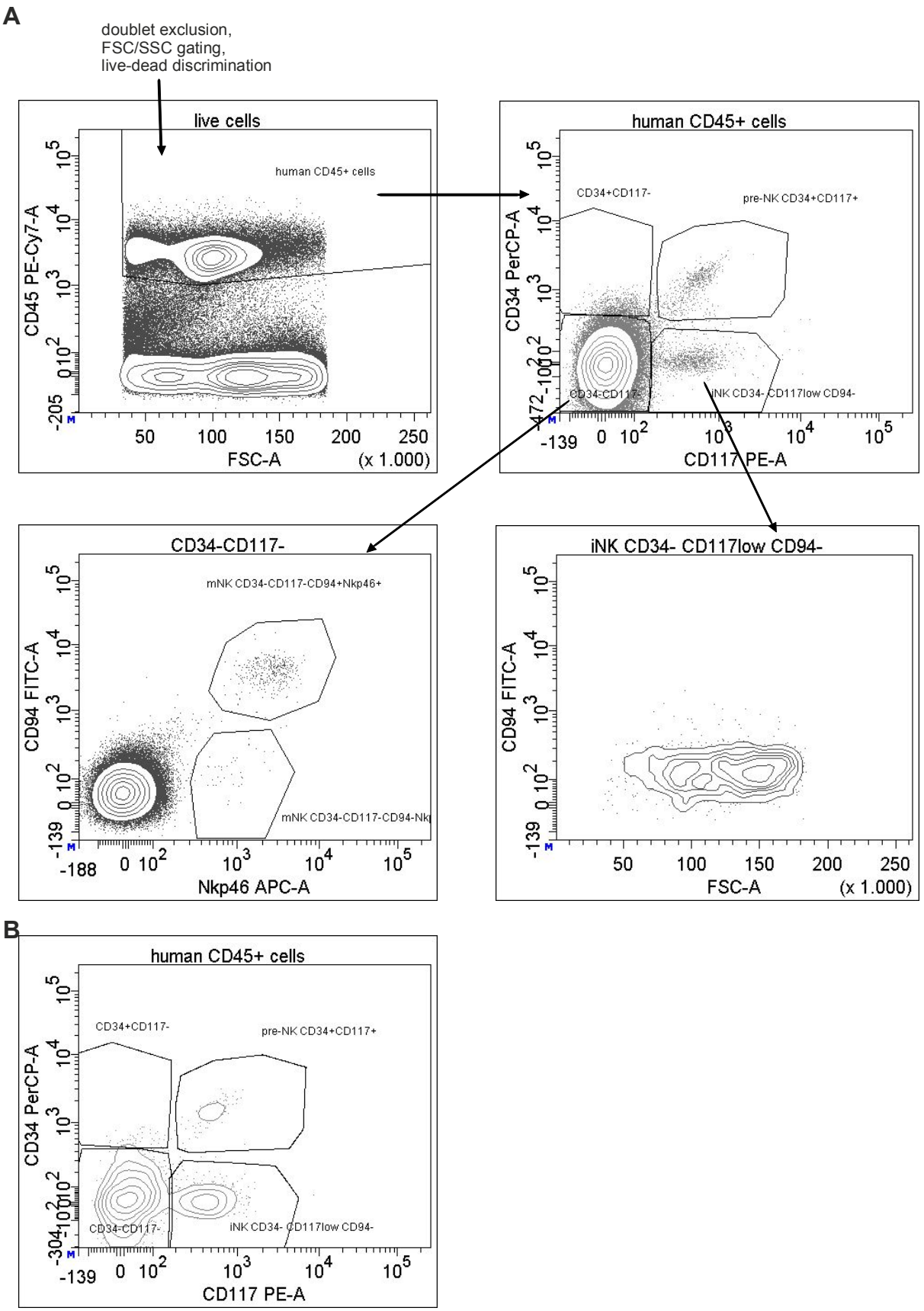

Suppl. Fig. 4: Exemplary gating of bone marrow-residing NK cell precursors. Gating strategy to identify NK cell precursors in huNSG mice (data shown in Fig. 24). (A) Hierarchical multicolour flow cytometric gating strategy to identify the following subsets in a 5-AzaC untreated huNSG (#592): preNK cells: $CD34^{+}CD117^{+}$, iNK cells: $CD34^{-}CD117^{low}CD94^{-}$, $CD94^{+}$ mNK cells: $CD34^{-}CD117^{-}CD94^{+}NKp46^{+}$, $CD94^{-}$ mNK cells: $CD34^{-}CD117^{-}CD94^{-}NKp46^{+}$). (B) exemplary plot from a 5-AzaC treated huNSG (#593), showing an increased abundance of preNK and iNK cell precursors compared to untreated huNSG shown in (A).

6.2 Supplemental tables

Suppl. Table 1: HLA class I genotype of NK cell donors (SNK), stem cell donors (SSC), and leukemias (P). Shown is HLA-typing data and the resulting HLA-determined KIRL assignment. HLA class I genotyping was performed at 4-digit resolution by sequence-based typing (SBT), except for P23T which was determined at 4-digit resolution by sequence-specific primer typing (SSP). * Only P18R HLA-typing was determined in 2-digit resolution (Kübler et al., 2014)[i].

	HLA-A allele		KIRL		HLA-B allele		Supertypic specificity / KIRL		HLA-C allele		KIRL	
SNK9A	01:01	33:03	-	-	15:25	55:01	Bw6	Bw6	03:03	07:01	C1	C1
SNK10P	01:01	02:01	-	-	08:01	40:01	Bw6	Bw6	07:01	03:04	C1	C1
SNK21BC	02:01	03:01	-	A3	07:02	08:01	Bw6	Bw6	07:02	07:01	C1	C1
SNK13B	02:01	24:02	-	Bw4	27:05	44:02	Bw4-80T	Bw4-80T	02:02	05:01	C2	C2
SNK14B	02:01	32:02	-	Bw4	27:02	44:02	Bw4-80I	Bw4-80T	02:02	05:01	C2	C2
SNK15B	02:01	31:01	-	-	27:05	44:02	Bw4-80T	Bw4-80T	02:02	05:01	C2	C2
SNK20B	02:01	03:01	-	A3	51:01	51:05	Bw4-80I	Bw4-80I	04:01	05:01	C2	C2
SSC18U	23:01	34:02	Bw4	-	44:03	44:03	Bw4-80T	Bw4-80T	04:01	07:01	C2	C1
SSC52G	02:01	02:01	-	-	15:01	18:01	Bw6	Bw6	01:02	07:01	C1	C1
P18R*	01	02	-	-	08	40	Bw6	Bw6	07	03	C1	C1
P3B relapse	02:01	26:01	-	-	18:03	14:14	Bw6	Bw6	07:01	08:02	C1	C1
P23T	24:02	24:02	Bw4	Bw4	49:01	51:01	Bw4-80I	Bw4-80I	02:02	07:01	C2	C1
P31G	03:01	03:01	A3	A3	27:05	35:01	Bw4-80T	Bw6	02:02	04:01	C2	C2
Nalm-16	30:01	-	-	-	44:02	-	Bw4-80T	-	07:04	-	C1	-
Kasumi-1	26:01	26:02	-	-	40:06	48:01	Bw6	Bw6	03:03	08:01	C1	C1

Suppl. Table 2: **KIR repertoire of NK cell donors (SNK) and stem cell donors (SSC).** Shown is the KIR DNA genotype and KIR RNA expression as determined by Q-(RT)-PCR, and KIR3DL1 surface expression of donors included in this work. The B-content score, KIR genotype group and the centromeric and telomeric gene content motif were assessed as described by (Cooley et al., 2010).* indicates KIR DNA genotype (Q-PCR), ° indicates KIR RNA expression (Q-RT-PCR) and # indicates 3DL1 protein expression (flow cytometry, clone DX9). ■ = present, □ = absent, ND = not determined. (+): very weak, +: low, ++: positive, +++: strong and -: absent expression (Kübler et al., 2014)[i].

	B-content score	KIR Geno-type	Cen	Tel	2DL1		2DL2		2DL3		2DL4		2DL5		3DL1			3DL2		3DL3		2DS1		2DS2		2DS3		2DS4		2DS5		3DS1	
					*	°	*	°	*	°	*	°	*	°	*	°	#	*	°	*	°	*	°	*	°	*	°	*	°	*	°	*	°
SNK9A	2	B/x	A/B	A/B	■	■	■	■	■	■	■	■	■	■	■	■	+	■	■	■	■	■	■	■	■	□	□	□	■	■	■	■	■
SNK10P	0	A/A	A/A	A/A	■	■	□	□	■	■	■	■	□	□	■	■	+	■	■	■	■	□	□	□	□	□	□	□	■	■	□	□	□	□
SNK21BC	1	B/x	A/B	A/A	■	■	■	■	■	■	■	■	■	■	■	■	++	■	■	■	■	□	□	■	■	■	■	■	■	■	□	□	□	□
SNK13B	2	B/x	A/B	A/B	■	■	■	■	■	■	■	■	■	■	■	■	-	■	■	■	□	■	■	■	■	■	■	■	■	■	□	□	□	□
SNK14B	1	B/x	A/B	A/A	■	■	■	■	■	■	■	■	□	□	■	■	++	■	■	■	■	□	□	■	■	□	□	□	■	■	□	□	□	□
SNK15B	0	A/A	A/A	A/A	■	■	□	□	■	■	■	■	□	□	■	■	+	■	■	■	■	□	□	□	□	□	□	□	■	■	□	□	□	□
SNK20B	1	B/x	A/B	A/A	■	■	■	■	■	■	■	■	□	□	■	■	++	■	■	■	■	□	□	■	■	□	□	□	■	■	□	□	□	□
SSC18U	0	A/A	A/A	A/A	■	■	□	□	■	■	■	■	□	□	■	■	(+)	■	■	■	□	□	□	□	□	□	□	□	■	■	□	□	□	□
SSC52G	1	B/x	A/B	A/A	■	ND	■	ND	■	ND	■	ND	■	ND	■	ND	-	■	ND	□	ND	□	ND	■	ND	■	ND	■	ND	□	ND	□	ND

REFERENCES

Abdul-Hamid, G. Classification of Acute Leukemia. Acute Leukemia - The Scientist's Perspective and Challenge, M. Antica (Ed.), InTech, 2011. Available from: http://www.intechopen.com/books/acute-leukemia-the-scientist-s-perspective-and-challenge/classification-ofacute-leukemia.

Alves, L.G.T., Rajalingam, R., and Canavez, F. A novel real-time PCR method for KIR genotyping. *Tissue Antigens*. 2008; 73: 188-191.

Andersson, S., Fauriat, C., Malmberg, J.-A., Ljunggren, H.-G., and Malmberg, K.-J. KIR acquisition probabilities are independent of self-HLA class I ligands and increase with cellular KIR expression. *Blood*. 2009; 114(1): 95-104.

André, M.C., Erbacher, A., Gille, C., Schmauke, V., Goecke, B., Hohberger, A., Mang, P., Wilhelm, A., Mueller, I., Herr, W., Lang, P., Handgretinger, R., and Hartwig, U.F. Long-Term Human CD34+ Stem Cell-Engrafted Nonobese Diabetic/SCID/IL-2Rγ null Mice Show Impaired CD8+ T Cell Maintenance and a Functional Arrest of Immature NK Cells. *J Immunol*. 2010; 185(5): 2710-2720.

Anfossi, N., André, P., Guia, S., Falk, C.S., Roetynck, S., Stewart, C.A., Breso, V., Frassati, C., Reviron, D., Middleton, D., Romagné, F., Ugolini, S., and Vivier, E. Human NK Cell Education by Inhibitory Receptors for MHC Class I. *Immunity*. 2006; 25(2): 331-342.

Annesley, C.E., and Brown, P. Novel agents for the treatment of childhood acute leukemia. *Therapeutic Advances in Hematology*. 2015; 6(2): 61-79.

Arase, H., Arase, N., and Saito, T. Fas-mediated cytotoxicity by freshly isolated natural killer cells. *J Exp Med*. 1995; 181(3): 1235-1238.

Arnon, T.I., Lev, M., Katz, G., Chernobrov, Y., Porgador, A., and Mandelboim, O. Recognition of viral hemagglutinins by NKp44 but not by NKp30. *Eur J Immunol*. 2001; 31(9): 2680-2689.

Auchincloss Jr, H., and Sultan, H. Antigen processing and presentation in transplantation. *Curr Opin Immunol*. 1996; 8(5): 681-687.

Babor, F., Fischer, J.C., and Uhrberg, M. The role of KIR genes and ligands in leukemia surveillance. *Front Immunol*. 2013; 4: 2248-2251.

Bargou, R., Leo, E., Zugmaier, G., Klinger, M., Goebeler, M., Knop, S., Noppeney, R., Viardot, A., Hess, G., Schuler, M., Einsele, H., Brandl, C., Wolf, A., Kirchinger, P., Klappers, P., Schmidt, M., Riethmüller, G., Reinhardt, C., Baeuerle, P.A., and Kufer, P. Tumor Regression in Cancer Patients by Very Low Doses of a T Cell–Engaging Antibody. *Science*. 2008; 321(5891): 974-977.

Baychelier, F., Sennepin, A., Ermonval, M., Dorgham, K., Debré, P., and Vieillard, V. Identification of a cellular ligand for the natural cytotoxicity receptor NKp44. *Blood*. 2013; 122(17): 2935-2942.

Bessoles, S., Angelov, G.S., Back, J., Leclercq, G., Vivier, E., and Held, W. Education of Murine NK Cells Requires Both cis and trans Recognition of MHC Class I Molecules. *J Immunol*. 2013; 191(10): 5044-5051.

Bessoles, S., Grandclément, C., Alari-pahissa, E., Gehrig, J., Jeevan-Raj, B., and Held, W. Adaptations of natural killer cells to self-MHC class I. *Front Immunol*. 2014; 5: 1-6.

Béziat, V., Descours, B., Parizot, C., Debre, P., and Vieillard, V. NK Cell Terminal Differentiation : Correlated Stepwise Decrease of NKG2A and Acquisition of KIRs. *PLoS ONE*. 2010; 5(8): 1-12.

Bonnema, J.D., Rivlin, K.A., Ting, A.T., Schoon, R.A., Abraham, R.T., and Leibson, P.J. Cytokine-enhanced NK cell-mediated cytotoxicity. Positive modulatory effects of IL-2 and IL-12 on stimulus-dependent granule exocytosis. *J Immunol*. 1994; 152(5): 2098-2104.

Bottino, C., Castriconi, R., Pende, D., Rivera, P., Nanni, M., Carnemolla, B., Cantoni, C., Grassi, J., Marcenaro, S., Reymond, N., Vitale, M., Moretta, L., Lopez, M., and Moretta, A. Identification of PVR (CD155) and Nectin-2 (CD112) as Cell Surface Ligands for the Human DNAM-1 (CD226) Activating Molecule. *J Exp Med*. 2003; 198(4): 557-567.

Brandt, C.S., Baratin, M., Yi, E.C., Kennedy, J., Gao, Z., Fox, B., Haldeman, B., Ostrander, C.D., Kaifu, T., Chabannon, C., Moretta, A., West, R., Xu, W., Vivier, E., and Levin, S.D. The B7 family member B7-H6 is a tumor cell ligand for the activating natural killer cell receptor NKp30 in humans. *J Exp Med*. 2009; 206(7): 1495-1503.

Braud, V.M., Allan, D.S.J., O'Callaghan, C.A., Soderstrom, K., D'Andrea, A., Ogg, G.S., Lazetic, S., Young, N.T., Bell, J.I., Phillips, J.H., Lanier, L.L., and McMichael, A.J. HLA-E binds to natural killer cell receptors CD94/NKG2A, B and C. *Nature*. 1998; 391: 795-799.

Brodin, P., Kärre, K., and Höglund, P. NK cell education : not an on-off switch but a tunable rheostat. *Trends Immunol*. 2009; 30(4): 143-149.

Brodin, P., Lakshmikanth, T., Johansson, S., Kärre, K., and Höglund, P. The strength of inhibitory input during education quantitatively tunes the functional responsiveness of individual natural killer cells. *Blood*. 2008; 113(11): 2434-2441.

Brown, M.H., Boles, K., Anton van der Merwe, P., Kumar, V., Mathew, P.A., and Neil Barclay, A. 2B4, the Natural Killer and T Cell Immunoglobulin Superfamily Surface Protein, Is a Ligand for CD48. *J Exp Med*. 1998; 188(11): 2083-2090.

Bryceson, Y.T., March, M.E., Barber, D.F., Ljunggren, H.-G., and Long, E.O. Cytolytic granule polarization and degranulation controlled by different receptors in resting NK cells. *J Exp Med*. 2005; 202(7): 1001-1012.

Burns, L.J., Weisdorf, D.J., DeFor, T.E., Vesole, D.H., Repka, T.L., Blazar, B.R., Burger, S.R., Panoskaltsis-Mortari, A., Keever-Taylor, C.A., Zhang, M.J., and Miller, J.S. IL-2-based immunotherapy after autologous transplantation for lymphoma and breast cancer induces immune activation and cytokine release: a phase I//II trial. *Bone Marrow Transplant*. 2003; 32(2): 177-186.

Caligiuri, M.A. Human natural killer cells. *Blood*. 2008; 112: 461-469.

Campana, D. Minimal Residual Disease in Acute Lymphoblastic Leukemia. *ASH Education Program Book*. 2010; 2010(1): 7-12.

Campbell, K.S., and Purdy, A.K. Structure / function of human killer cell immunoglobulin-like receptors: lessons from polymorphisms, evolution, crystal structures and mutations. *Immunology*. 2011; 132: 315-325.

Cannons, J.L., Lau, P., Ghumman, B., DeBenedette, M.A., Yagita, H., Okumura, K., and Watts, T.H. 4-1BB Ligand Induces Cell Division, Sustains Survival, and Enhances Effector Function of CD4 and CD8 T Cells with Similar Efficacy. *J Immunol*. 2001; 167(3): 1313-1324.

Castillo, E.F., Stonier, S.W., Frasca, L., and Schluns, K.S. Dendritic Cells Support the In Vivo Development and Maintenance of NK Cells via IL-15 Trans-Presentation. *J Immunol*. 2009; 183: 4948-4956.

Chan, H.-W., Kurago, Z.B., Stewart, C.A., Wilson, M.J., Martin, M.P., Mace, B.E., Carrington, M., Trowsdale, J., and Lutz, C.T. DNA Methylation Maintains Allele-specific KIR Gene Expression in Human Natural Killer Cells. *J Exp Med*. 2003; 197(2): 245-255.

Chan, H.-W., Miller, J.S., Moore, M.B., and Lutz, C.T. Epigenetic Control of Highly Homologous Killer Ig-Like Receptor Gene Alleles. *J Immunol*. 2005; 175(9): 5966-5974.

Chiaretti, S., and Foà, R. T-cell acute lymphoblastic leukemia. *Haematologica*. 2009; 94(2): 160-162.

Christman, J.K. 5-Azacytidine and 5-aza-2 '-deoxycytidine as inhibitors of DNA methylation : mechanistic studies and their implications for cancer therapy. *Oncogene*. 2002; 21: 5483-5495.

Clausen, J., Wolf, D., Petzer, A.L., Gunsilius, E., Schumacher, P., Kircher, B., Gastl, G., and Nachbaur, D. Impact of natural killer cell dose and donor killer-cell immunoglobulin-like receptor (KIR) genotype on outcome following human leucocyte antigen-identical haematopoietic stem cell transplantation. *Clin Exp Immunol*. 2007; 148(3): 520-528.

Colucci, F., Caligiuri, M.A., and Di Santo, J.P. What does it take to make a natural killer? *Nat Rev Immunol*. 2003; 3: 413-425.

Colucci, F., Samson, S.I., DeKoter, R.P., Lantz, O., Singh, H., and Di Santo, J.P. Differential requirement for the transcription factor PU.1 in the generation of natural killer cells versus B and T cells. *Blood*. 2001; 97(9): 2625-2632.

Cooley, S., Weisdorf, D.J., Guethlein, L.A., Klein, J.P., Wang, T., Le, C.T., Marsh, S.G.E., Geraghty, D., Spellman, S., Haagenson, M.D., Ladner, M., Trachtenberg, E., Parham, P., and Miller, J.S. Donor selection for natural killer cell receptor genes leads to superior survival after unrelated transplantation for acute myelogenous leukemia. *Blood*. 2010; 116(14): 2411-2419.

Cooper, M.A., Fehniger, T.A., and Caligiuri, M.A. The biology of human natural killer-cell subsets. *Trends Immunol*. 2001; 22(11): 633-640.

Curik, N., Burda, P., Vargova, K., Pospisil, V., Belickova, M., Vlckova, P., Savvulidi, F., Necas, E., Hajkova, H., Haskovec, C., Cermak, J., Krivjanska, M., Trneny, M., Laslo, P., Jonasova, A., and Stopka, T. 5-Azacitidine in aggressive myelodysplastic syndromes regulates chromatin structure at PU.1 gene and cell differentiation capacity. *Leukemia*. 2012; 26(8): 1804-1811.

De Lima, M., Giralt, S., Thall, P.F., de Padua Silva, L., Jones, R.B., Komanduri, K., Braun, T.M., Nguyen, H.Q., Champlin, R., and Garcia-Manero, G. Maintenance therapy with low-dose azacitidine after allogeneic hematopoietic stem cell transplantation for recurrent acute myelogenous leukemia or myelodysplastic syndrome. *Cancer*. 2010; 116(23): 5420-5431.

Derissen, E.J.B., Beijnen, J.H., and Schellens, J.H.M. Concise Drug Review: Azacitidine and Decitabine. *The Oncologist*. 2013; 18(5): 619-624.

Dick, J.E. Stem cell concepts renew cancer research. *Blood*. 2008; 112(13): 4793-4807.

DiSanto, J.P., Keever, C.A., Small, T.N., Nicols, G.L., O'Reilly, R.J., and Flomenberg, N. Absence of interleukin 2 production in a severe combined immunodeficiency disease syndrome with T cells. *J Exp Med*. 1990; 171(5): 1697-1704.

Dowell, A., Oldham, K., Bhatt, R., Lee, S., and Searle, P. Long-term proliferation of functional human NK cells, with conversion of CD56dim NK cells to a CD56bright phenotype, induced by carcinoma cells co-expressing 4-1BBL and IL-12. *Cancer Immunol Immunother*. 2012; 61(5): 615-628.

Dubois, S., Mariner, J., Waldmann, T.A., and Tagaya, Y. IL-15Rα Recycles and Presents IL-15 In trans to Neighboring Cells. *Immunity*. 2002; 17(5): 537-547.

Elliott, J.M., Wahle, J.A., and Yokoyama, W.M. MHC class I–deficient natural killer cells acquire a licensed phenotype after transfer into an MHC class I–sufficient environment. *J Exp Med*. 2010; 207(10): 2073-2079.

Fehniger, T.A., Cooper, M.A., Nuovo, G.J., Cella, M., Facchetti, F., Colonna, M., and Caligiuri, M.A. CD56bright natural killer cells are present in human lymph nodes and are activated by T cell–derived IL-2: a potential new link between adaptive and innate immunity. *Blood*. 2003; 101(8): 3052-3057.

Fenaux, P., Mufti, G.J., Hellstrom-Lindberg, E., Santini, V., Finelli, C., Giagounidis, A., Schoch, R., Gattermann, N., Sanz, G., List, A., Gore, S.D., Seymour, J.F., Bennett, J.M., Byrd, J., Backstrom, J., Zimmerman, L., McKenzie, D., Beach, C.L., and Silverman, L.R. Efficacy of azacitidine compared with that of conventional care regimens in the treatment of higher-risk myelodysplastic syndromes: a randomised, open-label, phase III study. *Lancet Oncol*. 2009; 10(3): 223-232.

Fernandez, N.C., Treiner, E., Vance, R.E., Jamieson, A.M., Lemieux, S., and Raulet, D.H. A subset of natural killer cells achieves self-tolerance without expressing inhibitory receptors specific for self-MHC molecules. *Blood*. 2005; 105: 4416-4423.

Feuchtinger, T., Pfeiffer, M., Pfaffle, A., Teltschik, H.M., Wernet, D., Schumm, M., Lotfi, R., Handgretinger, R., and Lang, P. Cytolytic activity of NK cell clones against acute childhood precursor-B-cell leukaemia is influenced by HLA class I expression on blasts and the differential KIR phenotype of NK clones. *Bone Marrow Transplant*. 2009; 43: 875-881.

Freireich, E.J., Wiernik, P.H., and Steensma, D.P. The Leukemias: A Half-Century of Discovery. *J Clin Oncol*. 2014; 32(31): 3463-3469.

Freud, A.G., and Caligiuri, M.A. Human natural killer cell development. *Immunol Rev*. 2006; 214: 56-72.

Freud, A.G., Yokohama, A., Becknell, B., Lee, M.T., Mao, H.C., Ferketich, A.K., and Caligiuri, M.A. Evidence for discrete stages of human natural killer cell differentiation in vivo. *J Exp Med*. 2006; 203(4): 1033-1043.

Frikeche, J., Clavert, A., Delaunay, J., Brissot, E., Grégoire, M., Gaugler, B., and Mohty, M. Impact of the hypomethylating agent 5-azacytidine on dendritic cells function. *Exp Hematol*. 2011; 39(11): 1056-1063.

Fujisaki, H., Kakuda, H., Shimasaki, N., Lockey, T., Eldridge, P., Leung, W.H., and Campana, D. Expansion of Highly Cytotoxic Human Natural Killer Cells for Cancer Cell Therapy. *Cancer Res*. 2009; 69(9): 4010-4017.

Gao, X.-n., Lin, J., Wang, L.-l., and Yu, L. Demethylating treatment suppresses natural killer cell cytolytic activity. *Mol Immunol*. 2009; 46: 2064-2070.

Gordon, S.M., Chaix, J., Rupp, L.J., Wu, J., Madera, S., Sun, J.C., Lindsten, T., and Reiner, S.L. The Transcription Factors T-bet and Eomes Control Key Checkpoints of Natural Killer Cell Maturation. *Immunity*. 2012; 36: 55-67.

Habib-Agahi, M., Phan, T.T., and Searle, P.F. Co-stimulation with 4-1BB ligand allows extended T-cell proliferation, synergizes with CD80/CD86 and can reactivate anergic T cells. *Int Immunol*. 2007; 19(12): 1383-1394.

Hagemann, S., Heil, O., Lyko, F., and Brueckner, B. Azacytidine and Decitabine Induce Gene-Specific and Non-Random DNA Demethylation in Human Cancer Cell Lines. *PLoS ONE*. 2011; 6(3): e17388.

Handgretinger, R. Negative depletion of CD3+ and TcR[alpha][beta]+ T cells. *Curr Opin Hematol*. 2012; 19(6): 434-439.

Howlader, N., Noone, A., Krapcho, M., Garshell, J., Miller, D., Altekruse, S., Kosary, C., Yu, M., Ruhl, J., Tatalovich, Z., Mariotto, A., Lewis, D., Chen, H., Feuer, E., and Cronin, K.e. SEER Cancer Statistics Review, 1975-2011, National Cancer Institute. Bethesda, MD, http://seer.cancer.gov/csr/1975_2011/, based on November 2013 SEER data submission, posted to the SEER web site, April 2014. 2014.

Hsu, K.C., Keever-Taylor, C.A., Wilton, A., Pinto, C., Heller, G., Arkun, K., Reilly, R.J., Horowitz, M.M., and Dupont, B. Improved outcome in HLA-identical sibling hematopoietic stem-cell transplantation for acute myelogenous leukemia predicted by KIR and HLA genotypes. *Blood*. 2005; 105(12): 4878-4884.

Hu, Z., Negrotto, S., Gu, X., Mahfouz, R., Ng, K.P., Ebrahem, Q., Copelan, E., Singh, H., Maciejewski, J.P., and Saunthararajah, Y. Decitabine Maintains Hematopoietic Precursor Self-Renewal by Preventing Repression of Stem Cell Genes by a Differentiation-Inducing Stimulus. *Mol Cancer Ther*. 2010; 9(6): 1536-1543.

Huergo-Zapico, L., Acebes-Huerta, A., López-Soto, A., Villa-Álvarez, M., Gonzalez-Rodriguez, A.P., and Gonzalez, S. Molecular bases for the regulation of NKG2D ligands in cancer. *Front Immunol*. 2014; 5(106.

Huntington, N.D., Legrand, N., Alves, N.L., Jaron, B., Weijer, K., Plet, A., Corcuff, E., Mortier, E., Jacques, Y., Spits, H., and Santo, J.P.D. IL-15 trans-presentation promotes human NK cell development and diff erentiation in vivo. *J Exp Med*. 2009; 206(1): 25-34.

Huntington, N.D., Vosshenrich, C.A.J., and Di Santo, J.P. Developmental pathways that generate natural-killer-cell diversity in mice and humans. *Nat Rev Immunol*. 2007; 7(9): 703-714.

Imai, C., Iwamoto, S., and Campana, D. Genetic modification of primary natural killer cells overcomes inhibitory signals and induces specific killing of leukemic cells. *Blood*. 2005; 106: 376-383.

Issa, J.-P.J. DNA Methylation as a Therapeutic Target in Cancer. *Clin Cancer Res*. 2007; 13(6): 1634-1637.

Issa, J.-P.J. The myelodysplastic syndrome as a prototypical epigenetic disease. *Blood*. 2013; 121(19): 3811-3817.

Jabbour, E., Giralt, S., Kantarjian, H., Garcia-Manero, G., Jagasia, M., Kebriaei, P., de Padua, L., Shpall, E.J., Champlin, R., and de Lima, M. Low-dose azacitidine after allogeneic stem cell transplantation for acute leukemia. *Cancer*. 2009; 115(9): 1899-1905.

Jarahian, M., Fiedler, M., Cohnen, A., Djandji, D., Hämmerling, G.J., Gati, C., Cerwenka, A., Turner, P.C., Moyer, R.W., Watzl, C., Hengel, H., and Momburg, F. Modulation of NKp30- and NKp46-Mediated Natural Killer Cell Responses by Poxviral Hemagglutinin. *PLoS Pathog*. 2011; 7(8): e1002195.

Joncker, N.T., Fernandez, N.C., Treiner, E., Vivier, E., and Raulet, D.H. NK Cell Responsiveness Is Tuned Commensurate with the Number of Inhibitory Receptors for Self-MHC Class I: The Rheostat Model. *J Immunol*. 2009; 182(8): 4572-4580.

Joncker, N.T., Shifrin, N., Delebecque, F., and Raulet, D.H. Mature natural killer cells reset their responsiveness when exposed to an altered MHC environment. *J Exp Med*. 2010; 207(10): 2065-2072.

Jones, P.A., and Baylin, S.B. The Epigenomics of Cancer. *Cell*. 2007; 128(4): 683-692.

Kaminskas, E., Farrell, A.T., Wang, Y.-C., Sridhara, R., and Pazdur, R. FDA Drug Approval Summary: Azacitidine (5-azacytidine, Vidaza™) for Injectable Suspension. *The Oncologist*. 2005; 10(3): 176-182.

Karre, K., Ljunggren, H.G., Piontek, G., and Kiessling, R. Selective rejection of H-2-deficient lymphoma variants suggests alternative immune defence strategy. *Nature*. 1986; 319(6055): 675-678.

Kayagaki, N., Yamaguchi, N., Nakayama, M., Takeda, K., Akiba, H., Tsutsui, H., Okamura, H., Nakanishi, K., Okumura, K., and Yagita, H. Expression and Function of TNF-Related Apoptosis-Inducing Ligand on Murine Activated NK Cells. *J Immunol*. 1999; 163(4): 1906-1913.

Kekre, N., and Antin, J.H. Hematopoietic stem cell transplantation donor sources in the 21st century: choosing the ideal donor when a perfect match does not exist. *Blood*. 2014; 124(3): 334-343.

Kennedy, M.K., Glaccum, M., Brown, S.N., Butz, E.A., Viney, J.L., Embers, M., Matsuki, N., Charrier, K., Sedger, L., Willis, C.R., Brasel, K., Morrissey, P.J., Stocking, K., Schuh, J.C.L., Joyce, S., and Peschon, J.J. Reversible Defects in Natural Killer and Memory CD8 T Cell Lineages in Interleukin 15–deficient Mice. *J Exp Med*. 2000; 191(5): 771-780.

Kim, S., Poursine-laurent, J., Truscott, S.M., Lybarger, L., Song, Y.-j., Yang, L., French, A.R., Sunwoo, J.B., Lemieux, S., Hansen, T.H., and Yokoyama, W.M. Licensing of natural killer cells by host major histocompatibility complex class I molecules. *Nature*. 2005; 436(4): 709-713.

Kim, S., Sunwoo, J.B., Yang, L., Choi, T., Song, Y.-J., French, A.R., Vlahiotis, A., Piccirillo, J.F., Cella, M., Colonna, M., Mohanakumar, T., Hsu, K.C., Dupont, B., and Yokoyama, W.M. HLA alleles determine differences in human natural killer cell responsiveness and potency. *Proc Natl Acad Sci USA*. 2008; 105(8): 3053-3058.

Kübler, A., Woiterski, J., Witte, K.-E., Bühring, H.-J., Hartwig, U.F., Ebinger, M., Oevermann, L., Mezger, M., Herr, W., Lang, P., Handgretinger, R., Münz, C., and André, M.C. Both mature KIR+ and immature KIR− NK cells control pediatric acute B-cell precursor leukemia in NOD.Cg-Prkdcscid IL2rgtmWjl/Sz mice. *Blood*. 2014; 124(26): 3914-3923.

Kundig, T.M., Schorle, H., Bachmann, M.F., Hengartner, H., Zinkernagel, R.M., and Horak, I. Immune Responses in Interleukin-2-Deficient Mice. *Science*. 1993; 262: 1059-1061.

Lamb, L.S., Jr., Gee, A.P., Henslee-downey, P.J., Geier, S.S., Hazlett, L., Pati, A.R., Godder, K., Abhyankar, S.A., Turner, M.W., Lee, C., Harris, W.G., and Parrish, R.S. Phenotypic and functional reconstitution of peripheral blood lymphocytes following T cell-depleted bone marrow transplantation from partially mismatched related donors. *Bone Marrow Transplant*. 1998; 21: 461-471.

Lanier, L.L., Corliss, B.C., Wu, J., Leong, C., and Phillips, J.H. Immunoreceptor DAP12 bearing a tyrosine-based activation motif is involved in activating NK cells. *Nature*. 1998; 391(6668): 703-707.

Lanier, L.L., Le, A.M., Civin, C.I., Loken, M.R., and Phillips, J.H. The relationship of CD16 (Leu-11) and Leu-19 (NKH-1) antigen expression on human peripheral blood NK cells and cytotoxic T lymphocytes. *J Immunol*. 1986; 136(12): 4480-4486.

Lanier, L.L., Testi, R., Bindl, J., and Phillips, J.H. Identity of Leu-19 (CD56) leukocyte differentiation antigen and neural cell adhesion molecule. *J Exp Med*. 1989; 169(6): 2233-2238.

Lapidot, T., Sirard, C., Vormoor, J., Murdoch, B., Hoang, T., Caceres-Cortes, J., Minden, M., Paterson, B., Caligiuri, M.A., and Dick, J.E. A cell initiating human acute myeloid leukaemia after transplantation into SCID mice. *Nature*. 1994; 367(6464): 645-648.

le Viseur, C., Hotfilder, M., Bomken, S., Wilson, K., Röttgers, S., Schrauder, A., Rosemann, A., Irving, J., Stam, R.W., Shultz, L.D., Harbott, J., Jürgens, H., Schrappe, M., Pieters, R., and Vormoor, J. In Childhood Acute Lymphoblastic Leukemia, Blasts at Different Stages of Immunophenotypic Maturation Have Stem Cell Properties. *Cancer Cell*. 2008; 14(1): 47-58.

Leung, W., Iyengar, R., Turner, V., Lang, P., Bader, P., Conn, P., Niethammer, D., and Handgretinger, R. Determinants of Antileukemia Effects of Allogeneic NK Cells. *J Immunol*. 2004; 172(1): 644-650.

Livak, K.J., and Schmittgen, T.D. Analysis of Relative Gene Expression Data Using Real- Time Quantitative PCR and the 2-ΔΔ CT Method. *Methods*. 2001; 25: 402-408.

Lowin-Kropf, B., Kunz, B., Beermann, F., and Held, W. Impaired Natural Killing of MHC Class I-Deficient Targets by NK Cells Expressing a Catalytically Inactive Form of SHP-1. *J Immunol*. 2000; 165: 1314-1321.

Lubbert, M., Bertz, H., Wasch, R., Marks, R., Ruter, B., Claus, R., and Finke, J. Efficacy of a 3-day, low-dose treatment with 5-azacytidine followed by donor lymphocyte infusions in older patients with acute

myeloid leukemia or chronic myelomonocytic leukemia relapsed after allografting. *Bone Marrow Transplant*. 2010; 45(4): 627-632.

Male, V., Nisoli, I., Kostrzewski, T., Allan, D.S.J., Carlyle, J.R., Lord, G.M., Wack, A., and Brady, H.J.M. The transcription factor E4bp4/Nfil3 controls commitment to the NK lineage and directly regulates Eomes and Id2 expression. *J Exp Med*. 2014; 211(4): 635-642.

Mandelboim, O., Lieberman, N., Lev, M., Paul, L., Arnon, T.I., Bushkin, Y., Davis, D.M., Strominger, J.L., Yewdell, J.W., and Porgador, A. Recognition of haemagglutinins on virus-infected cells by NKp46 activates lysis by human NK cells. *Nature*. 2001; 409(6823): 1055-1060.

McErlean, C., Gonzalez, A.A., Cunningham, R., Meenagh, A., Shovlin, T., and Middleton, D. Differential RNA expression of KIR alleles. *Immunogenetics*. 2010; 62: 431-440.

McGregor, S., McNeer, J., and Gurbuxani, S. Beyond the 2008 World Health Organization classification: the role of the hematopathology laboratory in the diagnosis and management of acute lymphoblastic leukemia. *Semin Diagn Pathol*. 2012; 29(1): 2-11.

Mengarelli, A., Zarcone, D., Caruso, R., Tenca, C., Rana, I., Pinto, R.M., Grossi, C.E., and Rossi, G.D. Adhesion Molecule Expression, Clinical Features and Therapy Outcome in Childhood Acute Lymphoblastic Leukemia. *Leukemia & Lymphoma*. 2001; 40(5-6): 625-630.

Milhem, M., Mahmud, N., Lavelle, D., Araki, H., DeSimone, J., Saunthararajah, Y., and Hoffman, R. Modification of hematopoietic stem cell fate by 5aza 2′deoxycytidine and trichostatin A. *Blood*. 2004; 103(11): 4102-4110.

Miller, J.S., and McCullar, V. Human natural killer cells with polyclonal lectin and immunoglobulinlike receptors develop from single hematopoietic stem cells with preferential expression of NKG2A and KIR2DL2/L3/S2. *Blood*. 2001; 98(3): 705-713.

Miller, J.S., Soignier, Y., Panoskaltsis-Mortari, A., McNearney, S.A., Yun, G.H., Fautsch, S.K., McKenna, D., Le, C., Defor, T.E., Burns, L.J., Orchard, P.J., Blazar, B.R., Wagner, J.E., Slungaard, A., Weisdorf, D.J., Okazaki, I.J., and McGlave, P.B. Successful adoptive transfer and in vivo expansion of human haploidentical NK cells in patients with cancer. *Blood*. 2005; 105(8): 3051-3057.

Moricke, A., Zimmermann, M., Reiter, A., Henze, G., Schrauder, A., Gadner, H., Ludwig, W.D., Ritter, J., Harbott, J., Mann, G., Klingebiel, T., Zintl, F., Niemeyer, C., Kremens, B., Niggli, F., Niethammer, D., Welte, K., Stanulla, M., Odenwald, E., Riehm, H., and Schrappe, M. Long-term results of five consecutive trials in childhood acute lymphoblastic leukemia performed by the ALL-BFM study group from 1981 to 2000. *Leukemia*. 2009; 24(2): 265-284.

Musch, T., Öz, Y., Lyko, F., and Breiling, A. Nucleoside Drugs Induce Cellular Differentiation by Caspase-Dependent Degradation of Stem Cell Factors. *PLoS ONE*. 2010; 5(5): e10726.

Nguyen, S., Dhedin, N., Vernant, J.-p., Kuentz, M., Al Jijakli, A., Carosella, E.D., Boudifa, A., Debré, P., and Vieillard, V. NK-cell reconstitution after haploidentical hematopoietic stem-cell transplantations : immaturity of NK cells and inhibitory effect of NKG2A override GvL effect. *Blood*. 2005; 105: 4135-4142.

North, J., Bakhsh, I., Marden, C., Pittman, H., Addison, E., Navarrete, C., Anderson, R., and Lowdell, M.W. Tumor-Primed Human Natural Killer Cells Lyse NK-Resistant Tumor Targets: Evidence of a Two-Stage Process in Resting NK Cell Activation. *J Immunol*. 2007; 178: 85-94.

Numoto, K., Yoshida, A., Sugihara, S., Kunisada, T., Morimoto, Y., Yoneda, Y., Fujita, Y., Nishida, K., Ouchida, M., and Ozaki, T. Frequent methylation of RASSF1A in synovial sarcoma and the anti-tumor effects of 5-aza-2'-deoxycytidine against synovial sarcoma cell lines. *J Cancer Res Clin Oncol*. 2010; 136: 17-25.

O'Shea, J.J., Ma, A., and Lipsky, P. Cytokines and autoimmunity. *Nat Rev Immunol*. 2002; 2(1): 37-45.

Oevermann, L., Michaelis, S.U., Mezger, M., Lang, P., Toporski, J., Bertaina, A., Zecca, M., Moretta, L., Locatelli, F., and Handgretinger, R. KIR B haplotype donors confer a reduced risk for relapse after haploidentical transplantation in children with ALL. *Blood*. 2014; 124(17): 2744-2747.

Olcese, L., Lang, P., Vély, F., Cambiaggi, A., Marguet, D., Bléry, M., Hippen, K.L., Biassoni, R., Moretta, A., Moretta, L., Cambier, J.C., and Vivier, E. Human and mouse killer-cell inhibitory receptors recruit PTP1C and PTP1D protein tyrosine phosphatases. *J Immunol*. 1996; 156(12): 4531-4534.

Orr, M.T., Murphy, W.J., and Lanier, L.L. ' Unlicensed ' natural killer cells dominate the response to cytomegalovirus infection. *Nat Immunol*. 2010; 11(4): 321-327.

Pando, M.J., Gardiner, C.M., Gleimer, M., McQueen, K.L., and Parham, P. The Protein Made from a Common Allele of KIR3DL1 (3DL1*004) Is Poorly Expressed at Cell Surfaces due to Substitution at Positions 86 in Ig Domain 0 and 182 in Ig Domain 1. *J Immunol*. 2003; 171: 6640-6649.

Pardo, J., Aguilo, J.I., Anel, A., Martin, P., Joeckel, L., Borner, C., Wallich, R., Müllbacher, A., Froelich, C.J., and Simon, M.M. The biology of cytotoxic cell granule exocytosis pathway: granzymes have evolved to induce cell death and inflammation. *Microbes Infect*. 2009; 11(4): 452-459.

Parham, P. MHC Class I Molecules and KIRs in Human History, Health and Survival. *Nat Rev Immunol*. 2005; 5: 201-214.

Parham, P., and Moffett, A. Variable NK cell receptors and their MHC class I ligands in immunity, reproduction and human evolution. *Nat Rev Immunol*. 2013; 13(2): 133-144.

Pende, D., Marcenaro, S., Falco, M., Martini, S., Bernardo, M.E., Montagna, D., Romeo, E., Cognet, C., Martinetti, M., Maccario, R., Mingari, M.C., Vivier, E., Moretta, L., Locatelli, F., and Moretta, A. Anti-leukemia activity of alloreactive NK cells in KIR ligand-mismatched haploidentical HSCT for pediatric patients: evaluation of the functional role of activating KIR and redefinition of inhibitory KIR specificity. *Blood*. 2009; 113(13): 3119-3129.

Pende, D., Spaggiari, G.M., Marcenaro, S., Martini, S., Rivera, P., Capobianco, A., Falco, M., Lanino, E., Pierri, I., Zambello, R., Bacigalupo, A., Mingari, M.C., Moretta, A., and Moretta, L. Analysis of the receptor-ligand interactions in the natural killer – mediated lysis of freshly isolated myeloid or lymphoblastic leukemias : evidence for the involvement of the Poliovirus receptor (CD155) and Nectin-2 (CD112). *Blood*. 2005; 105(5): 2066-2073.

Perussia, B., Tutt, M.M., Qiu, W.Q., Kuziel, W.A., Tucker, P.W., Trinchieri, G., Bennett, M., Ravetch, J.V., and Kumar, V. Murine natural killer cells express functional Fc gamma receptor II encoded by the Fc gamma R alpha gene. *J Exp Med*. 1989; 170(1): 73-86.

Petersdorf, E.W. HLA matching in allogeneic stem cell transplantation. *Curr Opin Hematol*. 2004; 11(6.

Pfeiffer, M., Schumm, M., Feuchtinger, T., Dietz, K., Handgretinger, R., and Lang, P. Intensity of HLA class I expression and KIR-mismatch determine NK-cell mediated lysis of leukaemic blasts from children with acute lymphatic leukaemia. *Br J Haematol*. 2007; 138: 97-100.

Pfeiffer, M.M., Feuchtinger, T., Teltschik, H.-M., Schumm, M., Müller, I., Handgretinger, R., and Lang, P. Reconstitution of natural killer cell receptors influences natural killer activity and relapse rate after haploidentical transplantation of T- and B-cell depleted grafts in children. *Haematologica*. 2010; 95(8): 1381-1388.

Pfeiffer, M.M., Schumm, M., Muller, I., Handgretinger, R., and Lang, P. IL-15-stimulated CD3/CD19-depleted stem-cell boosts in relapsed pediatric patients after haploidentical SCT. *Leukemia*. 2012; 26(11): 2435-2439.

Pískala, A., and Šorm, F. Nucleic acids components and their analogues. LI. Synthesis of 1-glycosyl derivatives of 5-azauracil and 5-azacytosine. *Collect Czech Chem C*. 1964; 29(9): 2060-2076.

Pui, C.-H., Carroll, W.L., Meshinchi, S., and Arceci, R.J. Biology, Risk Stratification, and Therapy of Pediatric Acute Leukemias: An Update. *J Clin Oncol*. 2011; 29(5): 551-565.

Pui, C.-H., and Evans, W.E. A 50-Year Journey to Cure Childhood Acute Lymphoblastic Leukemia. *Semin Hematol*. 2013; 50(3): 185-196.

Pui, C.-H., Robison, L.L., and Look, A.T. Acute lymphoblastic leukaemia. *The Lancet*. 2008; 371(9617): 1030-1043.

Rajagopalan, S., Fu, J., and Long, E.O. Cutting Edge: Induction of IFN-γ Production but Not Cytotoxicity by the Killer Cell Ig-Like Receptor KIR2DL4 (CD158d) in Resting NK Cells. *J Immunol*. 2001; 167(4): 1877-1881.

Ranson, T., Vosshenrich, C.A.J., Corcuff, E., Richard, O., Müller, W., and Di Santo, J.P. IL-15 is an essential mediator of peripheral NK-cell homeostasis. *Blood*. 2003; 101(12): 4887-4893.

Raulet, D.H., and Vance, R.E. Self-tolerance of natural killer cells. *Nat Rev Immunol*. 2006; 6(7): 520-531.

Ries, L.S., MA; Gurney, JG; Linet, M; Tamra, T; Young, JL; Bunin, GR; (eds). Cancer Incidence and Survival among Children and Adolescents: United States SEER Program 1975-1995, National Cancer Institute, SEER Program. *NIH Pub, Bethesda, MD*. 1999): No. 99-4649.

Rivera, G.K., Zhou, Y., Hancock, M.L., Gajjar, A., Rubnitz, J., Ribeiro, R.C., Sandlund, J.T., Hudson, M., Relling, M., Evans, W.E., and Pui, C.-H. Bone marrow recurrence after initial intensive treatment for childhood acute lymphoblastic leukemia. *Cancer*. 2005; 103(2): 368-376.

Rohner, A., Langenkamp, U., Siegler, U., Kalberer, C.P., and Wodnar-Filipowicz, A. Differentiation-promoting drugs up-regulate NKG2D ligand expression and enhance the susceptibility of acute myeloid leukemia cells to natural killer cell-mediated lysis. *Leuk Res*. 2007; 31(10): 1393-1402.

Romagné, F., André, P., Spee, P., Zahn, S., Anfossi, N., Gauthier, L., Capanni, M., Ruggeri, L., Benson, D.M., Blaser, B.W., Chiesa, M.D., Moretta, A., Vivier, E., Caligiuri, M.A., Velardi, A., and Wagtmann, N. Preclinical characterization of 1-7F9 , a novel human anti – KIR receptor therapeutic antibody that augments natural killer – mediated killing of tumor cells. *Blood*. 2009; 114(13): 2667-2677.

Rosenberg, S.A., Lotze, M.T., Muul, L.M., Chang, A.E., Avis, F.P., Leitman, S., Linehan, W.M., Robertson, C.N., Lee, R.E., Rubin, J.T., Seipp, C.A., Simpson, C.G., and White, D.E. A Progress Report on the Treatment of 157 Patients with Advanced Cancer Using Lymphokine-Activated Killer Cells and Interleukin-2 or High-Dose Interleukin-2 Alone. *N Engl J Med*. 1987; 316(15): 889-897.

Rubnitz, J.E., Inaba, H., Ribeiro, R.C., Pounds, S., Rooney, B., Bell, T., Pui, C.-H., and Leung, W. NKAML: A Pilot Study to Determine the Safety and Feasibility of Haploidentical Natural Killer Cell Transplantation in Childhood Acute Myeloid Leukemia. *J Clin Oncol*. 2010; 28(6): 955-959.

Ruggeri, L., Capanni, M., Casucci, M., Volpi, I., Tosti, A., Perruccio, K., Urbani, E., Negrin, R.S., Martelli, M.F., and Velardi, A. Role of Natural Killer Cell Alloreactivity in HLA-Mismatched Hematopoietic Stem Cell Transplantation. *Blood*. 1999; 94(1): 333-339.

Ruggeri, L., Capanni, M., Urbani, E., Perruccio, K., Shlomchik, W.D., Tosti, A., Posati, S., Rogaia, D., Frassoni, F., Aversa, F., Martelli, M.F., and Velardi, A. Effectiveness of Donor Natural Killer Cell Alloreactivity in Mismatched Hematopoietic Transplants. *Science*. 2002; 295(5562): 2097-2100.

Ruggeri, L., Mancusi, A., Capanni, M., Urbani, E., Carotti, A., Aloisi, T., Stern, M., Pende, D., Perruccio, K., Burchielli, E., Topini, F., Bianchi, E., Aversa, F., Martelli, M.F., and Velardi, A. Donor natural killer cell allorecognition of missing self in haploidentical hematopoietic transplantation for acute myeloid leukemia: challenging its predictive value. *Blood*. 2007; 110(1): 433-440.

Sánchez-Abarca, L.I., Gutierrez-Cosio, S., Santamaría, C., Caballero-Velazquez, T., Blanco, B., Herrero-Sánchez, C., García, J.L., Carrancio, S., Hernández-Campo, P., González, F.J., Flores, T., Ciudad, L., Ballestar, E., del Cañizo, C., San Miguel, J.F., and Pérez-Simon, J.A. Immunomodulatory effect of 5-azacytidine (5-azaC): potential role in the transplantation setting. *Blood*. 2009; 115(1): 107-121.

Sanchez-Correa, B., Morgado, S., Gayoso, I., Bergua, J., Casado, J., Arcos, M., Bengochea, M., Duran, E., Solana, R., and Tarazona, R. Human NK cells in acute myeloid leukaemia patients: analysis of NK cell-activating receptors and their ligands. *Cancer Immunol Immunother*. 2011; 60(8): 1195-1205.

Santourlidis, S., Graffmann, N., Christ, J., and Uhrberg, M. Lineage-Specific Transition of Histone Signatures in the Killer Cell Ig-Like Receptor Locus from Hematopoietic Progenitor to NK Cells. *J Immunol*. 2008; 180: 418-425.

Santourlidis, S., Trompeter, H.-I., Weinhold, S., Eisermann, B., Meyer, K.L., Wernet, P., and Uhrberg, M. Crucial Role of DNA Methylation in Determination of Clonally Distributed Killer Cell Ig-like Receptor Expression Patterns in NK Cells. *J Immunol*. 2002; 169: 4253-4261.

Schipper, R.F., Amaro, J., and Oudshoorn, M. The probability of finding a suitable related donor for bone marrow transplantation in extended families [see comments]. *Blood*. 1996; 87(2): 800-804.

Schmiedel, B.J., Arélin, V., Gruenebach, F., Krusch, M., Schmidt, S.M., and Salih, H.R. Azacytidine impairs NK cell reactivity while decitabine augments NK cell responsiveness toward stimulation. *Int J Cancer*. 2011; 128: 2911-2922.

Schroder, K., Hertzog, P.J., Ravasi, T., and Hume, D.A. Interferon-γ: an overview of signals, mechanisms and functions. *J Leukoc Biol*. 2004; 75(2): 163-189.

Shen, L., Kantarjian, H., Guo, Y., Lin, E., Shan, J., Huang, X., Berry, D., Ahmed, S., Zhu, W., Pierce, S., Kondo, Y., Oki, Y., Jelinek, J., Saba, H., Estey, E., and Issa, J.-P.J. DNA Methylation Predicts Survival and Response to Therapy in Patients With Myelodysplastic Syndromes. *J Clin Oncol*. 2010; 28(4): 605-613.

Shultz, L.D., Ishikawa, F., and Greiner, D.L. Humanized mice in translational biomedical research. *Nat Rev Immunol*. 2007; 7: 118-130.

Shultz, L.D., Lyons, B.L., Burzenski, L.M., Gott, B., Chen, X., Chaleff, S., Kotb, M., Gillies, S.D., King, M., Mangada, J., Greiner, D.L., and Handgretinger, R. Human Lymphoid and Myeloid Cell Development in NOD/LtSz- scid IL2R γ null Mice Engrafted with Mobilized Human Hemopoietic Stem Cells. *J Immunol*. 2005; 174: 6477-6489.

Shultz, L.D., Schweitzer, P.A., Christianson, S.W., Gott, B., Schweitzer, I.B., Tennent, B., McKenna, S., Mobraaten, L., Rajan, T.V., and Greiner, D.L. Multiple defects in innate and adaptive immunologic function in NOD/LtSz-scid mice. *J Immunol*. 1995; 154(1): 180-191.

Sivori, S., Carlomagno, S., Pesce, S., Moretta, A., Vitale, M., and Marcenaro, E. TLR/NCR/KIR: which ones to use and when? *Front Immunol*. 2014; 5: 1-10.

Sivori, S., Pende, D., Bottino, C., Marcenaro, E., Pessino, A., Biassoni, R., Moretta, L., and Moretta, A. NKp46 is the major triggering receptor involved in the natural cytotoxicity of fresh or cultured human NK cells. Correlation between surface density of NKp46 and natural cytotoxicity against autologous, allogeneic or xenogeneic target cells. *Eur J Immunol*. 1999; 29(5): 1656-1666.

Smith, M., Arthur, D., Camitta, B., Carroll, A.J., Crist, W., Gaynon, P., Gelber, R., Heerema, N., Korn, E.L., Link, M., Murphy, S., Pui, C.H., Pullen, J., Reamon, G., Sallan, S.E., Sather, H., Shuster, J., Simon, R., Trigg, M., Tubergen, D., Uckun, F., and Ungerleider, R. Uniform approach to risk classification and treatment assignment for children with acute lymphoblastic leukemia. *J Clin Oncol*. 1996; 14(1): 18-24.

Spits, H., Artis, D., Colonna, M., Diefenbach, A., Santo, J.P.D., Eberl, G., Koyasu, S., Locksley, R.M., McKenzie, A.N.J., Mebius, R.E., Powrie, F., and Vivier, E. Innate lymphoid cells - a proposal for uniform nomenclature. *Nat Rev Immunol*. 2013; 13: 145-149.

Stern, M., Ruggeri, L., Capanni, M., Mancusi, A., and Velardi, A. Human leukocyte antigens A23 , A24 , and A32 but not A25 are ligands for KIR3DL1. *Blood*. 2008; 112(3): 708-710.

Stresemann, C., and Lyko, F. Modes of action of the DNA methyltransferase inhibitors azacytidine and decitabine. *Int J Cancer*. 2008; 123: 8-13.

Strowig, T., Chijioke, O., Carrega, P., Arrey, F., Meixlsperger, S., Rämer, P.C., Ferlazzo, G., and Münz, C. Human NK cells of mice with reconstituted human immune system components require preactivation to acquire functional competence. *Blood*. 2010; 116: 4158-4167.

Sugamura, K., Asao, H., Kondo, M., Tanaka, N., Ishii, N., Ohbo, K., Nakamura, M., and Takeshita, T. The Interleukin-2 Receptor γ Chain: Its Role in the Multiple Cytokine Receptor Complexes and T Cell Development in XSCID. *Annu Rev Immunol*. 1996; 14(1): 179-205.

Takenouchi, M., Hirai, S., Sakuragi, N., Yagita, H., Hamada, H., and Kato, K. Epigenetic Modulation Enhances the Therapeutic Effect of Anti − IL-13Rα2 Antibody in Human Mesothelioma Xenografts. *Clin Cancer Res*. 2011; 17: 2819-2829.

Tang, K.-F., He, C.-X., Zeng, G.-L., Wu, J., Song, G.-B., Shi, Y.-S., Zhang, W.-g., Huang, A.-L., Steinle, A., and Ren, H. Induction of MHC class I-related chain B (MICB) by 5-aza-2′-deoxycytidine. *Biochem Biophys Res Commun*. 2008; 370(4): 578-583.

Tang, X., Mo, C., Wang, Y., Wei, D., and Xiao, H. Anti-tumour strategies aiming to target tumour-associated macrophages. *Immunology*. 2013; 138(2): 93-104.

Thomas, L.M., Peterson, M.E., and Long, E.O. Cutting Edge: NK Cell Licensing Modulates Adhesion to Target Cells. *J Immunol*. 2013; 191: 3981-3985.

Thorburn, A. Death receptor-induced cell killing. *Cell Signal*. 2004; 16(2): 139-144.

Triozzi, P., Aldrich, W., Achberger, S., Ponnazhagan, S., Alcazar, O., and Saunthararajah, Y. Differential effects of low-dose decitabine on immune effector and suppressor responses in melanoma-bearing mice. *Cancer Immunol Immunother*. 2012; 61(9): 1441-1450.

Troetel, W., Weiss, A., Stambaugh, J., Laucius, J., and Manthei, R. Absorption, distribution, and excretion of 5-azacytidine (NSC-102816) in man. *Cancer Chemother Rep* 1972; 56(3): 405-411.

Uhrberg, M., Valiante, N.M., Shum, B.P., Shilling, H.G., Lienert-Weidenbach, K., Corliss, B., Tyan, D., Lanier, L.L., and Parham, P. Human Diversity in Killer Cell Inhibitory Receptor Genes. *Immunity*. 1997; 7(6): 753-763.

Vago, L., Forno, B., Sormani, M.P., Crocchiolo, R., Zino, E., Di Terlizzi, S., Lupo Stanghellini, T.M., Mazzi, B., Perna, S.K., Bondanza, A., Middleton, D., Palini, A., Bernardi, M., Bacchetta, R., Peccatori, J., Rossini, S., Roncarolo, M.G., Bordignon, C., Bonini, C., Ciceri, F., and Fleischhauer, K. Temporal , quantitative , and functional characteristics of single-KIR – positive alloreactive natural killer cell recovery account for impaired graft-versus-leukemia activity after haploidentical hematopoietic stem cell transplantation. *Blood*. 2008; 112: 3488-3499.

Valiante, N.M., Uhrberg, M., Shilling, H.G., Lienert-Weidenbach, K., Arnett, K.L., D'Andrea, A., Phillips, J.H., Lanier, L.L., and Parham, P. Functionally and Structurally Distinct NK Cell Receptor Repertoires in the Peripheral Blood of Two Human Donors. *Immunity*. 1997; 7(6): 739-751.

Vardiman, J.W., Thiele, J., Arber, D.A., Brunning, R.D., Borowitz, M.J., Porwit, A., Harris, N.L., Le Beau, M.M., Hellström-Lindberg, E., Tefferi, A., and Bloomfield, C.D. The 2008 revision of the World Health Organization (WHO) classification of myeloid neoplasms and acute leukemia: rationale and important changes. *Blood*. 2009; 114(5): 937-951.

Venturelli, S., Armeanu, S., Pathil, A., Hsieh, C.-J., Weiss, T.S., Vonthein, R., Wehrmann, M., Gregor, M., Lauer, U.M., and Bitzer, M. Epigenetic combination therapy as a tumor-selective treatment approach for hepatocellular carcinoma. *Cancer*. 2007; 109(10): 2132-2141.

Vey, N., Bourhis, J.-H., Boissel, N., Bordessoule, D., Prebet, T., Charbonnier, A., Etienne, A., Andre, P., Romagne, F., Benson, D., Dombret, H., and Olive, D. A phase 1 trial of the anti-inhibitory KIR mAb IPH2101 for AML in complete remission. *Blood*. 2012; 120(22): 4317-4323.

Vilches, C., Castan, J., and Estefanı, E. Facilitation of KIR genotyping by a PCR-SSP method that amplifies short DNA fragments. *Tissue Antigens*. 2007; 70: 415-422.

Vilches, C., and Parham, P. KIR : Diverse , Rapidly Evolving Receptors of Innate and Adaptive Immunity. *Annu Rev Immunol*. 2002; 20: 217-251.

Welte, S., Kuttruff, S., Waldhauer, I., and Steinle, A. Mutual activation of natural killer cells and monocytes mediated by NKp80-AICL interaction. *Nat Immunol*. 2006; 7(12): 1334-1342.

Welte, S.A., Sinzger, C., Lutz, S.Z., Singh-Jasuja, H., Sampaio, K.L., Eknigk, U., Rammensee, H.-G., and Steinle, A. Selective intracellular retention of virally induced NKG2D ligands by the human cytomegalovirus UL16 glycoprotein. *Eur J Immunol*. 2003; 33(1): 194-203.

Wende, H., Colonna, M., Ziegler, A., and Volz, A. Organization of the leukocyte receptor cluster (LRC) on human Chromosome 19q13.4. *Mamm Genome*. 1999; 10: 154-160.

Woiterski, J., Ebinger, M., Witte, K.E., Goecke, B., Heininger, V., Philippek, M., Bonin, M., Schrauder, A., Röttgers, S., Herr, W., Lang, P., Handgretinger, R., Hartwig, U.F., and Andre, M.C. Engraftment of low numbers of pediatric acute lymphoid and individual leukemogenecity and highly correlates with clinical outcome. *Int J Cancer*. 2013; 133: 1547-1557.

Yang, Q., Tian, Y., Ostler, K., Chlenski, A., Guerrero, L., Salwen, H., Godley, L., and Cohn, S. Epigenetic alterations differ in phenotypically distinct human neuroblastoma cell lines. *BMC Cancer*. 2010; 10(1): 286.

Yokota, Y., Mansouri, A., Mori, S., Sugawara, S., Adachi, S., Nishikawa, S.-I., and Gruss, P. Development of peripheral lymphoid organs and natural killer cells depends on the helix-loop-helix inhibitor Id2. *Nature*. 1999; 397(6721): 702-706.

Yokoyama, W.M., and Kim, S. Licensing of natural killer cells by self-major histocompatibility complex class I. *Immunol Rev*. 2006; 214: 143-154.

Zamai, L., Ahmad, M., Bennett, I.M., Azzoni, L., Alnemri, E.S., and Perussia, B. Natural Killer (NK) Cell–mediated Cytotoxicity: Differential Use of TRAIL and Fas Ligand by Immature and Mature Primary Human NK Cells. *J Exp Med*. 1998; 188(12): 2375-2380.

Zhang, Y., Wallace, D.L., De Lara, C.M., Ghattas, H., Asquith, B., Worth, A., Griffin, G.E., Taylor, G.P., Tough, D.F., Beverley, P.C.L., and Macallan, D.C. In vivo kinetics of human natural killer cells: the effects of ageing and acute and chronic viral infection. *Immunology*. 2007; 121(2): 258-265.

Zhou, H., Bao, X., Wu, X., Tang, X., Wang, M., Wu, D., and He, J. Donor Selection for Killer Immunoglobulin-like Receptors B Haplotype of the Centromeric Motifs Can Improve the Outcome after HLA-Identical Sibling Hematopoietic Stem Cell Transplantation. *Biol Blood Marrow Transplant*. 2014; 20(1): 98-105.

Zwaan, M., C., and M. van den Heuvel-Eibrink, M. Pediatric Acute Myeloid Leukemia. Acute Leukemia - The Scientist's Perspective and Challenge, M. Antica (Ed.), InTech, 2011. Available from: http://www.intechopen.com/books/acute-leukemia-the-scientist-s-perspectiveand-challenge/pediatric-acute-myeloid-leukemia.

OWN PUBLICATIONS

Publications (international journals, peer-reviewed)

Dannenmann, B.*, Lehle, S.*, Hildebrand, DG., **Kübler, A.**, Grondona, P., Schmid, V., Holzer, K., Fröschl, M., Essmann, F., Rothfuss, O., and Schulze-Osthoff, K. *Co-first author. High Glutathione and Glutathione Peroxidase-2 Levels Mediate Cell-Type-Specific DNA Damage Protection in Human Induced Pluripotent Stem Cells. *Stem Cell Reports*. 2015; 4(5): 886-898.

Steinbacher J., Baltz-Ghahremanpour K., Schmiedel B.J., Steinle A., Jung G., **Kübler A.**, André M.C., Grosse-Hovest L. Salih H.R. (2015). An Fc-optimized NKG2D-IgG fusion protein for induction of natural killer cell reactivity against leukemia. *Int J Cancer. 2015;* 136, 1073-1084.

Kübler A., Woiterski J., Witte K.E., Bühring H.J., Hartwig U.F., Ebinger M., Oevermann L., Mezger M., Herr W., Lang P., Handgretinger R., Münz C., André M.C. Both mature KIR+ but also immature KIR- NK control pediatric acute B cell precursor leukemia NOD.Cg-Prkdcscid IL2rgtmWjl/Sz mice. *Blood.* 2014; 124, 3914-3923.

Gille C., Orlikowsky T.W., Spring B., Hartwig U.F., **Wilhelm A.**, Wirth A., Goecke B., Handgretinger R., Poets C.F., André M.C. Monocytes derived from humanized neonatal NOD/SCID/IL2Rγ(null) mice are phenotypically immature and exhibit functional impairments. *Hum Immunol*. 2012; 73 (4): 346–354.

André M.C., Erbacher A., Gille C., Schmauke V., Goecke B., Hohberger A., Mang P., **Wilhelm A.**, Mueller I., Herr W., Lang P., Handgretinger R., Hartwig U.F. Long-term human CD34+ stem cell-engrafted nonobese diabetic/SCID/IL-2R gamma(null) mice show impaired CD8+ T cell maintenance and a functional arrest of immature NK cells. *J. Immunol*. 2010; 185(5):2710-20.

Contributions to (international) conferences

A. Kübler, J. Woiterski, K.-E. Witte, U.F. Hartwig, M. Ebinger, W. Herr, P. Lang, R. Handgretinger, C. Münz, M.C. André. More than direct cytotoxicity: increased natural killer cell differentiation promotes antileukemic activity of 5-azacytidine. Poster at the EMBO conference on Innate Lymphoid Cells, October 2014, Institut Pasteur, Paris, France. Travel Grant from the German Academic Exchange Service.

A. Kübler, J. Woiterski, K.-E. Witte, H.-J. Bühring, U.F. Hartwig, M. Ebinger, L. Oevermann, M. Mezger, W. Herr, P. Lang, R. Handgretinger, C. Münz, M.C. André. KIR-KIRL mismatch constellations promote NK cell-mediated GvL effects against pediatric acute B cell precursor leukaemia. Poster at the Natural Killer Cell Symposium September 2014 Hannover, Germany.

A. Wilhelm, J. Woiterski, K. E. Witte, M. Mezger, L. Oevermann, U. F. Hartwig, M. Ebinger, B. Goecke, M. M. Pfeiffer, W. Herr, P. Lang, R. Handgretinger, M. C. André. Induction of killer immunoglobulin-like receptor (KIR) expression on NK cells potentiates *in vivo* alloreactivity against pediatric B cell precursor leukemia in a NOD/SCID/IL2Rγ^{null} xenotransplantation model. Poster at the 7th International Symposium on the Clinical Use of Cellular Products, March 2013 Erlangen, Germany.

A. Wilhelm, O. Rothfuss, K. Schulze-Osthoff. Cell cycle arrest upon DNA damage in human induced pluripotent stem cells. Poster at the international conference “Stem Cells in Development and Disease”, September 2011, Max-Delbrueck-Center for Molecular Medicine Berlin, Germany.

CONTRIBUTIONS

The data presented in this thesis is a result of my own work with the following exceptions/contributions:

Data from functional response stainings were obtained together with Dr. Jeanette Woiterski who established and mainly performed functional response stainings (Fig. 15,Fig. 16). The antibody panel for discrimination of the alloreactive and non-alloreactive NK cell subsets for the degranulation assay Fig. 16 was planned by myself, as well as the evaluation in Fig. 13B.

FACS sorting of KIR+ and KIR- NKAES cells was performed with the help and advice of Kai Witte and Prof. Dr. Hans-Jörg Bühring, together with Dr. Jeanette Woiterski in the Sorting Facility at the Department of Internal Medicine II, Eberhard Karls University Tuebingen.

Kai Witte helped in designing, evaluation and interpretation of the patient-specific antibody panels for detection of MRD in huNSG mice and contributed to performing the MRD data in one of the 5-AzaC *in vivo* experiments.

5-AzaC *in vivo* experiments were performed together with Dr. Jeanette Woiterski, but the experimental layout, planning of antibody panels and data analysis was performed by myself.

Dr. Markus Mezger and Dr. Lena Oevermann established the KIR-Q-PCR at the Children's University Hospital in Tuebingen. Dr. Markus Mezger helped with interpreting the KIR-Q-PCR data.

Maximilian Rentschler performed NKAES expansion and 5-AzaC treatment and KIR-Q-PCR for 5 out of 12 donors (Fig. 21) during his Master Thesis under my supervision.

Kathrin Stauß and Barbara Goecke provided technical assistance.

Dr. Dr. Maya André as direct supervisor was involved in planning, analysis, discussion, presentation, and interpretation of all data.

Parts of this research are published in (Kübler et al. 2014).

ACKNOWLEDGMENTS

My sincere thanks go to Dr. Dr. Maya André for her exceptional supervision and support that enabled pursuing my PhD thesis. She is always available to discuss ideas, projects and to help solving problems, I am very grateful for her remarkable engagement. I would like to thank her for the interesting discussions, personal conversations and continuous support!

I am grateful to Dr. Jeanette Woiterski for the good teamwork! I thank her and the other current and former members of the André lab but also all other researchers from floor C02 (especially AG Holzer, AG Ebinger, AG Mezger) of the University Children's Hospital Tuebingen who contributed to a good atmosphere for the good teamwork and the great time!

I would like to thank Prof. Dr. Rupert Handgretinger for his support and the opportunity to perform research in his department.

I am very grateful for the excellent technical assistance from Kathrin Stauß and Barbara Goecke and to all who contributed to this work.

I would like to thank Kai Witte for his help in designing antibody panels, solving problems with the LSRII FACS and the Aria cell sorter, and the interesting discussions.

I am grateful for the advice from Dr. Markus Mezger for the KIR-Q-PCR and the help of Maximilian Rentschler during his internship and master thesis. Thank you also for the nice time with the other interns, MD or diploma students (Dorothea Köthe, Ruhila Zahin, Richard Baumgartner, Sabrina Eilenberger, David Volpini, Dennis Clement).

Further, I am grateful for the interesting and fruitful cooperation with the lab of Prof. Dr. H. Salih (Department of Hematology and Oncology, Eberhard Karls University, Tuebingen, Germany), especially with Julia Steinbacher, Samuel Körner and Dr. Phil Kousis.

I would like to thank Dr. Martin Ebinger for providing patient samples and to all who contributed to establish and maintain the "Blastenbank" (AG André, AG Ebinger) at the University Children's Hospital Tuebingen.

I would also like to thank all children from the University Children's Hospital Tuebingen who donated bone marrow samples at the time of diagnosis, their parents for donating HSCs and the healthy volunteers for donating large blood volumes for NK cell isolation or expansion!

Thank you to Dr. Martin Thunemann and Dr. Katharina Hammer for reading and commenting the manuscript of this thesis.

Finally, I am very grateful for my fantastic husband Andreas who is always there for me. Thank you for your encouraging words in difficult times and your support and understanding that enables me to continue!

[i] This research was originally published in *Blood*. Kübler, A., Woiterski, J., Witte, K.-E., Bühring, H.-J., Hartwig, U.F., Ebinger, M., Oevermann, L., Mezger, M., Herr, W., Lang, P., Handgretinger, R., Münz, C., and André, M.C. Both mature KIR+ and immature KIR− NK cells control pediatric acute B-cell precursor leukemia in NOD.Cg-Prkdcscid IL2rgtmWjl/Sz mice. *Blood*. 2014; 124(26): 3914-3923. © The American Society of Hematology.

[ii] This research was originally published in *Blood,* see [i]. Data displayed in Fig. 12 of this work is shown in Fig. 2C in a different representation.